Microalgal-Bacterial Membrane Photobioreactor (MB-MPBR) for Wastewater Treatment and Membrane Fouling Characterization

A Thesis

Presented to

The Faculty of Graduate Studies

of

Lakehead University

by

Mei-jia Zhang

In partial fulfilment of requirements

for the degree of

Doctor of Philosophy

September 2020

Abstract

This thesis investigated the effects of combined hydraulic retention time (HRT) and nitrogen/phosphorus (N/P) ratio variation, and solo solids retention time (SRT) variation on the biological performance and membrane fouling of microalgal-bacterial membrane photobioreactor (MB-MPBR) for wastewater treatment.

The results showed that both HRT and N/P ratio significantly affected biomass production, nutrient removal, and biological micromorphology. The reason was attributed to the different nutrient loading rates resulted from the various combinations of HRT and N/P ratio. Controlling nutrient loading rate below the nutrients removal capacity threshold was critical to achieving superior effluent quality meeting the discharge standards.

A lower N/P ratio of 3.9:1 led to a more quickly transmembrane pressure increase under the same HRT and total influent nitrogen concentration. Characterization of mixed liquor showed that smaller particle size under the lower N/P ratio was the primary contributor to the faster increase in membrane fouling. X-ray photoelectron spectroscopy (XPS), fourier transform infrared spectroscopy (FTIR), and microscopic analysis demonstrated that the underlying reason for the decreased floc size was attributed to the strengthened competitiveness and overgrowth of microalgae at P-rich conditions.

The application of MB-MPBR for the treatment of high strength anaerobic digestion effluent at three SRTs of 10, 20, and 30 d was evaluated. Longer SRT led to a higher biomass concentration and increased total phosphorus removal efficiency, which was attributed to the enhanced surface-adsorption under higher biomass concentration. The total nitrogen removal relied on microalgae assimilation, whereas they nonlinearly correlated to SRT. SRT had significant influences on the particle size distribution and microscopic morphology of microalgal-bacterial consortium.

Membrane fouling rate in MB-MPBR nonlinearly correlated with SRT and the highest membrane fouling was observed at SRT of 20 d. It was mainly attributed to the higher

concentration of extracellular polymeric substances (EPSs) and soluble microbial products (SMPs). Environmental stress and fierce competition between microalgae and bacteria were considered as the underlying reason for the increased production of EPSs and SMPs.

The results suggest that MB-MPBR is a promising technology for simultaneous removals of organics and nutrients from wastewater. Optimizing the operating conditions to balance the microalgae and bacteria at an appropriate rate is the key to achieve high-quality effluent meeting the discharge standards and effective membrane fouling control in MB-MPBRs.

Keywords: Microalgal-bacterial membrane photobioreactor; Hydraulic retention time; Solids retention time; N/P ratio; Nutrients removal; Characterization; Membrane fouling; Wastewater treatment; Anaerobic digestion effluent

Acknowledgements

On the completion of this thesis, I would like to express my deep gratitude to many people who gave their help to my research and made this thesis possible.

I would like first to express my sincere appreciation to my Ph.D. supervisors Dr. Baoqiang Liao and Dr. Kam Tin Leung, for their careful guidance and continuous supports to my research. Their active academic thoughts, pragmatic work style, and rigorous scientific research attitude have benefited me a lot.

I also want to express my deep gratitude to my supervisory committee membranes, Dr. Pedram Fatehi and Dr. Wa Gao, for their time, suggestions, and guidance. I am also thankful to Dr. Siamak Elyasi, who served as the external member for my comprehensive examination, Dr. Wensheng Qin, who chaired the comprehensive examination, as well as Dr. Qiuyan Yuan, who served as the external examiner for my doctoral dissertation.

Also, I must thank Lakehead University for offering me the opportunity and Natural Sciences and Engineering Research Council of Canada (NSERC) for providing funding to this research. Other financial assistance from the University and Government are also much appreciated. Besides, many thanks also go to Dr. Brenda Magajna, Dr. Jinan Fiaidhi, Maegen Lavallee, and the Faculty of Graduate Studies for administrative support. Thank all the professors, staffs, and classmates in the Program of Biotechnology, communications with you make me grow a lot.

Special thanks to Dr. Guosheng Wu, Mr. Greg Krepka, and Mr. Michael Sorokopud for their training and testing services. I also wish to express my sincere thanks to Dr. Weijue Gao and my team members Alnour Bokhary, Yichen Liao, Lishan Yao, Zhe Feng, and Maryam Amini for their great help and support in the lab. Great thanks also go to all other team membranes for their help and kindness.

Finally, I want to express my sincere gratitude to my family, especially my husband (Mengyong Ruan), who always stands behind me to provide companionship, support, care, and encouragement

to help me get through the difficult times. His unconditional understanding and encouragement are the biggest motivation for my study.

Tables of Contents

List of Figures

List of Tables

List of Nomenclature and Abbreviations

Nomenclature

r_x	productivity of the biomass
X	average biomass concentration
Q_{waste}	biomass wasting rate
$V_{MB\text{-}MPBR}$	working volume of the bioreactor
C_{inf}	concentration of TN or TP in the feed
C_{eff}	concentration of TN or TP in the effluent
Q	flow rate
V	working volume
R	filtration resistance
R_t	total filtration resistance
R_m	virgin membrane filtration resistance
R_p	pore-clogging filtration resistance
R_c	cake layer filtration resistance
ΔP	trans-membrane pressure difference
J	permeate flux
μ	permeate dynamic viscosity
R_g	gel layer filtration resistance

Abbreviations

ADF	average daily flow
ADW	anaerobically digested wastewater
AnMBR	anaerobic membrane bioreactor
ANOVA	analysis of variance
AW	aquaculture wastewater
BAP	biomass-associated products
BOD	biochemical oxygen demand
CAS	conventional activated sludge
C-MBR	conventional membrane bioreactor
CO_2	carbon dioxide
COD	chemical oxygen demand
COD/N	chemical oxygen demand/nitrogen
ECs	emerging contaminants
EPS	extracellular polymeric substances
F/M	food-microorganisms
FO	forward osmosis
FS	flat sheet
FTIR	fourier transform infrared spectroscopy
HF	hollow fiber
HRT	hydraulic retention time
HU	human urine
IC	inorganic carbon
IEM	ion-exchange-membrane
IEM-PBR	ion-exchange-membrane photobioreactor
LLW	landfill leachate wastewater
MB-MPBR	microalgal-bacterial membrane photobioreactor

MBR	membrane bioreactor
MF	microfiltration
MLSS	mixed liquor suspended solids
MPBR	membrane photobioreactor
MSM	mineral salt medium
N/P	nitrogen/phosphorus
OLR	organic lading rate
PAC	powdered activated carbon
PAFC	polymeric aluminum ferric chloride
PACI	polymeric aluminum chloride
PAN	polyacrylonitrile
PBR	photobioreactor
PE	polyethylene
PES	polyethersulfone
PFS	polymeric ferric sulphate
PSD	particle size distribution
PVDF	polyvinylidene fluoride
QQ	quorum quenching
QS	quorum sensing
RES	real secondary treated wastewater
S/V	surface to volume ratio
SMP	soluble microbial products
SRT	solids retention time
SSE	synthetic secondary treated effluent
TMP	transmembrane pressure
TN	total nitrogen
TOC	total organic carbon

TP	total phosphorus
UAP	substrate-utilization-associated products
UMW	untreated municipal wastewater
XPS	X-ray photoelectron spectroscopy

Chapter 1 Introduction

1.1 Overview

Water shortage is one of the most pervasive and severe problems throughout the world. With the rapid growth in human population and the global economy, the issue of water scarcity is expected to grow worse, and the discrepancies between water supply and demand become increasingly aggravated. While the overall water demand grows, the available water is decreasing due to water pollution from wastewater. With the accelerated urbanization and industrialization, the wastewater production from human activities continuously increases. Wastewater contains pollutants and requires proper treatment before disposal. However, it was reported over 80% of wastewater overall the world is discharged directly into the environment without adequate treatment (WWAP, 2017), which leads to water pollution, ecological damage, and health hazards. In the coming decades, water scarcity is believed may become the fuse of war, unless new ways to supply clean water are found (Shannon et al., 2008).

In the face of the ever-growing severe problem of water shortage, wastewater reuse, recycling and resource recovery are considered as a part of the solution to the problem. Therefore, numerous processes have been developed to recover energy, nutrients, and clean water from sewage. Among the multiple wastewater treatment processes, membrane bioreactor (MBR) is an advance technology being considered as one the most promising technology for wastewater treatment and reuse over the coming decades (Shannon et al., 2008). In comparison with conventional activated sludge (CAS) process, MBR technology not only can produce high-quality effluent but also has broad potential application in improving environmental sanitation and recycling valuable resources from wastewater (Daigger et al., 2005). To date, MBRs have been extensively applied in more than 200 countries for municipal and industrial wastewater treatment.

Although MBR technology takes many distinctive advantages, a broader application of this technology requires further research and development. In traditional MBR systems, the bacteria mainly play a role for organics removal and the nutrients (nitrogen and phosphorus) removal

efficiency is low. The excessive disposal of nutrients into the water body will cause the problem of eutrophication. Therefore, other processes should be integrated with traditional MBR systems to improve nutrient removal efficiency and meet the wastewater discharge standards. However, these processes require additional equipment, which will result in an increase in capital costs (Marbelia et al., 2014). Besides, membrane fouling is inevitable in MBRs and becomes the primary obstacle to the widespread application of MBR. To date, membrane fouling problem is still not fully understood. Therefore, for MBR research, it is necessary to take actions from a new perspective to improve the treatment performance, deeper understand fouling mechanisms, and develop more cost-effective strategies.

Characteristics of microalgae provide new ideas for the improvement of MBR technology. Microalgae can fix carbon in the form of CO_2, assimilate inorganic nitrogen and phosphorus, and realize biomass accumulation through photosynthesis (Jia & Yuan, 2016; Yao et al., 2019). As a new sustainable bio-based feedstock, the wasted microalgae biomass can be used for biofuels production. Therefore, microalgae have been extensively applied for wastewater treatment (Gao et al., 2016; Honda et al., 2017; Luo et al., 2017; Xu et al., 2015). A superior kind of biomass is algal-bacterial consortia, which can simultaneously remove organic matters and inorganic nutrients from wastewater with high efficiency (Alcántara et al., 2015; de Godos et al., 2011; Karya et al., 2013; Lee et al., 2015; Posadas et al., 2013). The idea of using microalgae-bacteria symbiosis system for sewage treatment was first proposed by Oswald and Gotaas in the 1960s (Zhang et al., 2020). Nowadays, the feasibility, effectiveness, and potential of microalgae-bacteria for wastewater treatment also have been broadly proven in conventional membrane-free systems (Alcántara et al., 2015; Lee et al., 2015; Medina & Neis, 2007; Posadas et al., 2013). In the microalgal-bacterial consortium, CO_2 produced by bacteria is used to support the growth of microalgae for inorganic nutrient removal and O_2 produced by microalgae is used for bacterial decomposition of organic compounds (Oswald, 1988). This synergy reduces the energy demand of mechanical aerations for CO_2 and O_2 deliveries, and hence be regarded as a safer and more cost-effective alternative of mechanical aeration. Nevertheless, conventional algal-related systems

associated with a problem of biomass washout due to the coupling solids retention time (SRT) and hydraulic retention time (HRT), which will result in the poor effluent quality, unstable or even failed system. A simple and efficient solution to prevent microalgae washout is the integration of membrane separation within the photobioreactor to retain all algae cells.

To date, the application of membrane photobioreactors (MPBR, integration of membrane module within microalgal solo systems) in wastewater treatment has been widely reported. The relationships between MPBR performance and operating conditions have been summarized in previous literature (Luo et al., 2017). According to the previous literature, MPBRs are mainly used for the treatment of secondary effluent, where most of the organic carbon substances have been removed. Other wastewaters with a high level of organic matters are not good selections for MPBR system due to the severe inhibitory action to microalgae growth.

In recent years, microalgal-bacterial membrane photobioreactor (MB-MPBR), a novel system combing membrane separation system with the microalgal-bacterial consortium, has been developed. It was reported that MB-MPBR has a higher nutrient removal rate than traditional MBR and can significantly reduce membrane fouling (Sun et al., 2018a; Sun et al., 2018c). Another two studies figured out that the microalgae/bacteria inoculating ratio and SRT have important influences on the biological performance as well as membrane performance and microorganism community in MB-MPBR (Sun et al., 2018b; Yang et al., 2018). Like MBRs, the biological performance and membrane fouling in MB-MPBRs depend on various factors, including feed composition, nutrients loading rate, HRT, SRT, etc. In MB-MPBR, the introduction of microalgae not only varies the biological communities in the bioreactor but also changes the effects law of operating conditions on processing performance and membrane fouling. Therefore, previous rules regarding MBRs cannot be directly adopted for MB-MPBRs. For such a novel system, we have limited knowledge about it. Therefore, more studies are required to understand MB-MBPR and promote its development.

1.2 Objectives

The long-term goal of this study is to develop a novel system of MB-MPBR for wastewater treatment and resource recovery with a high efficiency that is not achievable with current technologies. Therefore, this thesis intends to study the feasibility of MB-MPBRs, identify the critical influence factors, and investigate the membrane fouling performance. The specific research objectives were as follows:

(1) develop an MB-MPBR process for the treatment of municipal wastewater and investigate the effects of HRT and N/P ratio on the biological performance of the MB-MPBR for simultaneous removals of COD and nutrients (N and P) from municipal wastewater;

(2) investigate the impacts of N/P ratio on the properties of microalgal-bacterial consortium and their role in membrane fouling for the MB-MPBR system;

(3) identify the effects of SRT on the biological performance of an MB-MPBR for the treatment of anaerobic digestion effluent with high strength organics and nutrients; and

(4) investigate the effects of SRT variations on the biomass properties and membrane fouling of the MB-MPBR treating high-strength anaerobic digestion effluent with enriched nutrients.

1.3 Scope of this thesis

This thesis developed a novel system of MB-MPBR and investigated the application of this system for the treatment of municipal wastewater and anaerobic digestion effluent. The effects of conditions variation (HRT and N/P ratio variation, and SRT variation) on the process performance and membrane fouling were studies. Based on the experimental results, the feasibility and potential of MB-MPBR for simultaneous removals of COD and nutrients from wastewaters were briefly evaluated.

In **Chapter 1**, the research background and study objectives are presented.

Chapter 2 covers a literature review about the wastewater treatment status. The literature review is structured into four sections. The first section briefly introduces the conventional processes developed for wastewater treatment as well as their main drawbacks. The second and

third sections discuss the application of MBR and MPBR in wastewater treatment, respectively. Furthermore, the current understanding of membrane fouling and fouling control strategies are discussed in the fourth section.

In **Chapter 3**, a submerged MB-MPBR was developed and operated over 350 days for synthetic municipal wastewater treatment. The variations of MB-MPBR performance with HRT and N/P ratio were evaluated based on the evaluations of series parameters, including biomass production, biomass productivity, COD removal, nutrient (N and P) removal, and partial consortium properties.

Chapter 4 compares the physic-chemical properties of microalgal-bacterial consortium and its membrane fouling propensity under different combinations of HRT and N/P ratio. Various characterizations, including transmembrane pressure (TMP), filtration resistance composition, soluble microbial products (SMP), extracellular polymeric substances (EPS), X-ray photoelectron spectroscopy (XPS), fourier transform infrared spectroscopy (FTIR), particle size distribution (PSD), and microscopic observation, were conducted.

Chapter 5 deals with the application of an MB-MPBR treating anaerobic digestion effluent at three SRTs of 10, 20, and 30 d. Influences of SRT on the MB-MPBR performance and biomass properties were investigated.

Chapter 6 discusses the effects of SRT on membrane fouling based on a series of characterizations, including TMP, filtration resistance composition, PSD, micromorphology, SMP, EPS, XPS, and FTIR.

Chapter 7 states the overall conclusions and recommendations for future work.

1.4 References

Alcántara, C., Domínguez, J. M., García, D., Blanco, S., Pérez, R., García-Encina, P. A., Muñoz, R., 2015. Evaluation of wastewater treatment in a novel anoxic–aerobic algal–bacterial photobioreactor with biomass recycling through carbon and nitrogen mass balances.

Bioresource Technology. 191, 173-186.

Daigger, G. T., Rittmann, B. E., Adham, S., Andreottola, G., 2005. Are membrane bioreactors ready for widespread application? *Environmental Science and Technology*. 39(19), 399a-406a.

de Godos, I., Guzman, H. O., Soto, R., García-Encina, P. A., Becares, E., Muñoz, R., Vargas, V. A., 2011. Coagulation/flocculation-based removal of algal–bacterial biomass from piggery wastewater treatment. *Bioresource Technology*. 102(2), 923-927.

Gao, F., Li, C., Yang, Z.-H., Zeng, G.-M., Feng, L.-J., Liu, J.-z., Liu, M., Cai, H.-w., 2016. Continuous microalgae cultivation in aquaculture wastewater by a membrane photobioreactor for biomass production and nutrients removal. *Ecological Engineering*. 92, 55-61.

Honda, R., Teraoka, Y., Noguchi, M., Yang, S., 2017. Optimization of Hydraulic Retention Time and Biomass Concentration in Microalgae Biomass Production from Treated Sewage with a Membrane Photobioreactor. *Journal of Water and Environment Technology*. 15(1), 1-11.

Jia, H., Yuan, Q., 2016. Removal of nitrogen from wastewater using microalgae and microalgae–bacteria consortia. *Cogent Environmental Science*. 2(1), 1275089.

Karya, N. G. A. I., van der Steen, N. P., Lens, P. N. L., 2013. Photo-oxygenation to support nitrification in an algal–bacterial consortium treating artificial wastewater. *Bioresource Technology*. 134, 244-250.

Lee, C. S., Lee, S.-A., Ko, S.-R., Oh, H.-M., Ahn, C.-Y., 2015. Effects of photoperiod on nutrient removal, biomass production, and algal-bacterial population dynamics in lab-scale photobioreactors treating municipal wastewater. *Water Research*. 68, 680-691.

Luo, Y., Le-Clech, P., Henderson, R. K., 2017. Simultaneous microalgae cultivation and wastewater treatment in submerged membrane photobioreactors: A review. *Algal Research*. 24, 425-437.

Marbelia, L., Bilad, M. R., Passaris, I., Discart, V., Vandamme, D., Beuckels, A., Muylaert, K., Vankelecom, I. F. J., 2014. Membrane photobioreactors for integrated microalgae cultivation and nutrient remediation of membrane bioreactors effluent. *Bioresource Technology*. 163, 228-235.

Medina, M., Neis, U., 2007. Symbiotic algal bacterial wastewater treatment: effect of food to microorganism ratio and hydraulic retention time on the process performance. *Water Science and Technology*. 55(11), 165-171.

Oswald, W. J., 1988. Micro-algae and wastewater treatment. in: *Micro-algal Biotechnology*, (Eds.) Borowitska, M. A., Borowitzka, L. J., Cambridge, pp. 305-328.

Posadas, E., García-Encina, P.-A., Soltau, A., Domínguez, A., Díaz, I., Muñoz, R., 2013. Carbon and nutrient removal from centrates and domestic wastewater using algal–bacterial biofilm bioreactors. *Bioresource Technology*. 139, 50-58.

Shannon, M. A., Bohn, P. W., Elimelech, M., Georgiadis, J. G., Mariñas, B. J., Mayes, A. M., 2008. Science and technology for water purification in the coming decades. *Nature*. 452(7185), 301-310.

Sun, L., Tian, Y., Zhang, J., Cui, H., Zuo, W., Li, J., 2018a. A novel symbiotic system combining algae and sludge membrane bioreactor technology for wastewater treatment and membrane fouling mitigation: Performance and mechanism. *Chemical Engineering Journal*. 344, 246-253.

Sun, L., Tian, Y., Zhang, J., Li, H., Tang, C., Li, J., 2018b. Wastewater treatment and membrane fouling with algal-activated sludge culture in a novel membrane bioreactor: Influence of inoculation ratios. *Chemical Engineering Journal*. 343, 455-459.

Sun, L., Tian, Y., Zhang, J., Li, L., Zhang, J., Li, J., 2018c. A novel membrane bioreactor inoculated with symbiotic sludge bacteria and algae: Performance and microbial community analysis. *Bioresource Technology*. 251, 311-319.

WWAP (United Nations World Water Assessment Programme). 2017. The United Nations World Water Development Report 2017. Wastewater: The Untapped Resource. Paris, UNESCO.

Xu, M., Li, P., Tang, T., Hu, Z., 2015. Roles of SRT and HRT of an algal membrane bioreactor system with a tanks-in-series configuration for secondary wastewater effluent polishing. *Ecological Engineering*. 85, 257-264.

Yang, J., Gou, Y., Fang, F., Guo, J., Ma, H., Wei, X., Shahmoradi, B., 2018. Impacts of sludge

retention time on the performance of an algal-bacterial bioreactor. *Chemical Engineering Journal*. 343, 37-43.

Yao, S., Lyu, S., An, Y., Lu, J., Gjermansen, C., Schramm, A., 2019. Microalgae–bacteria symbiosis in microalgal growth and biofuel production: a review. *Journal of Applied Microbiology*. 126(2), 359-368.

Zhang, M., Lee, E., Vonghia, E., Hong, Y., Liao, B., 2020. 1 - Introduction to aerobic membrane bioreactors: Current status and recent developments. in: *Current Developments in Biotechnology and Bioengineering*, (Eds.) Ng, H. Y., Ng, T. C. A., Ngo, H. H., Mannina, G., Pandey, A., Elsevier, pp. 1-23.

Chapter 2 Literature Review

2.1 Conventional processes for wastewater treatment

The lack of clean water is a worldwide problem afflicting human beings. It was reported 1.2 billion people lack access to safe drinking water all over the world (Shannon et al., 2008). The rapid growth of the global economy and human population promotes the production of wastewater. The amount of municipal and industrial sewage reached approximately 450 km^3 in 2010 and ever-grew every year (Mateo-Sagasta et al., 2015). The wastewater from human activities contains pollutants and requires proper treatment before disposal. However, globally, over 80% of all wastewater directly enters water bodies before adequate treatment (WWAP, 2017). This wastewater into the environment causes not only the immediate impacts of degraded water quality and ecological damage but also significant health issues. It was reported over 3900 children died from diseases every day due to the unsafe water (Shannon et al., 2008). On the other hand, global water demand significantly increases with the accelerated urbanization and industrialization (WWAP, 2017). Consequently, applying effective wastewater treatment technologies to recover the energy, nutrients, and organic matters from the wastewater and realize the reuse of sewage is significantly essential.

The CAS process is the most common technique for organics removal and has been widely applied in the treatment of municipal and industrial sewage (Jenkins, 2014). It consists of an aeration tank for biological degradation and a secondary clarifier for physical separation. Activated sludge process is a cost-effective technology that possesses high efficiency of biodegradation and COD/BOD removal. However, the effluent quality of this process highly depends on the settling properties of the activated sludge (Martins et al., 2004). Bulking and foaming, mainly provoked by the overgrowth of filamentous microorganisms, are the frequently observed problems in activated sludge plants (Wanner, 1995). The occurrence of these problems would lead to the deterioration of sludge settleability, loss of activated sludge, reduction of effluent quality, and worse still, the fail of the system (Madoni et al., 2000; Martins et al., 2004). Therefore,

considerable efforts have been made to investigate the mechanisms of sludge bulking and foaming and expect to develop effective control strategies (Jenkins et al., 2004; Martins et al., 2004). Although the frequency and degree of sludge bulking and foaming can be reduced, bulking and foaming are ongoing problems in wastewater treatment plants operation since the possibility of sludge washout remains at some points.

In addition to activated sludge, microalgae are also considered as a promising alternative for wastewater treatment. Microalgae are a group of prokaryotic or eukaryotic photosynthetic microorganisms that exist in nature and can survive in various manners. They can convert solar energy into chemical energy and realize biomass accumulation through photosynthesis. Therefore, microalgae are regarded as the new sustainable biobased feedstock for the production of the third-generation biofuels which have the potential to replace the fossil fuels (Jesus et al., 2016; Maity et al., 2014). Besides, microalgae reveal a considerable potential in wastewater treatment and greenhouse gas mitigation (Brennan & Owende, 2010; Chen et al., 2015; Gao et al., 2014; Maity et al., 2014; Mata et al., 2010). As we all know, apart from organic matters, wastewater generally contains a high concentration of nutrients. The high-nutrient sewage discharged into the water bodies would result in eutrophication and an unhealthy aquatic ecosystem (Chen et al., 2015). Although CAS process has been widely used in nutrient removal, its economy was significantly weakened by the low removal efficiency and high requirement of aeration supply (Jia & Yuan, 2016). In comparison, microalgae possess higher efficiency for nutrients assimilation and offer a cheaper means for nutrients removal from wastewater than conventional activated sludge process. However, the microalgal processes need a long HRT to ensure enough nutrients uptake, which will increase the footprint of the system (Ting et al., 2017). Another way by increasing the flow rate of feed supply would cause the problem of microalgae washout (Gao et al., 2016a).

A simple and efficient solution to solve the above issues of sludge bulking and microalgae washout is the integration of membrane separation within the bioreactors to completely retain the biomass (activated sludge or microalgae) and decouple SRT and HRT. To date, the feasibility and effectiveness of membrane technology to solve the above problems have been verified by

numerous studies (Abass et al., 2015; Deowan et al., 2015; Drexler & Yeh, 2014; Kraume & Drews, 2010; Lin et al., 2012; Luo et al., 2017b).

2.2 Current status of membrane bioreactors for wastewater treatment

The MBR is a process integrating the membrane module into a biological process. The biological unit and the membrane module are responsible for the biodegradation of waste compounds and the physical solids/liquid separation, respectively (Deowan et al., 2015). According to configurations, the MBRs can be classified into external/side-stream MBR (Figure 2-1(a)) and submerged/immersed MBR (Figure 2-1(b)). In the external configuration, the membrane module is placed outside the MBR. This configuration has the advantages of flexible operation, easier membrane replacement, and high fluxes (Deowan et al., 2015; Lin et al., 2012). For submerged configuration, the membrane module is directly immersed in the reactor. In comparison to external MBR, submerged MBR possessed simpler configuration and lower energy consumption.

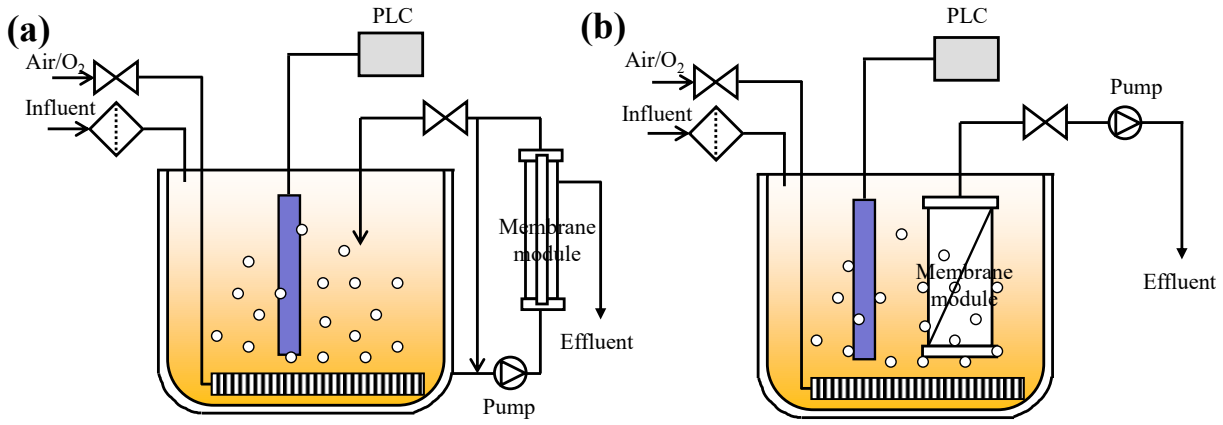

Figure 2-1 Membrane bioreactor configurations: (a) external configuration and (b) submerged configuration (drawn after Lin et al. (2012)).

The application of membrane in MBR offers some distinctive advantages over CAS processes, including excellent effluent quality, independent HRT and SRT, good disinfection capability, and reduced sludge production (Judd, 2008; Lin et al., 2012). With these advantages, MBR has been extensively applied in municipal and industrial wastewater treatment (Chan et al., 2009; Mutamim

et al., 2012; van Nieuwenhuijzen et al., 2008). Today, the MBR market is predominated by submerged membrane modules with configurations of the flat-sheet and hollow fibers (Fane et al., 2011). According to the recent reports, MBR systems have been installed in more than 200 countries, and the global market of MBR would grow from $ 1.9 billion in 2018 to reach $ 3.8 billion by 2023 (GVR report, 2017; BCC report, 2019). Table 2-1 summarizes the large MBR plants which have been commissioned during the last ten years with an average daily flow (ADF) greater than 175,000 m^3/d. It was reported that both the largest design capacity of MBR and the number of large-scale (≥ 10,000 m^3/d) and super-large-scale (≥ 100,000 m^3/d) plants gradually increase (Krzeminski et al., 2017; Xiao et al., 2019). The increase of MBR design capacity and large-scale number demonstrates the significant growth of MBR technology in recent years and reveals its promising momentum in the future.

Recently, many efforts have been conducted to improve membranes and MBR configurations to obtain a better effluent quality, lower operating cost, better membrane fouling control, and higher membrane lifespan. Membrane development targets a reduction in membrane module cost or the enhancement of membrane anti-fouling capacity. Currently, PVDF is the most prevalent commercial membrane chemistry used in aerobic MBR systems due to its superior chemical and fouling tolerance, comparably low cost, mechanical strength, and biological stability (Abass et al., 2015). However, research on new membrane development is constantly underway to challenge the status quo and extend membrane performance to more extreme conditions, stronger anti-fouling capacity or improved permeate quality. The associated studies involve the inorganic membranes, nano-composite membranes, and polymer-based osmotic membranes for MBR applications, which provides more ground for the potential use of MBR (Holloway et al., 2015; Jhaveri & Murthy, 2016; Wang et al., 2016).

Table 2-1 Summary of large-scale MBR plants in the world that have a design capacity higher than 200,000 m^3/d. Adopted from http://www.thembrsite.com/about-mbrs/largest-mbr-plants/ on June 20, 2020.

Installation	Location, Country	Peak daily flow (m^3/d)	Year of commissioning	Technology supplier
Tuas Water Reclamation Plant	Singapore	1,200,000	2025	TBC
Beihu WWTP	Hubei, China	1,040,000	2019	BOW
Henriksdal	Stockholm, Sweden	864,000	2019-2026	SUEZ
Huaifang Water Recycling Project	Beijing, China	780,000	2016	Memstar
Water Affairs Integrative EPC	Xingyi, Guizhou, China	399,000	2016-2017	BOW
Seine Aval	Acheres, France	357,000	2016	SUEZ
Canton WWTP	Ohio, USA	333,000	2015-2017	Ovivo
9th and 10th WWTP	Kunming, Yunnan, China	325,000	2013	BOW
Wuhan Sanjintan WWTP	Hubei, China	260,000	2015	BOW
Jilin WWTP (Phase 1, upgrade)	Jilin Province, China	260,000	2015	BOW
Caotan WWTP PPP project	Xi'an, Shanxi, China	260,000	2015-2017	BOW
Huhehaote Xinxinban WWTP	Mongolia, China	260,000	2016	BOW
Weibei Industrial Park Wanzi WWTP	Xi'an, China	260,000	2016	BOW
Liaoyang City Centre WWTP Phase 2	Liaoyang, China	260,000	2014	Memstar
Fuzhou Yangli WWTP (Phase 4)	Fuzhou, China	260,000	2015	Memstar
Chengdu Xingrong Project #3	Chengdu, China	260,000	2016	Memstar
Chengdu Xingrong Project #5	Chengdu, China	260,000	2016	Memstar
Chengdu Xingrong Project #8	Chengdu, China	260,000	2016	Memstar
Gaoyang Textile Industrial Park WWTP Phase 1 & 2 & 3	Gaoyang, Hebei, China	260,000	2016	Memstar
Euclid	Ohio, USA	250,000	2018	SUEZ
Shunyi	Beijing, China	234,000	2016	SUEZ

In addition, many types of novel MBRs with different purposes have been proposed and developed up to now. The configurational schematics of these MBRs have been summarized previously (Meng et al., 2012). According to the literature, these configurations are developed by integrating the MBR process with other technology or optimizing their configuration design. They can be roughly classified into four groups according to the purpose of 1) enhanced pollutants removal and fouling mitigation, 2) wastewater reuse, 3) energy reduction and 4) specific foulants removal (Krzeminski et al., 2017; Luo et al., 2017a; Meng et al., 2012; Morrow et al., 2018; Phattaranawik et al., 2008; Wang et al., 2017; Wang et al., 2011). Like the membrane development, the development of new MBR process configurations can improve market competition and broaden the MBR application to the areas like emerging contaminants (ECs) removal and sludge reduction (Besha et al., 2017; Do et al., 2009; Kim et al., 2018; Li et al., 2015; Na et al., 2017; Yoon et al., 2004).

2.3 Membrane photobioreactors

2.3.1 Description of membrane photobioreactor (MPBR)

MPBR is a system that combines a membrane module with a closed or semi-closed photobioreactor (PBR). Depending on the function of the membrane in the PBR system, the MPBR can be classified into carbonation MPBR and biomass retention MPBR (Bilad et al., 2014; Drexler & Yeh, 2014). The biomass retention MPBR can be further classified into submerged biomass retention MPBR and external biomass retention MPBR, depending on the position of the membrane module in the PBR. In the carbonation MPBR system, the membrane plays a role as a contactor or sparger to improve the carbon dioxide (CO_2) delivery in the cultivation medium. In the biomass retention MPBR, the membrane exerts a barrier to separate solids from the liquid, which can reduce the footprint of the reactor (due to the decoupled SRT and HRT) and enhance the microalgae concentration (due to the reduced washout of biomass) in PBRs (Bilad et al., 2014; Marbelia et al., 2014).

2.3.2 Application of MPBRs in wastewater treatment

Although MPBR can be separated into two types of carbonation MPBR and biomass retention MPBR, current studies associated with wastewater treatment are mainly conducted in biomass retention MPBR. Therefore, MPBR is used to signify biomass retention MPBR in the subsequent sections.

2.3.2.1 Wastewater types

In addition to microalgal biomass production, in recent studies, the MPBR has been extensively used for nutrients recovery in wastewater (Luo et al., 2017b). The integration of microalgae cultivation and wastewater treatment can produce microalgal biomass for biofuel production, and it is cost-effective (Marbelia et al., 2014). As shown in Table 2-2, recent studies regarding MPBR for wastewater treatment have mainly focused on the optimization of operating conditions, as well as improvement of biomass productivity and nutrients removal rate. As listed in Table 2-2, secondary effluent (either synthetic or real) was mostly used in the MPBR for microalgae cultivation. Compared with primary effluents, secondary effluents generally have a low level of organic carbon substances (Table 2-2), which can effectively inhibit the growth of heterotrophic bacteria and enhance the accumulation of algae biomass (Xu et al., 2015). As a result, the nutrients in the wastewater can be effectively removed. It is worth noting that the MPBR is suitable for the treatment of sewage with low nutrients concentrations (e.g., secondary effluent and recovered cultivation medium) because a high nutrients loading can be achieved by the separation function of the membrane (Luo et al., 2017b).

In comparison with synthetic secondary effluent, real secondary effluent was reported to be rich in trace nutrients and, therefore, led to higher microalgal biomass productivity (Xu et al., 2015). However, the growth of microalgae might be affected by the microorganisms that exist in the real secondary effluent, which would negatively impact the nutrient removal efficiency. Therefore, the selection of sewage as MPBR feed should comprehensively weigh the positive and negative effects.

In addition, many studies have been conducted to examine the feasibility of MPBR for the treatment of raw municipal wastewater and other wastewaters (e.g., landfill leachate wastewater, anaerobically digested wastewater, and human urine) with a high level of organic carbon substances and nutrients (Table 2-2). Unlike secondary effluents, the raw sewage generally contains high concentrations of pollutants, like suspended solids, ammonia nitrogen and heavy colour (Chang et al., 2019; Chang et al., 2017; Chang et al., 2018; Chen et al., 2018; Van Thuan et al., 2018), which can lead to growth inhibition or death of microalgae through photoinhibition and toxicity. Therefore, an appropriate pre-treatment or a specific system design is necessary for the treatment of the above wastewater with microalgae. For instance, an ion-exchange-membrane (IEM), which can retain pollutants but allows nutrients to pass, was adopted in a traditional PBR system to integrate microalgae cultivation into the treatment of un-pretreated municipal wastewater and landfill leachate (Chang et al., 2019; Chang et al., 2017; Chang et al., 2018). The results showed that the microalgae growth and lipid productivity, as well as the nutrients removal, were greatly improved because the membrane has effectively avoided the inhibition effects from un-pretreated sewage (Chang et al., 2019; Chang et al., 2017; Chang et al., 2018). In another study, the ammonium toxicity of anaerobic digestate was alleviated by nitrification-based pre-treatment and eventually achieved a high microalgae biomass accumulation of about 5 g/L and excellent nitrogen and phosphorus recovery from the sewage (Praveen et al., 2018). Moreover, appropriate dilution with low nutrients loading wastewater or permeate is another feasible approach for the treatment of high nutrients loading wastewater with microalgae (Van Thuan et al., 2018).

2.3.2.2 Microalgae species

In conventional microalgae cultivation, the primary target is high biomass productivity. While, for the selection of microalgae species for nutrients recovery from wastewater, its adaptability should also be considered because the composition of wastewater (especially the real raw sewage) is generally very complicated and variable. Among numerous species of microalgae, *Chlorella vulgaris* was the most frequently used microalgae for biomass production and wastewater treatment, because of its high productivity and strong adaptability (Table 2-2). According to Table

2-2, the biomass concentration and productivity of *Chlorella vulgaris* in BR-MPBRs can reach as high as 5000 mg/L and 151.93 mg/L/d) respectively, which are much higher than that in traditional PBRs (Luo et al., 2017b). Apart from *Chlorella vulgaris*, some other species, such as *Chlorella* sp., *Chlorella emersonii*, *Chlorella sorokiniana*, *Scenedesmus obliquus*, *Scenedesmus dimorphus*, and *Scenedesmus quadricauda*, also have been adopted for wastewater treatment due to some outstanding strong points. For example, it was reported that *Chlorella* sp. ADE4 exhibited higher adaptability and viability than *Chlorella vulgaris* when treating secondary sewage effluent with low nutrients concentration (Boonchai & Seo, 2015). Also, *Scenedesmus obliquus* accumulated more lipid than *Chlorella vulgaris* when cultivated with a low-nutrients secondary effluent (Boonchai & Seo, 2015).

2.3.2.3 Membranes in MPBR

As a barrier for solid/liquid separation, the selection of membrane mainly depends on the size of the microalgae cells. Since the cell size of microalgae varies between 3 to 30 μm, a microfiltration (MF) membrane with an average pore size of ≤ 0.45 μm has been selected in almost all BR-MPBR studies (Table 2-2). In general, the membrane pore size has no significant impact on the growth of microalgae and performance of the MPBR when the membrane pore size is smaller than the size of the microalgae cell. However, the pore size becomes significant for the MPBR performance when the membrane is used for nutrients permeation rather than biomass retention. Chen et al. (2018) examined the effect of pore size on the performance of the MPBR with a novel configuration. They found that when the membrane pore size increased from 0.1 μm to 1 μm, the ammonia and phosphate removal efficiencies remarkably dropped from 43.9% to 20.1% and 64.9% to 21%, respectively (Chen et al., 2018). They ascribed the deteriorated performance to the higher light shading caused by the increased suspended solids and microscale competitors (Chen et al., 2018). As summarized in Table 2-2, the hollow fiber (HF) membrane was mostly used in BR-MPBR for wastewater treatment although it is more prone to fouling (Liao et al., 2018), which might be due to the higher packing densities of this kind of module. Many membrane materials, including polyvinylidene fluoride (PVDF), cellulose triacetate, polyethylene (PE),

polyacrylonitrile (PAN), and polyethersulfone (PES), have been examined in MPBR systems (Liao et al., 2018), while the application of PVDF membrane in BR-MPBR is predominant (Table 2-2). In addition to the commonly used membranes, membranes with specific functions, like IEM, have been applied in wastewater microalgae cultivation systems to isolate the suspended solids and toxic compounds and enhance the biomass accumulation and lipid productivity (Chang et al., 2019; Chang et al., 2017; Chang et al., 2018).

Table 2-2 Summary of the wastewater types, microalgae species, and membranes in the MPBRs for wastewater treatment in recent studies (modified from Zhang et al. (2019)).

Research purpose	Wastewater types [1]	Microalgae species	Membrane [2]	Cell concentration (g/L)	Ref.
Role of SRT and HRT for secondary effluent polishing	SSE	*Chlorella vulgaris*	HF PVDF MF 0.1 μm	0.69-1.473 g COD/L	(Xu et al., 2015)
Optimization of HRT and biomass concentration for improvement of microalgae production	SSE	*Chlorella vulgaris*	HF PVDF MF 0.1 μm	~ 0.9	(Honda et al., 2017)
Effect of HRT on MPBR	SSE	*Chlorella vulgaris*	HF PVDF MF 0.1 μm	~ 1.2	(Gao et al., 2018)
Long-term operation of MPBR	SSE	*Chlorella vulgaris*	HF PVDF MF 0.1 μm	1.035-1.524	(Gao et al., 2018)
Assessment of MPBR performance and operation	SSE	*Chlorella vulgaris*	HF PVDF MF 0.04 μm	0.47-1.22	(Luo et al., 2018)

Biodegradation of atrazine and nutrients by MPBR	SSE	Algae-bacteria	HF PVDF MF 0.1 µm	~ 6	(Derakhshan et al., 2018)
Comparison of hybrid MPBR and MPBR system	SSE	Microalgae-bacteria	HF PVDF MF 0.1 µm	~ 4	(Derakhshan et al., 2019)
Effects of water composition on nutrients removal	SSE	*Graesiella emersonii*	FS Cellulose triacetate FO	0.017-0.382	(Praveen & Loh, 2019)
Effects of light/dark cycle on nutrients removal	SSE	*Graesiella emersonii*	FS Cellulose triacetate FO	0.018-0.143	(Praveen & Loh, 2019)
Impact of SRT	SSE	Mixed algae (dominated by *Chaetophora sp.* and *Navicula sp.*)	HF PVDF MF 0.45 µm	0.354-1.025	(Solmaz & Işik, 2019)
Phosphorus removal	SSE	Chlorella emersonii	HF PVDF MF 0.1 µm	0.385-4.84	(Xu et al., 2014)
Microalgae cultivation in batch flow mode	RSE	*Chlorella vulgaris*	HF PVDF MF 0.1 µm	0.1-0.659	(Gao et al., 2014)
MPBR for real secondary effluent polishing	RSE	*Chlorella vulgaris*	HF PVDF MF 0.1 µm	1.289 g COD/L	(Xu et al., 2015)
Nutrients removal in secondary sewage effluent with MPBR	RSE	*Chlorella sp.*	HF PE MF 0.4 µm	0.3-1.22	(Boonchai & Seo, 2015)

Removal of nutrients, organic matter, and metal by MPBR	RSE	*Chlorella vulgaris*	HF PVDF MF 0.1 μm	0.03-1.724	(Gao et al., 2016b)
Biomass production assessment with SB-MPBR for real wastewater polishing	RSE	Native microalgae (pre-dominated by *Euglena sp*.)	FS PVDF 0.16 ± 0.01 μm	0.58-1 (Max)	(Sheng et al., 2017)
Biodegradation of atrazine and nutrients by MPBR	RSE	Algae-bacteria	HF PVDF MF 0.1 μm	N/A	(Derakhshan et al., 2018)
Lipid accumulation in MPBR	RSE	*Chlorella vulgaris*	HF PVDF MF 0.1 μm	0.3-1.84	(Gao et al., 2019)
Lipid accumulation in MPBR	RSE	*Scenedesmus obliquus*	HF PVDF MF 0.1 μm	0.3-1.72	(Gao et al., 2019)
Continues cultivation in aquaculture wastewater	AW	*Chlorella vulgaris*	HF PVDF MF 0.1 μm	0.44-1.1	(Gao et al., 2016a)
Improvement of microalgae lipid productivity	UMW	*Chlorella vulgaris*	IEM	~ 1.71	(Chang et al., 2017)
Improvement of microalgae lipid productivity	UMW	*Scenedesmus obliquus*	IEM	~ 2.19	(Chang et al., 2017)
Nutrients reclamation	LLW	*Chlorella vulgaris*	IEM	0.1-0.95	(Chang et al., 2018)

Microalgal lipids production and nutrients recovery from landfill leachate	LLW	*Chlorella vulgaris*	IEM	0.1-2.13	(Chang et al., 2019)
Nutrients removal from anaerobically digested wastewater with different microalgae	ADW	-*Scenedesmus dimorphus* -*Scenedesmus quadricauda* -*Chlorella sorokiniana* -*Chlorella vulgaris*	HF PVDF MF 0.1 μm	0.1-0.54	(Chen et al., 2018)
Nutrients removal from anaerobically digested wastewater with different ammonia concentration	ADW	*Chlorella sorokiniana*	HF PVDF MF 0.1 μm	0.1-1.15	(Chen et al., 2018)
Enhancing microalgae cultivation in anaerobic digestate through nitrification	ADW	*Chlorella vulgaris*	FS PVDF MF 0.1 μm	0.11-5	(Praveen et al., 2018)
Impact of SRT on biomass production	HU	*Chlorella vulgaris*	HF PVDF MF 0.4 μm	0.08-0.86	(Van Thuan et al., 2018)

[1] SSE: synthetic secondary treated effluent; RES: real secondary treated wastewater; AW: aquaculture wastewater; UMW: untreated municipal wastewater; LLW: landfill leachate wastewater; ADW: anaerobically digested wastewater; HU: human urine

[2] HF: hollow fiber; PVDF: polyvinylidene fluoride; MF: micro-filtration; FS: flat sheet; FO: forward osmosis; PE: polyethylene; IEM: ion exchange membrane

2.3.3 Factors affecting MPBR performance

The microalgae growth and nutrients removal rates in MPBRs are highly dependent on various operating conditions, including lighting, CO_2, nutrients concentrations, HRT, and SRT. All these factors interact and have a far-reaching impact on the photosynthesis, cellular metabolism, and cell composition of microalgae, exhibiting as differences in microalgal productivity and nutrients removal. Due to the utilization of a membrane, the effects of the above factors on microalgae growth and nutrients reduction in MPBRs might be of some unique characteristics, which will affect the biological and membrane performance of MPBRs. Table 2-3 summarizes the studies regarding MPBR in microalgae cultivation with wastewater in recent years. A detailed analysis of the impact of different factors on microalgae growth and nutrients removal in MPBRs is provided as follows.

2.3.3.1 Lighting

Light is the energy source for microalgal photosynthesis and, therefore, plays a vital role in wastewater treatment with microalgae. Generally, the optimized light intensity can improve the uptake efficiency of nutrients and CO_2 (Sforza et al., 2012; Simionato et al., 2013). The source of light can be classified into the natural source (sunlight) and artificial sources (e.g., LED and fluorescence). The natural source is free but unstable. Therefore, artificial lighting has been extensively used to keep a stable operation, especially for indoor and lab-scale cultivation systems. For MPBR systems, LED and fluorescent lamps are both artificial sources that have been mostly used (Table 2-3). Light intensity and wavelength, as well as the light/dark cycle, affect the growth of microalgae. Light intensity and the light/dark cycle are two factors that are affected by the presence of a membrane in MPBR systems.

Light intensity is a critical factor impacting carbon dioxide fixation, biomass productivity and nutrients removal in microalgae cultivation systems. The growth of microalgae can be inhibited by both photo-inhibition (for the top layers with too much light) and photo limitation (for the bottom shaded parts with too little light) (Kesaano & Sims, 2014). Microalgae have the capacity to change their synthetic pathway to adapt to the light intensity, to enhance the efficiency of

photosynthesis, and prevent photodamage (Chang et al., 2019; Chang et al., 2018; Gao et al., 2016b; Sheng et al., 2017; Xu et al., 2014). However, it has been extensively reported that light penetration is decreased and becomes a limiting factor for microalgae growth, due to the gradual increase in biomass concentration. Due to utilization of a membrane in the MPBR, for complete retention of biomass and decoupling of SRT from HRT, a higher cell density can be achieved in comparison to conventional PBR systems. Therefore, photoinhibition would more easily take place in MPBRs. From Table 2-3, it is clear that the light intensity used in MPBRs differs between studies, which might be dependent on the microalgae species and biomass concentrations (Luo et al., 2017b). Generally, increasing the light intensity can improve carbon dioxide fixation, while nutrients removal and biomass productivity can be improved (Dechatiwongse et al., 2014; Judd et al., 2015). For MPBRs, an optimized design for the illumination is desired in order to reduce the negative impacts of photoinhibition caused by self-shading by the high cell density. It is worth noting that, except for the self-shading from the microalgae, the turbidity and color of the wastewater can also limit the light availability (Chang et al., 2019; Chang et al., 2017; Chang et al., 2018; Chen et al., 2018). Therefore, an appropriate pre-treatment or optimized design of the reactor is necessary when using MPBR systems for simultaneous wastewater treatment and microalgae cultivation.

The light/dark cycle is another factor affecting biomass production and energy savings. Continuous lighting and 12 h dark/12 h light cycle are two lighting modes that have been extensively applied in MPBRs for wastewater treatment and microalgae cultivation (Table 2-3). In MPBR systems, the application of a membrane enables a continuous and stable supply of nutrients into the bioreactor, and continuous illumination is preferred for continuous microalgae growth and nutrients removal. Praveen and Loh (2019) investigated the effects of the light/dark cycle on wastewater treatment by operating an MPBR under continuous lighting versus light/dark cycle of 12/12 h and found that both the biomass accumulation and nutrients removal were substantially decreased under light/dark cycle conditions. Nevertheless, for some species, like *Nannochloropsis salina,* that need a dark period for re-oxidation of the electron transporters of the photosynthetic apparatus, a light/dark cycle rather than continuous lighting, is reported as an excellent choice (Luo

et al., 2017b).

2.3.3.2 CO_2

For photoautotrophic cultivation, CO_2 is the main source of carbon for microalgae growth. Generally, an increase in the CO_2 carbonation rate can effectively improve the biomass productivity and nutrients assimilation (Abdulhameed et al., 2017; Mortezaeikia et al., 2016a; Mortezaeikia et al., 2016b; Yoshihiko et al., 2016). In MPBR systems, CO_2 is generally provided through aeration, and the concentration can be controlled by either the aeration rate or the CO_2 concentration in the supplied gas (Table 2-3). From Table 2-3, the aeration rate has been varied over a wide range (0.15-8.0 L/min) for MPBR systems. It is worth noting that, in MPBR systems, the aeration rate not only affects the CO_2 supply but also impacts membrane fouling control. Therefore, a higher aeration rate can increase CO_2 supply and generally reduce membrane fouling, while too high aeration rate is not preferred because the intensive shear force may cause cell lysis and severe membrane fouling by microalgal floc-deflocculation. Consequently, a moderate aeration rate is an optimized option, and insufficient CO_2 can be supplemented by high CO_2 concentration additives, such as pure CO_2 or flue gases (Derakhshan et al., 2019; Gao et al., 2019; Gao et al., 2016a; Gao et al., 2018; Luo et al., 2017b; Van Thuan et al., 2018). Some early studies have demonstrated that concentrated CO_2 led to higher biomass productivity and nutrients assimilation, as compared with atmospheric air, because of the higher CO_2 concentration in conventional microalgae cultivation systems (Posadas et al., 2015; Razzak et al., 2015). However, no related studies have been conducted for MPBR systems in the past several years (Table 2-3). Therefore, more investigations are required for the optimization of CO_2 supply in MPBR systems for microalgae cultivation and nutrients removal.

2.3.3.3 Nutrients

Total nitrogen (TN) and total phosphorus (TP) are two vital nutrients for microalgal biomass production. As summarized in Table 1, both TN and TP concentrations of MPBR feeds varied over a wide range, from 4 mg/L to more than 2360 mg/L (2106.5 ± 114.7 mg/L NO_3^- plus 253.6 ± 25.3

mg/L NH_4^+) for TN, and from 0.3 mg/L to 18.6 mg/L for TP, depending on the type of wastewater treated. As compared with common cultivation media, such as BG11, the TN concentration in the secondary effluent is much lower (varying from 4 mg/L to 24.7 mg/L) (Table 2-3). Like the TN, the secondary effluents also possess lower TP concentrations, ranging from 0.3 mg/L to 12.75 mg/L (Table 2-3). It is universally accepted that the biomass productivity of microalgae can be limited by low concentrations of TN or TP (Boonchai & Seo, 2015; Chang et al., 2019; Chen et al., 2018; Honda et al., 2017). However, in MPBR systems, the use of a membrane enables a high supply flow rate of secondary effluent to maintain high nutrients loading for microalgae production, due to the complete decoupling of the HRT from the SRT. Therefore, secondary treated sewage is still an appropriate nutrients alternative for microalgal production in MPBRs and to decrease nutrient cost.

On the other hand, a high concentration of TN and TP can also inhibit the growth of microalgae. Many early articles have demonstrated that excessive ammonia-nitrogen (NH_3-N) concentration reduced the growth rate and productivity of microalgae (Luo et al., 2017b). In a recent study, Chen et al. (2018) applied anaerobically digested wastewater, containing different initial NH_3-N concentration, for *Chlorella sorokiniana* cultivation in an MPBR. They found that the highest biomass concentration of 1.15 g/L was obtained at an NH_3-N concentration of 128.5 mg/L, and a further increase in NH_3-N concentration led to a dramatic drop in biomass concentration (dropped to 0.16 g/L with 514.0 mg/L NH_3-N) (Chen et al., 2018). Similarly, Chang et al. (2019) reported that after the TP concentration exceeds the inhibition saturation, a further increase in TP concentration will not promote higher yield and concentration of microalgae biomass. The results above indicate that raw wastewater with high nutrients concentration would not be appropriate and should be diluted for microalgae cultivation. For the conventional PBR and common MPBR systems, a proper pretreatment (e.g., dilution, nitrification, and pH adjustment) was required for the high nutrients loading wastewaters before being pumped into the bioreactor, in order to avoid the inhibitory impact from the high levels of nutrients (Boonchai & Seo, 2015; Chang et al., 2019; Chang et al., 2017; Chang et al., 2018; Chen et al., 2018; Praveen et al., 2018;

Van Thuan et al., 2018).

In contrast to conventional microalgae cultivation systems, the MPBR has been reported to treat raw wastewater with high nutrients concentration and achieve high biomass productivity, using a specially designed membrane and bioreactor design (Chang et al., 2019; Chang et al., 2017; Chang et al., 2018). For instance, the productivity and quality of microalgae were significantly improved in an ion-exchange-membrane photobioreactor (IEM-PBR) when using municipal wastewater as the source of the nutrients. It is because the harmful effects of pollutants, like inhibitors, were eliminated by the IEM (Chang et al., 2017). In another study, it was reported that microalgae biomass concentration was improved from 0.66 g/L in a traditional photobioreactor to 0.95 g/L in IEM-PBR when treating landfill leachate (Chang et al., 2018). In other words, the utilization of membrane allows the MPBR to be adaptable for the treatment of wider types of sewage.

2.3.3.4 HRT

A suitable HRT is essential to the microalgal cultivation system because too long or too short HRT worsens the performance of MPBR. Generally, a longer HRT can improve the nutrients removal efficiency but slows down the growth rate of microalgae due to the limitation of nutrients. Conversely, a shorter HRT can increase the microalgae growth rate but reduces the nutrients removal rate because of the shortage of reaction time (Luo et al., 2017b). In comparison to conventional PBRs (HRT of 2-5 d), the HRT in MPBR varied over a broader range of 6 h to 8 d (Table 2-3) due to the utilization of a membrane for effective decoupling of HRT from SRT. It is apparent that the selection of HRT in an MPBR should carefully consider various factors, including feed characteristics, cultivation targets, and environmental conditions.

To date, many studies have investigated the effect of HRT on biomass production in MPBRs. Gao et al. (2018) operated four MPBRs with HRTs of 1, 2, 4 and 6 d, respectively, and they found that the highest biomass concentration (0.878 ± 0.007 g/L) and productivity (48.78 ± 0.39 mg/L/d) were obtained at an HRT of 2 d. Similarly, Luo et al. (2018) observed that the cell counts significantly decreased when the HRT was extended from 1 d to 4 d. Another study reported that

the biomass concentration and algal productivity increased from 690 ± 19 mg COD/L to 1023 ± 15 mg COD/L and 92.3 ± 5.2 mg/L/d to 131.7 ± 6.9 mg/L/d, respectively with the HRT decreased from 12 h to 6 h (Xu et al., 2015). However, Honda et al. (2017) claimed that the microalgae biomass concentration was almost comparable regardless of HRT conditions. The inconsistent results suggest that the impact of HRT on biomass production may be controlled by other conditions such as SRT, nutrients concentration, and light.

In addition to biomass productivity, HRT also plays a crucial role in nutrients removal. Honda et al. (2017) reported that the ratio of consumed nitrogen and phosphorus increased from 67.5% to 70.0% and 82.5% to 96.7%, respectively when the HRT increased from 8 h to 24 h. Derakhshan et al. (2019) have reported similar results that the maximal removal efficiency of TN (98%) and TP (98%) was observed at an HRT of 12 h, as compared to the HRTs of 4 h and 8 h. Also, Gao et al. (2018) found that the removal rate of inorganic nitrogen and phosphorus at an HRT of 6 d (92.1% and 94.0%, respectively) was higher than those at an HRT of 1 d (35.9% and 76.9%, respectively). Luo et al. (2018) also presented that the removal rate of both nitrogen and phosphorus at an HRT of 4 d was much higher than that at HRT of 1 d. All the above results indicate that a higher nutrients removal rate can be achieved under a longer HRT as a longer HRT provides a longer reaction time. However, some other studies reported inconsistent results. For instance, Xu et al. (2015) reported that the removal rate of nitrogen and phosphorus at an HRT of 12 h (54.0 ± 4.7% and 84.4 ± 3.9%, respectively) was lower than that at an HRT of 6 h (66.1 ± 2.4% and 87.9 ± 3.1%, respectively). In another study, the highest nitrogen removal (95.95%), phosphorus removal (70.00%), and lipid content (10.79%) was achieved at an HRT of 4 d rather than an HRTs of 2 d and 8 d. The poor performance at an HRT of 8 d was caused by the light limitation (Sheng et al., 2017). All in all, similar to biomass production, the effect of HRT on nutrients removal also depends on other conditions, although longer HRT generally leads to higher nutrients removal.

2.3.3.5 SRT

The SRT, which is related to the microalgal concentration, algae species, and growth rate, is also crucial for microalgal cultivation. In the MPBR system, due to the decoupling of HRT from

SRT, a shorter HRT combined with a longer SRT can be applied to achieve a higher microalgae concentration (Table 2-3). This is desired for downstream microalgal harvesting and dewatering, to reduce cost. The variation of SRT can directly impact the biomass concentration of microalgae, and then indirectly influence the microalgal productivity and nutrients removal. It was reported that the MPBR with a longer SRT of 10 d reached higher biomass productivity (105.2 ± 6.7 mg/L/d) than that with a shorter SRT of 5 days (92.3 ± 5.2 mg/L/d), under the same HRT of 12 hours (Xu et al., 2015). In another study, Van Thuan et al. (2018) pointed out that the biomass concentration dramatically decreased from 0.759 g/L to 0.082 g/L when the SRT decreased from 5 d to 1.5 d at an HRT of 2 d. Consequently, the biomass productivity also significantly reduced due to the low microalgal concentration retained in the MPBR (Van Thuan et al., 2018). Similarly, Solmaz and Işik (2019) found that the microalgae concentration increased from 0.354 g/L to 1.025 g/L when the SRT increased from 3 d to 24 d, even though the biomass productivity decreased from 118 mg/L/d to 43 mg/L/d. Besides, Luo et al. (2018) reported that the microalgae concentration and biomass productivity would increase and decrease, respectively, with an increase in SRT.

In comparison with the biomass concentration, the effect of SRT on nutrients removal can be more complicated. Xu et al. (2015) reported that the TN and TP removal at an SRT of 10 d were 58.3 ± 3.4% and 90.1 ± 0.1%, respectively, which were higher than that at SRT of 5 d (i. e., 54.0 ± 4.7%, and 84.4 ± 3.9%, respectively). However, another study found that the removal of TN and TP was 31%, 36%, 32% and 30%, 31%, 25%, respectively, for SRTs of 9 d, 18 d, and 30 d (Luo et al., 2018). Similar results also were observed by Solmaz and Işik (2019). In summary, too long and too short SRTs are not appropriate for microalgae cultivation in MPBR systems, and a moderate range of SRT from 15 to 25 d is recommended to avoid self-shading and obtain high nutrients removal (Luo et al., 2017b).

Table 2-3 Effectiveness of membrane photobioreactors for wastewater treatment (modified from Zhang et al. (2019)).

Components concentrations in the wastewater (mg/L)			MPBR operation conditions				Results			Ref.
C [1]	N	P	Light intensity ($\mu mol/m^2/s$) Lamp type Photoperiod [2]	Aeration (air type, aeration rate)	HRT (d)	SRT (d)	Productivity (mg/L/d)	N removal (%)	P removal (%)	
0	12.2	6.1	150 Fluorescence 12 h dark/12 h light	Air	0.25-1	5-10	72.4-131.7	54.0-73.4	84.4-91.3	(Xu et al., 2015)
5 (TOC) 30 (IC)	15	0.3	92 LED Continuous lighting *	1% CO_2 200 mL/min	0.33-1	12	26.2-39.0 (Average) 65.5-72.7 (Max)	65.9-70	82.5-96.8	(Honda et al., 2017)
40 (COD)	15	0.8	101.5-112.3 LED Continuous lighting *	Air, 500 mL/min Pure CO_2 (99.9%)	1-6	∞	26.69-48.78	35.9-92.1	76.9-94.0	(Gao et al., 2018)
40 (COD)	15	0.8	101.5-112.3 LED Continuous lighting *	Air, 500 mL/min Pure CO_2 (99.9%)	2	21.1	49.12-72.39	81.4	90.8	(Gao et al., 2018)
9.0 ± 0.7 (TOC)	14.1 ± 0.5	2.5 ± 0.2	85 Fluorescence Continuous lighting *	Air, 2000 mL/min	1-4	9-30	28-52	31-84	25-80	(Luo et al., 2018)

48 (COD)	8	12	143.9 ± 0.2 LED 12h dark/12h light	Air	0.25-1	N/A	N/A	~ 93.7	~ 94.4	(Derakhshan et al., 2018)
30-90	5	1	152.9 ± 0.2 LED 12h dark/12h light	Air, 67-83 mL/min 5% CO_2, 4 vvm	0.17-0.5	N/A	N/A	54.9-83.7	61.3-89.0	(Derakhshan et al., 2019)
0	4-16	2.4	125.9-143.9 Fluorescence Continuous lighting	3% CO_2, 0.4 vvm	1.5	∞	26.5-30.4	~ 99.8	~ 100	(Praveen & Loh, 2019)
0	16	2.4	125.9-143.9 Fluorescence 12h dark/12h light	3% CO_2, 0.4 vvm	1.5	∞	10.4	81	N/A	(Praveen & Loh, 2019)
32.89 ± 2.3 (COD)	18.35 ± 0.30	8.81 ± 0.17	107.9 Fluorescence 12h dark/12h light	Air	1	2-24	43-118	4.02-5.55 mg/L/d (Removal rate)	0.29-1.61 mg/L/d (Removal rate)	(Solmaz & Işik, 2019)
0	12.04	5.0 ± 0.1	80 ± 5 Fluorescence 12h dark/12h light	Air, 8000 mL/min	1	180	12.5-39.5	N/A	52-83	(Xu et al., 2014)
55.6 ± 10.9 (COD)	19.12 ± 0.52	1.24 ± 0.12	143.9 LED Continuous lighting *	Air, 1500 mL/min	2.5	N/A	39.93±0.73	50.1-62.3	72.6-91.9	(Gao et al., 2014)
28 ± 3 (COD)	9.51 ± 0.82	1.81 ± 0.47	150 Fluorescence 12h dark/12h light	Air	1	10	98.2 ± 4.5	95.3 ± 0.9	94.9 ± 3.6	(Xu et al., 2015)

10.5 (COD)	18.8	1.01	50 Fluorescence 10h dark/14h light	Air, 4000 mL/min	2	N/A	55	66.5	94.5	(Booncha i & Seo, 2015)
39.91 ± 5.41 (COD)	14.12 ± 0.95	0.78 ± 0.11	< 120.8 LED Continuous lighting *	4% CO_2 mixed air, 500 mL/min	2	∞	50.72	87.7	76.7	(Gao et al., 2016b)
N/A	24.7 ± 0.5	3.5 ± 0.5	179.9 Fluorescence	Air, 1800 mL/min	2-8	60	10.5-16.7	~ 95.95	~ 70	(Sheng et al., 2017)
48.0 ± 0.5 (COD)	9.85 ± 0.6	7.4 ± 0.7	143.9 ± 0.2 LED 12h dark/12h light	Air	1	N/A	N/A	94.8 ± 0.1	95.1 ± 0.2	(Derakhs han et al., 2018)
25.62 ± 3.92 (COD)	12.75 ± 0.88	0.62 ± 0.13	101.5-112.3 LED Continuous lighting	Air, 500 mL/min Pure CO_2 (99.9%)	2	∞	88.8-96.3	N/A	N/A	(Gao et al., 2019)
8.5 ± 1.9 (BOD_5)	6.81 ± 0.68	0.42 ± 0.05	< 161.9 LED Continuous lighting *	Air, 500 mL/min Pure CO_2 (99.9%)	1	∞	42.6	86.1	82.7	(Gao et al., 2016a)
310 ± 11 (COD)	40.5 ± 1.1	9.3 ± 0.6	90 Continuous lighting	5% CO_2, 0.3 vvm	N/A	N/A	244.3-312.9	85.7-89.9 (NH_4^+-N)	100	(Chang et al., 2017)
341.5 ± 7.6 (COD)	632.4 ± 10.8 (NO_3^-) 135.9 ± 4.3 (NH_4^+)	15.3 ± 0.8	161.9 Continuous lighting	5% CO_2, 0.3 vvm	N/A	N/A	106.25	99.1	100	(Chang et al., 2018)

1446.5 ± 73.4 (COD)	2106.5 ± 114.7 (NO_3^-) 253.6 ± 25.3 (NH_4^+)	18.6 ± 1.4	170.9 µmol Continuous lighting	3% CO_2, 150 mL/min	N/A	N/A	169.17	57.5 (NO_3^-) 83.0 (NH_4^+)	100	(Chang et al., 2019)
N/A	64.3 (NH_4^+)	13.1	110 12h dark/12h light	5% CO_2, 0.3 vvm	N/A	N/A	48.9	> 75 (NH_4^+-N)	~ 99.2	(Chen et al., 2018)
N/A	64.3-514.0 (NH_4^+)	13.1	110 12h dark/12h light	5% CO_2, 0.3 vvm	N/A	N/A	6.67-116.7	N/A	~ 66.2	(Chen et al., 2018)
190 ± 50 (COD)	25-70 (NH_4^+) 25-51 (NO_3^-)	6-17	143.9-287.8 Fluorescence Continuous lighting *	3% CO_2, 1000 mL/min	3	> 200	49.6-167.0	< 75	< 99	(Praveen et al., 2018)
N/A	180-350	8-15	79.1 Fluorescence Continuous lighting	Air, 4000 mL/min Pure CO_2 (99.9%), 100 mL/min	2	1.5-5	146.4-151.9	N/A	N/A	(Van Thuan et al., 2018)

[1] TOC: total organic carbon; IC: inorganic carbon; COD: chemical oxygen demand; BOD: biochemical oxygen demand

[2] The photoperiod labelled with "*" indicates the author didn't provide a direct description of the illumination time in the original article, while all these MPBRs were operated under continuous mode.

2.4 Membrane fouling

2.4.1 Mechanisms of membrane fouling

Membrane fouling is defined as the unwanted deposition and accumulation of various pollutants, including biological cells, colloids, solutes, and debris, within/on the membrane. Although the foulants composition and content in different types of MBR are different, the mechanisms of membrane fouling are similar. The basic mechanisms associated with membrane fouling generally consist of pore blocking, gel layer formation, and cake layer formation (Figure 2-2) (Lin et al., 2020). The cooperative effect of these mechanisms leads to a three-stage membrane fouling. Under the constant-flux operation mode, the profile of transmembrane pressure (TMP) can be illustrated as an initial short-term rapid rise (stage 1) followed by a long-term slow rise (stage 2) and a sharp TMP jump (stage 3) in sequence (Wang et al., 2008; Zhang et al., 2006).

The TMP increase at the first stage is usually attributed to pore blocking. As shown in Figure 2-2(a), pore-blocking depends on the matching of membrane pore size and foulant size. In general, pollutants with size larger than the membrane pore size will be rejected. Therefore, the subvisible particles colloids in the supernatant, which have a comparable or smaller size than membrane pore size, are considered as the main contributor to pore blocking (Lin et al., 2020). It worth noting that, in some cases, gel layer will form in the start-up period due to the unstable conditions at that time.

The slow rise of TMP at the second stage results from cake layer formation. In an MBR system operated under sub-critical flux, cake layer formation requires a long time because of the restrictive interactions between dynamics and thermodynamics (Hong et al., 2013). Thermodynamic forces drive the biological flocs to adhere onto the membrane surface, while a partial of biomass will be stripped by the shear force over the membrane surface. Such a dynamic process eventually leads to the long and slow transition process of TMP.

The TMP jump at the third stage is the consequence of constant flux operation and may be caused by several mechanisms (Le-Clech et al., 2006). After long-term operation, a significant reduction of local flux in some specific area on the membrane surface will result in a redistribution

of the overall permeability productivity, which will increase the local flux of the low fouled area, and thus accelerating the formation of membrane fouling (Le-Clech et al., 2006). Besides, cake layer formation is accompanied by compression due to the continuous filtration and material deposition within the cake layer. The loss of connectively and resistance results in the rapid increase in TMP.

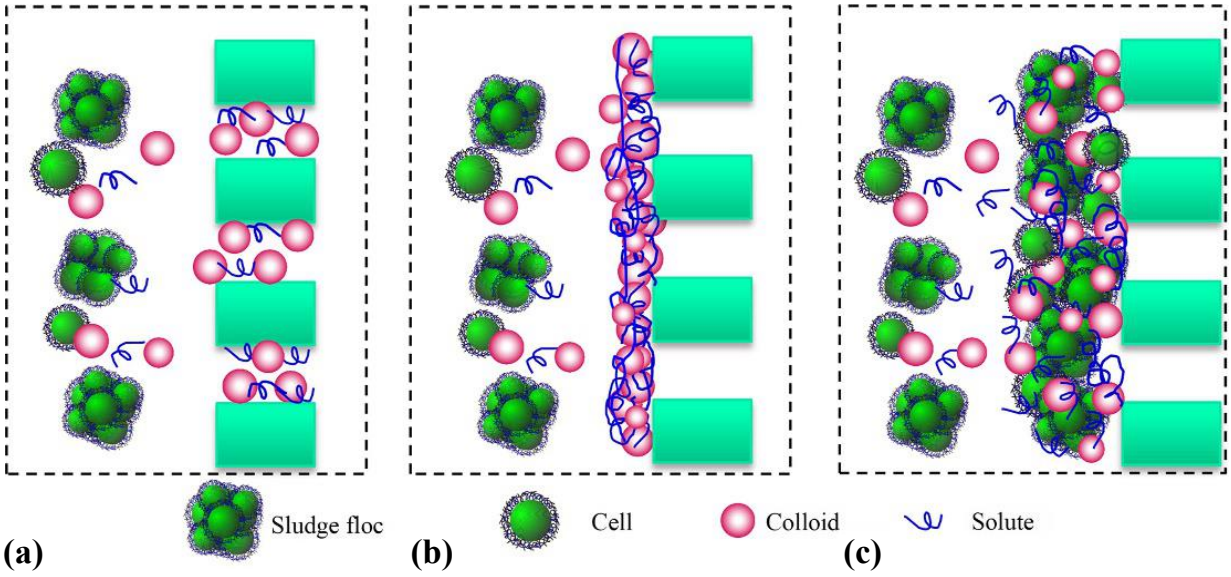

Figure 2-2 Schematic of basic membrane fouling mechanisms: (a) pore-clogging, (b) gel layer formation, and (c) cake layer formation (Lin et al., 2020).

2.4.2 Factors affecting membrane fouling

Membrane fouling is strongly affected by four categories of factors, including feedwater characteristics, operating conditions, membrane properties, and biomass characteristics. For a given membrane, membrane fouling is directly controlled by biomass characteristics and hydrodynamic conditions, while other conditions have indirect impacts on membrane fouling by modifying biomass characteristics. In this Section, the effects of feedwater characteristics, operating conditions, membrane properties, and biologic characteristics are briefly reviewed. Detailed relationships between these factors and membrane fouling in MBRs and MPBRs can refer to the previous publications (Hamedi et al., 2019; Iorhemen et al., 2016; Meng et al., 2009).

2.4.2.1 Feedwater characteristics

Feedwater characteristics including organic loading rate (OLR), food-microorganisms (F/M) ratio, chemical oxygen demand/nitrogen (COD/N) ratio, and salinity have significant impacts on membrane fouling by affecting the physicochemical characters of biological characteristics. According to previous studies, membrane fouling rate increases with the increase in OLR, F/M ratio, and salinity (Dvorák et al., 2011; Hamedi et al., 2019; Iorhemen et al., 2016; Jang et al., 2013; Johir et al., 2012). However, the investigation results about influences of the COD/N ratio on membrane fouling are inconsistent (Han et al., 2015; Hao et al., 2016). It is reasonable since all these factors indirectly influence membrane fouling by changing the sludge suspension. Their effect may also depend on other variables such as wastewater type. Besides, the feedwater with extreme pH and temperature, or containing heavy metals may also accelerate the membrane fouling rate (Hu et al., 2015; Sanguanpak et al., 2015). Overall, all the above parameters exert their influences by altering metabolic activity and microbial growth, which will promote or prevent the release of fouling substances like EPS and SMP.

2.4.2.2 Operating conditions

The operating conditions affecting membrane fouling consists of aeration, SRT, HRT, and temperature. To date, numerous studies have been conducted to investigate their impacts on membrane fouling, which have been summarized in previous publications (Hamedi et al., 2019; Iorhemen et al., 2016). Most of the studies regarding the above parameters suggested that high aeration rate, SRT, HRT, and temperature benefit the reduction of membrane fouling (Hamedi et al., 2019; Iorhemen et al., 2016; Meng et al., 2009). However, the extremely high value of these factors will, in turn, aggravate the formation of membrane fouling with different reasons (Hamedi et al., 2019; Iorhemen et al., 2016). In general, high aeration intensity and temperature will cause the breakage of biological flocs and generation of SMP, which enhances the formation of membrane fouling. The rapid membrane fouling under extremely high SRT and HRT is associated with the variation of biomass viscosity and accumulation of foulants.

2.4.2.3 Membrane properties

A series of membrane properties, including pore size, membrane material, and surface roughness, have significant impacts on membrane fouling. The effect of pore size on membrane fouling is controversial, which mainly depends on the matching of membrane pore size and particle size. Generally, increasing membrane pore size tends to increase the pore blocking due to the easier entrance and trapping of fine particles (Van den Broeck et al., 2012). In addition, the membranes made with different materials possess different filtration properties because of the difference in hydrophobicity, zeta potential and other properties. In comparison, ceramic membranes are hydrophilic and have lower fouling propensity, while polymeric membranes are mostly hydrophobic and thus foul more (Hofs et al., 2011; Jin et al., 2010). Furthermore, the membrane with smooth morphology was reported can slow down fouling development (Hashino et al., 2011; Vrijenhoek et al., 2001).

2.4.2.4 Biologic characteristics

The biological suspension in MBRs and MPBRs is the substance source of membrane fouling and thus plays a vital role in the membrane. The major characteristics include mixed liquor suspended solids (MLSS) concentration, floc size, EPS, and SMP.

MLSS concentration is one of the major factors affecting membrane fouling, but the results regarding the effect of MLSS concentration on membrane fouling is controversial. Many studies have reported that the membrane fouling rate positively correlates with MLSS concentration (Hamedi et al., 2019; Iorhemen et al., 2016; Le-Clech et al., 2006). Domínguez Chabaliná et al. (2012) confirmed the increased membrane fouling under higher MLSS concentration resulted from the reduction in sludge settleability. However, Lee et al. (2001) believed that under high sludge concentration, the filter cake layer on the membrane surface could act as a dynamic membrane, which can effectively adsorb and degrade SMP and colloidal particles on the membrane surface, thereby slowing the formation rate of membrane fouling. Moreover, some other studies reported MLSS concentration has no or little impact on membrane fouling (Domínguez Chabaliná et al.,

2012; Le-Clech et al., 2003).

In MBRs and MPBRs, the size of biological flocs has a great effect on membrane fouling. Shen et al. (2015) investigated the impact of floc size on membrane fouling and found that small flocs exhibited higher fouling propensity due to their stronger adhesion ability to the membrane surface. In addition, the cake layer formed by small flocs generally has a denser and less porous structure as compared to that formed by large flocs, which will lead to a higher filtration resistance and fouling rate (Lin et al., 2011; Meng et al., 2007; Su et al., 2013).

Currently, bound EPSs are considered as the predominant cause of membrane fouling in MBRs and MPBRs. Bound EPSs are different classes of network-like biopolymers that secreted by microorganisms during the metabolic processes and present outside the microbial cells (Lin et al., 2014). Bound EPSs exhibit a three-dimensional, gel-like, highly hydrated matrix and can protect the microorganisms against external stress and toxicity (Lin et al., 2014). The main components of bound EPS include polysaccharides and proteins as well as nucleic acids, lipids, and humic acids. The differences in composition and concentration of bound EPSs have significant influences on the physicochemical properties of microbial aggregates, which will then impact the formation of membrane fouling (Hamedi et al., 2019; Iorhemen et al., 2016; Le-Clech et al., 2006; Meng et al., 2009). It is generally considered that higher bound EPS concentration corresponds to a higher membrane fouling rate. Nevertheless, several studies reported that there has little correlation between bound EPS and membrane fouling (Rosenberger & Kraume, 2003; Yamato et al., 2006). The inconsistent results suggested EPSs are not the sole cause for membrane fouling. Considering EPSs play an essential role in biological properties and membrane fouling, controlling the concentration of bound EPS is still of significant importance for membrane fouling mitigation.

SMPs are identified as soluble EPSs. SMPs are the organic substances generated from substrate metabolism and biomass decay. According to the different production pathway, SMPs can be divided into substrate-utilization-associated products (UAP) from substrate metabolism and biomass-associated products (BAP) from biomass decay (Meng et al., 2009). The predominant

compositions of SMP include proteins, carbohydrates, humic acids, and nucleic acids. In MBRs and MPBRs, the rejection capacity of membrane favors the accumulation of SMP in the bioreactors, which will weaken the filterability of the biological suspension (Le-Clech et al., 2006; Liao et al., 2018). SMPs have complicated relationships with EPS and other membrane foulants and attract widespread attention from researchers (Lin et al., 2014). It is generally believed that a high concentration of SMP will lead to a high membrane fouling due to the enhanced pore blocking, cake layer, or gel layer formation (Hamedi et al., 2019; Iorhemen et al., 2016).

2.4.3 Membrane fouling control

Membrane fouling can be minimized through various control strategies of feedwater pretreatment, operating conditions control, membrane surface modification, biological properties adjustment, and membrane cleaning.

2.4.3.1 Pretreatment of feedwater

The properties of feedwater have profound effects on membrane fouling because they can modify the hydrodynamics conditions or biomass properties in the bioreactors. For example, the unpretreated sewage contained a high amount of trash may deteriorate the diffuser of bubbles (Cote & Thompson, 2000). Some wastewaters especially industrial sewages, which have extreme conditions (e.g., extreme pH, temperature, and ionic strength) or contain toxic substances, would seriously affect the biomass properties, and then influence membrane fouling (Jang et al., 2013; Zhang et al., 2014). Therefore, a careful check of feedwater properties before the system operation is all-important for the selection of an appropriate pretreatment strategy. Current strategies of feedwater pretreatment mainly include screening, pH adjustment, desalination, and settlement (Lin et al., 2020).

2.4.3.2 Control of operating conditions

Aeration is a critical factor for membrane fouling because it controls not only hydrodynamic conditions but also biological properties. The efficiency of aeration is governed by the aeration intensity, aeration mode, and bubble size. In general, high aeration intensity, unsteady aeration

mode, and course bubble size are more conducive to the generation of high scoring force on the membrane surface and thus contribute to membrane fouling mitigation (Lin et al., 2020). However, too high aeration intensity will cause the breakage of biological flocs and production of SMP, which will, in turn, deteriorate the filterability of biomass (Meng et al., 2009). Moreover, an increase in aeration intensity will also increase energy demand. Therefore, the establishment of a favorable hydrodynamic condition should comprehensively consider the three factors and their interactions.

The application of sustainable flux operation is a common strategy for membrane fouling control. The sustainable flux is theoretically defined as the flux below which no fouling occurs. In practice, membrane fouling cannot be avoided. Nevertheless, operating MBRs or MPBRs with sustainable flux can effectively prolong the operation period, slow the fouling formation, and decrease energy consumption (Hamedi et al., 2019).

In addition to aeration and membrane flux, other operating conditions (e.g., HRT, SRT, temperature, etc.) involve in membrane fouling by adjusting the characteristics of biological flocs. The purpose of fouling mitigation can be achieved under optimized operational conditions because of the ameliorated biomass properties.

2.4.3.3 Modification of membrane characteristics

As a media directly contact with biological suspension, the characters of membrane play a vital role in membrane fouling. It was reported the anti-fouling properties of the membrane could be significantly improved with the modification of the membrane surface. As mentioned above (Section 2.4.2.3), hydrophilic membranes possess lower fouling propensity. Therefore, numerous works have been done to improve the hydrophilicity of the hydrophobic membrane by implanting/generating hydrophilic groups onto the membrane surface (Lin et al., 2020). For instance, two types of TiO_2-immobilized membranes showed lower flux decline compared to that of unmodified membranes (Bae et al., 2006; Bae & Tak, 2005). Besides, modification of surface topography by 3D printing or engraving techniques was reported can reduce colloids adhesion.

2.4.3.4 Adjustment of biological properties

As membrane fouling results from the interactions between biomass and membrane, adjustment of biomass properties can directly control the membrane fouling. Addition of flocculants, adsorbents, and granular particles in the biological suspension is effective and the most commonly used technique for membrane fouling mitigation.

Powdered activated carbon (PAC) is a typical adsorbent applied to mitigate membrane fouling in MBRs. The addition of PAC can adsorb SMPs and colloids (Lesage et al., 2008; Li et al., 2005), hence reducing membrane fouling propensity. PAC also acts as a media for biological attachment and growth, which can prevent the accumulation of biomass on membranes (Mutamim et al., 2013; Wang et al., 2008). Moreover, the addition of coagulants, such as aluminum sulfate, ferric chloride, polymeric ferric sulphate (PFS), polymeric aluminum chloride (PACI), and polymeric aluminum ferric chloride (PAFC), can alleviate membrane fouling by enlarging the floc size and restraining the gel layer formation (Iorhemen et al., 2016). It worth noting that, although the use of additives takes distinctive advantages, the dosage is a key factor determining the performance of these additives. High dosage may be counterproductive for membrane fouling control because of the increased viscosity and EPS levels (Hamedi et al., 2019).

Quorum quenching (QQ) is a biological strategy for membrane fouling control. It was developed based on bacterial quorum sensing (QS) system. For biological communities, the production of EPS depended on the transcription of specific genes, which is controlled by intercellular communication (quorum sensing). Accordingly, effective mitigation of membrane fouling with QQ is realized by blocking intercellular communications (Jiang et al., 2013; Lee et al., 2016; Weerasekara et al., 2014). The utilization of enzymes is another biological strategy for fouling control in MBRs. The enzymes in the systems can degrade EPSs and then result in the detachment of the cake layer (te Poele & van der Graaf, 2005). Other biological strategies for MBR membrane fouling control include the application of D-amino acids, protozoan, and metazoan (Bagheri & Mirbagheri, 2018).

2.4.3.5 Membrane cleaning

Although membrane fouling can be effectively minimized with the above strategies, membrane fouling can only be postponed and will eventually happen. At this time, membrane cleaning should be conducted to recover the membrane permeability. Membrane cleaning methods can be categorized into physical, chemical, and biological cleaning. Backwashing and relaxation are the most common physical cleaning approaches for membrane cleaning (Le-Clech et al., 2003). In general, most of the removable fouling can be effectively removed through physical cleaning. Chemical cleaning is conducted to eliminate the biological, organic, and inorganic foulants that cannot be removed by physical cleaning (Meng et al., 2009). The most-commonly used chemical reagents are acids, bases, oxidants, and other in-situ and/or ex-situ chemicals (Wang et al., 2014). It should be noted that some chemicals would damage the membrane surface and shorten the membrane lifespan. Therefore, the selection of cleaning reagents should target predominant foulants and reduce the damage.

2.5 References

Abass, O., Wu, X., Guo, Y., Zhang, K., 2015. Membrane Bioreactor in China: A Critical Review. *International of Membrane Science and Technology*. 2, 29-47.

Abdulhameed, M. A., Othman, M. H. D., Ismail, A. F., Matsuura, T., Harun, Z., Rahman, M. A., Puteh, M. H., Jaafar, J., Rezaei, M., Hubadillah, S. K., 2017. Carbon dioxide capture using a superhydrophobic ceramic hollow fibre membrane for gas-liquid contacting process. *Journal of Cleaner Production*. 140, 1731-1738.

Bae, T.-H., Kim, I.-C., Tak, T.-M., 2006. Preparation and characterization of fouling-resistant TiO2 self-assembled nanocomposite membranes. *Journal of Membrane Science*. 275(1-2), 1-5.

Bae, T.-H., Tak, T.-M., 2005. Effect of TiO2 nanoparticles on fouling mitigation of ultrafiltration membranes for activated sludge filtration. *Journal of Membrane Science*. 249(1-2), 1-8.

Bagheri, M., Mirbagheri, S. A., 2018. Critical review of fouling mitigation strategies in membrane bioreactors treating water and wastewater. *Bioresource Technology*. 258, 318-334.

BCC, Membrane Bioreactors: Global Markets, BCC Report MST047E, BCC Research,

https://www.bccresearch.com/market-research/membrane-and-separation-technology/membrane-bioreactors.html, 2019.

Besha, A. T., Gebreyohannes, A. Y., Tufa, R. A., Bekele, D. N., Curcio, E., Giorno, L., 2017. Removal of emerging micropollutants by activated sludge process and membrane bioreactors and the effects of micropollutants on membrane fouling: A review. *Journal of Environmental Chemical Engineering*. 5(3), 2395-2414.

Bilad, M. R., Arafat, H. A., Vankelecom, I. F. J., 2014. Membrane technology in microalgae cultivation and harvesting: A review. *Biotechnology Advances*. 32(7), 1283-1300.

Boonchai, R., Seo, G., 2015. Microalgae membrane photobioreactor for further removal of nitrogen and phosphorus from secondary sewage effluent. *Korean Journal of Chemical Engineering*. 32(10), 2047-2052.

Brennan, L., Owende, P., 2010. Biofuels from microalgae—A review of technologies for production, processing, and extractions of biofuels and co-products. *Renewable and Sustainable Energy Reviews*. 14(2), 557-577.

Chan, Y. J., Chong, M. F., Law, C. L., Hassell, D. G., 2009. A review on anaerobic-aerobic treatment of industrial and municipal wastewater. *Chemical Engineering Journal*. 155(1-2), 1-18.

Chang, H., Fu, Q., Zhong, N., Yang, X., Quan, X., Li, S., Fu, J., Xiao, C., 2019. Microalgal lipids production and nutrients recovery from landfill leachate using membrane photobioreactor. *Bioresource Technology*. 277, 18-26.

Chang, H., Huang, Y., Xia, A., Liao, Q., Zhu, X., 2017. Improvement of microalgae lipid productivity and quality in an ion-exchange-membrane photobioreactor using real municipal wastewater. *International Journal of Agricultural and Biological Engineering*. 10(1), 97.

Chang, H., Quan, X., Zhong, N., Zhang, Z., Lu, C., Li, G., Cheng, Z., Yang, L., 2018. High-efficiency nutrients reclamation from landfill leachate by microalgae Chlorella vulgaris in membrane photobioreactor for bio-lipid production. *Bioresource Technology*. 266, 374-381.

Chen, G., Zhao, L., Qi, Y., 2015. Enhancing the productivity of microalgae cultivated in

wastewater toward biofuel production: A critical review. *Applied Energy*. 137, 282-291.

Chen, X., Li, Z., He, N., Zheng, Y., Li, H., Wang, H., Wang, Y., Lu, Y., Li, Q., Peng, Y., 2018. Nitrogen and phosphorus removal from anaerobically digested wastewater by microalgae cultured in a novel membrane photobioreactor. *Biotechnology for Biofuels*. 11(1), 190.

Cote, P., Thompson, D., 2000. Wastewater treatment using membranes: the North American experience. *Water Science and Technology*. 41, 209-215.

Dechatiwongse, P., Srisamai, S., Maitland, G., Hellgardt, K., 2014. Effects of light and temperature on the photoautotrophic growth and photoinhibition of nitrogen-fixing cyanobacterium Cyanothece sp. ATCC 51142. *Algal Research*. 5, 103-111.

Deowan, S. A., Bouhadjar.], S. I., Hoinkis, J., 2015. Membrane bioreactors for water treatment. in: *Advances in Membrane Technologies for Water Treatment: Materials, Processes and Applications*, (Eds.) Basile, A., Cassano, A., Rastogi, N.

Derakhshan, Z., Ehrampoush, M. H., Mahvi, A. H., Dehghani, M., Faramarzian, M., Eslami, H., 2019. A comparative study of hybrid membrane photobioreactor and membrane photobioreactor for simultaneous biological removal of atrazine and CNP from wastewater: A performance analysis and modeling. *Chemical Engineering Journal*. 355, 428-438.

Derakhshan, Z., Mahvi, A. H., Ehrampoush, M. H., Mazloomi, S. M., Faramarzian, M., Dehghani, M., Yousefinejad, S., Ghaneian, M. T., Abtahi, S. M., 2018. Studies on influence of process parameters on simultaneous biodegradation of atrazine and nutrients in aquatic environments by a membrane photobioreactor. *Environmental Research*. 161, 599-608.

Do, K.-U., Banu, J. R., Chung, I.-J., Yeom, I.-T., 2009. Effect of thermochemical sludge pretreatment on sludge reduction and on performances of anoxic-aerobic membrane bioreactor treating low strength domestic wastewater. *Journal of Chemical Technology & Biotechnology*. 84(9), 1350-1355.

Domínguez Chabaliná, L., Baeza Ruiz, J., Rodríguez Pastor, M., Prats Rico, D., 2012. Influence of EPS and MLSS concentrations on mixed liquor physical parameters of two membrane bioreactors. *Desalination and Water Treatment*. 46(1-3), 46-59.

Drexler, I. L. C., Yeh, D. H., 2014. Membrane applications for microalgae cultivation and harvesting: a review. *Reviews in Environmental Science and Bio/Technology*. 13(4), 487-504.

Dvorák, L., Gómez, M., Dvoráková, M., Ruzicková, I., Wanner, J., 2011. The impact of different operating conditions on membrane fouling and EPS production. *Bioresource Technology*. 102(13), 6870-6875.

Fane, A. G., Wang, R., Jia, Y., 2011. Membrane Technology: Past, Present and Future. in: *Membrane and Desalination Technologies*, (Eds.) Wang, L. K., Chen, J. P., Hung, Y.-T., Shammas, N. K., Humana Press. Totowa, NJ, pp. 1-45.

Gao, F., Cui, W., Xu, J.-P., Li, C., Jin, W.-H., Yang, H.-L., 2019. Lipid accumulation properties of Chlorella vulgaris and Scenedesmus obliquus in membrane photobioreactor (MPBR) fed with secondary effluent from municipal wastewater treatment plant. *Renewable Energy*. 136, 671-676.

Gao, F., Li, C., Yang, Z.-H., Zeng, G.-M., Feng, L.-J., Liu, J.-z., Liu, M., Cai, H.-w., 2016a. Continuous microalgae cultivation in aquaculture wastewater by a membrane photobioreactor for biomass production and nutrients removal. *Ecological Engineering*. 92, 55-61.

Gao, F., Li, C., Yang, Z.-H., Zeng, G.-M., Mu, J., Liu, M., Cui, W., 2016b. Removal of nutrients, organic matter, and metal from domestic secondary effluent through microalgae cultivation in a membrane photobioreactor. *Chemical Technology and Biotechnology*. 91(10), 2717-2719.

Gao, F., Peng, Y.-Y., Li, C., Cui, W., Yang, Z.-H., Zeng, G.-M., 2018. Coupled nutrient removal from secondary effluent and algal biomass production in membrane photobioreactor (MPBR): Effect of HRT and long-term operation. *Chemical Engineering Journal*. 335, 169-175.

Gao, F., Yang, Z.-H., Li, C., Wang, Y.-j., Jin, W.-h., Deng, Y.-b., 2014. Concentrated microalgae cultivation in treated sewage by membrane photobioreactor operated in batch flow mode. *Bioresource Technology*. 167, 441-446.

Grand View Research, Membrane Bioreactor (MBR) Market Analysis By Product (Hollow Fiber, Flat Sheet, Multi-Tubular), By Configuration (Submerged, Side Stream), By Application, And Segment Forecasts, 2017, pp. 2018–2025. https://www.grandviewresearch.com/

industry-analysis/membrane-bioreactor-mbr-market.

Hamedi, H., Ehteshami, M., Mirbagheri, S. A., Rasouli, S. A., Zendehboudi, S., 2019. Current Status and Future Prospects of Membrane Bioreactors (MBRs) and Fouling Phenomena: A Systematic Review. *The Canadian Journal of Chemical Engineering*. 97(1), 32-58.

Han, X., Wang, Z., Ma, J., Zhu, C., Li, Y., Wu, Z., 2015. Membrane bioreactors fed with different COD/N ratio wastewater: impacts on microbial community, microbial products, and membrane fouling. *Environmental Science and Pollution Research*. 22(15), 11436-11445.

Hao, L., Liss, S. N., Liao, B. Q., 2016. Influence of COD:N ratio on sludge properties and their role in membrane fouling of a submerged membrane bioreactor. *Water Research*. 89, 132-141.

Hashino, M., Katagiri, T., Kubota, N., Ohmukai, Y., Maruyama, T., Matsuyama, H., 2011. Effect of surface roughness of hollow fiber membranes with gear-shaped structure on membrane fouling by sodium alginate. *Journal of Membrane Science*. 366(1-2), 389-397.

Hofs, B., Ogier, J., Vries, D., Beerendonk, E. F., Cornelissen, E. R., 2011. Comparison of ceramic and polymeric membrane permeability and fouling using surface water. *Separation and Purification Technology*. 79(3), 365-374.

Holloway, R. W., Achilli, A., Cath, T. Y., 2015. The osmotic membrane bioreactor: a critical review. *Environmental Science: Water Research & Technology*. 1, 581-605.

Honda, R., Teraoka, Y., Noguchi, M., Yang, S., 2017. Optimization of Hydraulic Retention Time and Biomass Concentration in Microalgae Biomass Production from Treated Sewage with a Membrane Photobioreactor. *Journal of Water and Environment Technology*. 15(1), 1-11.

Hong, H., Peng, W., Zhang, M., Chen, J., He, Y., Wang, F., Weng, X., Yu, H., Lin, H., 2013. Thermodynamic analysis of membrane fouling in a submerged membrane bioreactor and its implications. *Bioresource Technology*. 146(0), 7-14.

Hu, D., Zhou, Z., Shen, X., Wei, H., Jiang, L.-M., Lv, Y., 2015. Effects of alkalinity on membrane bioreactors for reject water treatment: Performance improvement, fouling mitigation and microbial structures. *Bioresource Technology*. 197, 217-226.

Iorhemen, O. T., Hamza, R. A., Tay, J. H., 2016. Membrane Bioreactor (MBR) Technology for

Wastewater Treatment and Reclamation: Membrane Fouling. *Membranes*. 6(2), 33.

Jang, D., Hwang, Y., Shin, H., Lee, W., 2013. Effects of salinity on the characteristics of biomass and membrane fouling in membrane bioreactors. *Bioresource Technology*. 141(0), 50-56.

Jenkins, D., 2014. Activated Sludge – 100 Years and Counting.

Jenkins, D., G. Richard, M., T. Daigger, G., 2004. Manual on the Causes and Control of Activated Sludge Bulking, Foaming, and other Solids Separation Problems 3rd Edition. Lewis

Jesus, R., Giuseppe, O., Jeroen de, V., Rouke, B., Philippe, W., J.Hans, R., Eppink, M. H. M., Kleinegris, D. M. M., Wijffels, F. H., Maria J. , B., 2016. Towards industrial products from microalgae. Energy & Environmental Science. *Energy and Environmental Science*. 9, 3036-3043.

Jhaveri, J. H., Murthy, Z. V. P., 2016. A comprehensive review on anti-fouling nanocomposite membranes for pressure driven membrane separation processes. *Desalination*. 379, 137-154.

Jia, H., Yuan, Q., 2016. Removal of nitrogen from wastewater using microalgae and microalgae–bacteria consortia. *Cogent Environmental Science*. 2(1), 1275089.

Jiang, W., Xia, S., Liang, J., Zhang, Z., Hermanowicz, S. W., 2013. Effect of quorum quenching on the reactor performance, biofouling and biomass characteristics in membrane bioreactors. *Water Research*. 47(1), 187-196.

Jin, L., Ong, S. L., Ng, H. Y., 2010. Comparison of fouling characteristics in different pore-sized submerged ceramic membrane bioreactors. *Water Research*. 44(20), 5907-18.

Johir, M. A. H., Vigneswaran, S., Sathasivan, A., Kandasamy, J., Chang, C. Y., 2012. Effect of organic loading rate on organic matter and foulant characteristics in membrane bio-reactor. *Bioresource Technology*. 113, 154-160.

Judd, S., 2008. The status of membrane bioreactor technology. *Trends in Biotechnology*. 26(2), 109-116.

Judd, S., van den Broeke, L. J. P., Shurair, M., Kuti, Y., Znad, H., 2015. Algal remediation of CO2 and nutrient discharges: A review. *Water Research*. 87, 356-366.

Kesaano, M., Sims, R. C., 2014. Algal biofilm based technology for wastewater treatment. *Algal*

Research. 5, 231-240.

Kim, S., Chu, K. H., Al-Hamadani, Y. A. J., Park, C. M., Jang, M., Kim, D.-H., Yu, M., Heo, J., Yoon, Y., 2018. Removal of contaminants of emerging concern by membranes in water and wastewater: A review. *Chemical Engineering Journal*. 335, 896-914.

Kraume, M., Drews, A., 2010. Membrane Bioreactors in Waste Water Treatment – Status and Trends. *Chemical Engineering & Technology*. 33(8), 1251-1259.

Krzeminski, P., Leverette, L., Malamis, S., Katsou, E., 2017. Membrane bioreactors – A review on recent developments in energy reduction, fouling control, novel configurations, LCA and market prospects. *Journal of Membrane Science*. 527, 207-227.

Le-Clech, P., Chen, V., Fane, T. A. G., 2006. Fouling in membrane bioreactors used in wastewater treatment. *Journal of Membrane Science*. 284(1), 17-53.

Le-Clech, P., Jefferson, B., Judd, S. J., 2003. Impact of aeration, solids concentration and membrane characteristics on the hydraulic performance of a membrane bioreactor. *Journal of Membrane Science*. 218(1-2), 117-129.

Lee, J., Ahn, W.-Y., Lee, C.-H., 2001. Comparison of the filtration characteristics between attached and suspended growth microorganisms in submerged membrane bioreactor. *Water Research*. 35(10), 2435-2445.

Lee, S., Park, S. K., Kwon, H., Lee, S. H., Lee, K., Nahm, C. H., Jo, S. J., Oh, H. S., Park, P. K., Choo, K. H., Lee, C. H., Yi, T., 2016. Crossing the Border between Laboratory and Field: Bacterial Quorum Quenching for Anti-Biofouling Strategy in an MBR. *Environmental Science and Technology*. 50(4), 1788-1795.

Lesage, N., Sperandio, M., Cabassud, C., 2008. Study of a hybrid process: Adsorption on activated carbon/membrane bioreactor for the treatment of an industrial wastewater. *Chemical Engineering and Processing: Process Intensification*. 47(3), 303-307.

Li, C., Cabassud, C., Guigui, C., 2015. Evaluation of membrane bioreactor on removal of pharmaceutical micropollutants: a review. *Desalination and Water Treatment*. 55(4), 845-858.

Li, Y.-Z., He, Y.-L., Liu, Y.-H., Yang, S.-C., Zhang, G.-J., 2005. Comparison of the filtration

characteristics between biological powdered activated carbon sludge and activated sludge in submerged membrane bioreactors. *Desalination*. 174(3), 305-314.

Liao, Y., Bokhary, A., Maleki, E., Liao, B., 2018. A review of membrane fouling and its control in algal-related membrane processes. *Bioresource Technology*. 264, 343-358.

Lin, H., Gao, W., Meng, F., Liao, B.-Q., Leung, K.-T., Zhao, L., Chen, J., Hong, H., 2012. Membrane Bioreactors for Industrial Wastewater Treatment: A Critical Review. *Critical Reviews in Environmental Science and Technology*. 42(7), 677-740.

Lin, H., Liao, B.-Q., Chen, J., Gao, W., Wang, L., Wang, F., Lu, X., 2011. New insights into membrane fouling in a submerged anaerobic membrane bioreactor based on characterization of cake sludge and bulk sludge. *Bioresource Technology*. 102(3), 2373-2379.

Lin, H., Yu, G., Shen, L., Li, R., Xu, Y., 2020. 10 - Advanced membrane bioreactor fouling control and prevention strategies. in: *Current Developments in Biotechnology and Bioengineering*, (Eds.) Ng, H. Y., Ng, T. C. A., Ngo, H. H., Mannina, G., Pandey, A., Elsevier, pp. 209-224.

Lin, H., Zhang, M., Wang, F., Meng, F., Liao, B.-Q., Hong, H., Chen, J., Gao, W., 2014. A critical review of extracellular polymeric substances (EPSs) in membrane bioreactors: Characteristics, roles in membrane fouling and control strategies. *Journal of Membrane Science*. 460(0), 110-125.

Luo, W., Phan, H. V., Li, G., Hai, F. I., Price, W. E., Elimelech, M., Nghiem, L. D., 2017a. An Osmotic Membrane Bioreactor–Membrane Distillation System for Simultaneous Wastewater Reuse and Seawater Desalination: Performance and Implications. *Environmental Science & Technology*. 51(24), 14311-14320.

Luo, Y., Le-Clech, P., Henderson, R. K., 2018. Assessment of membrane photobioreactor (MPBR) performance parameters and operating conditions. *Water Research*. 138, 169-180.

Luo, Y., Le-Clech, P., Henderson, R. K., 2017b. Simultaneous microalgae cultivation and wastewater treatment in submerged membrane photobioreactors: A review. *Algal Research*. 24, 425-437.

Madoni, P., Davoli, D., Gibin, G., 2000. Survey of filamentous microorganisms from bulking and

foaming activated-sludge plants in Italy. *Water Research*. 34(6), 1767-1772.

Maity, J. P., Bundschuh, J., Chen, C.-Y., Bhattacharya, P., 2014. Microalgae for third generation biofuel production, mitigation of greenhouse gas emissions and wastewater treatment: Present and future perspectives – A mini review. *Energy*. 78, 104-113.

Marbelia, L., Bilad, M. R., Passaris, I., Discart, V., Vandamme, D., Beuckels, A., Muylaert, K., Vankelecom, I. F. J., 2014. Membrane photobioreactors for integrated microalgae cultivation and nutrient remediation of membrane bioreactors effluent. *Bioresource Technology*. 163, 228-235.

Martins, A. M. P., Pagilla, K., Heijnen, J. J., van Loosdrecht, M. C. M., 2004. Filamentous bulking sludge—a critical review. *Water Research*. 38(4), 793-817.

Mata, T. M., Martins, A. A., Caetano, N. S., 2010. Microalgae for biodiesel production and other applications: A review. *Renewable and Sustainable Energy Reviews*. 14(1), 217-232.

Mateo-Sagasta, J., Raschid-Sally, L., Thebo, A., 2015. Global Wastewater and Sludge Production, Treatment and Use. in: *Wastewater: Economic Asset in an Urbanizing World*, (Eds.) Drechsel, P., Qadir, M., Wichelns, D., Springer Netherlands. Dordrecht, pp. 15-38.

Meng, F., Chae, S.-R., Drews, A., Kraume, M., Shin, H.-S., Yang, F., 2009. Recent advances in membrane bioreactors (MBRs): Membrane fouling and membrane material. *Water Research*. 43(6), 1489-1512.

Meng, F., Chae, S.-R., Shin, H.-S., Yang, F., Zhou, Z., 2012. Recent Advances in Membrane Bioreactors: Configuration Development, Pollutant Elimination, and Sludge Reduction. *Environmental Engineering Science*. 29(3), 139-160.

Meng, F., Zhang, H., Yang, F., Liu, L., 2007. Characterization of cake layer in submerged membrane bioreactor. *Environmental Science and Technology*. 41(11), 4065-4070.

Morrow, C. P., Furtaw, N. M., Murphy, J. R., Achilli, A., Marchand, E. A., Hiibel, S. R., Childress, A. E., 2018. Integrating an aerobic/anoxic osmotic membrane bioreactor with membrane distillation for potable reuse. *Desalination*. 432, 46-54.

Mortezaeikia, V., Tavakoli, O., Yegani, R., Faramarzi, M., 2016a. Cyanobacterial CO2 biofixation

in batch and semi-continuous cultivation, using hydrophobic and hydrophilic hollow fiber membrane photobioreactors. *Greenhouse Gases: Science and Technology*. 6(2), 218-231.

Mortezaeikia, V., Yegani, R., Tavakoli, O., 2016b. Membrane-sparger vs. membrane contactor as a photobioreactors for carbon dioxide biofixation of Synechococcus elongatus in batch and semi-continuous mode. *Journal of CO2 Utilization*. 16, 23-31.

Mutamim, N. S. A., Noor, Z. Z., Hassan, M. A. A., Olsson, G., 2012. Application of membrane bioreactor technology in treating high strength industrial wastewater: a performance review. *Desalination*. 305(0), 1-11.

Mutamim, N. S. A., Noor, Z. Z., Hassan, M. A. A., Yuniarto, A., Olsson, G., 2013. Membrane bioreactor: Applications and limitations in treating high strength industrial wastewater. *Chemical Engineering Journal*. 225(0), 109-119.

Na, J.-H., Nam, D.-H., Ko, B.-G., Lee, C.-Y., Kang, K.-H., 2017. Reduced sludge production in a membrane bioreactor by uncoupling metabolism and its effect on phosphorus accumulation in the biomass. *Environmental Technology*. 38(23), 3007-3015.

Phattaranawik, J., Fane, A. G., Pasquier, A. C. S., Bing, W., 2008. A novel membrane bioreactor based on membrane distillation. *Desalination*. 223(1), 386-395.

Posadas, E., Morales, M. d. M., Gomez, C., Acién, F. G., Muñoz, R., 2015. Influence of pH and CO2 source on the performance of microalgae-based secondary domestic wastewater treatment in outdoors pilot raceways. *Chemical Engineering Journal*. 265, 239-248.

Praveen, P., Guo, Y., Kang, H., Lefebvre, C., Loh, K.-C., 2018. Enhancing microalgae cultivation in anaerobic digestate through nitrification. *Chemical Engineering Journal*. 354, 905-912.

Praveen, P., Loh, K.-C., 2019. Nutrient removal in an algal membrane photobioreactor: effects of wastewater composition and light/dark cycle. *Applied Microbiology and Biotechnology*.

Razzak, S. A., Ilyas, M., Ali, S. A. M., Hossain, M. M., 2015. Effects of CO2 Concentration and pH on Mixotrophic Growth of Nannochloropsis oculata. *Applied Biochemistry and Biotechnology*. 176(5), 1290-1302.

Rosenberger, S., Kraume, M., 2003. Filterability of activated sludge in membrane bioreactors.

Desalination. 151(2), 195-200.

Sanguanpak, S., Chiemchaisri, C., Chiemchaisri, W., Yamamoto, K., 2015. Influence of operating pH on biodegradation performance and fouling propensity in membrane bioreactors for landfill leachate treatment. *International Biodeterioration & Biodegradation*. 102(0), 64-72.

Sforza, E., Simionato, D., Giacometti, G. M., Bertucco, A., Morosinotto, T., 2012. Adjusted Light and Dark Cycles Can Optimize Photosynthetic Efficiency in Algae Growing in Photobioreactors. *PLOS ONE*. 7(6), e38975.

Shannon, M. A., Bohn, P. W., Elimelech, M., Georgiadis, J. G., Mariñas, B. J., Mayes, A. M., 2008. Science and technology for water purification in the coming decades. *Nature*. 452(7185), 301-310.

Shen, L.-g., Lei, Q., Chen, J.-R., Hong, H.-C., He, Y.-M., Lin, H.-J., 2015. Membrane fouling in a submerged membrane bioreactor: Impacts of floc size. *Chemical Engineering Journal*. 269(0), 328-334.

Sheng, A. L. K., Bilad, M. R., Osman, N. B., Arahman, N., 2017. Sequencing batch membrane photobioreactor for real secondary effluent polishing using native microalgae: Process performance and full-scale projection. *Journal of Cleaner Production*. 168, 708-715.

Simionato, D., Basso, S., Giacometti, G. M., Morosinotto, T., 2013. Optimization of light use efficiency for biofuel production in algae. *Biophysical Chemistry*. 182, 71-78.

Solmaz, A., Işik, M., 2019. Effect of Sludge Retention Time on Biomass Production and Nutrient Removal at an Algal Membrane Photobioreactor. *BioEnergy Research*.

Su, X., Tian, Y., Li, H., Wang, C., 2013. New insights into membrane fouling based on characterization of cake sludge and bulk sludge: An especial attention to sludge aggregation. *Bioresource Technology*. 128(0), 586-592.

te Poele, S., van der Graaf, J., 2005. Enzymatic cleaning in ultrafiltration of wastewater treatment plant effluent. *Desalination*. 179(1), 73-81.

Ting, H., Haifeng, L., Shanshan, M., Yuanhui, Z., Zhidan, L., Na, D., 2017. Progress in Microalgae cultivation photobioreactors and applications in wastewater treatment: A review.

International Journal of Agricultural and Biological Engineering. 10(1), 1-29.

Van den Broeck, R., Van Dierdonck, J., Nijskens, P., Dotremont, C., Krzeminski, P., van der Graaf, J. H. J. M., van Lier, J. B., Van Impe, J. F. M., Smets, I. Y., 2012. The influence of solids retention time on activated sludge bioflocculation and membrane fouling in a membrane bioreactor (MBR). *Journal of Membrane Science*. 401–402(0), 48-55.

van Nieuwenhuijzen, A. F., Evenblij, H., Uijterlinde, C. A., Schulting, F. L., 2008. Review on the state of science on membrane bioreactors for municipal wastewater treatment. *Water Science and Technology*. 57(7), 979-86.

Van Thuan, N., Thi Thanh Thuy, N., Hong Hai, N., Nguyen, N. C., Bui, X.-T., 2018. Influence of microalgae retention time on biomass production in membrane photobioreactor using human urine as substrate. *2018*. 60(4), 5.

Vrijenhoek, E. M., Hong, S., Elimelech, M., 2001. Influence of membrane surface properties on initial rate of colloidal fouling of reverse osmosis and nanofiltration membranes. *Journal of Membrane Science*. 188(1), 115-128.

Wang, J., Pathak, N., Chekli, L., Phuntsho, S., Kim, Y., Li, D., Shon, H. K., 2017. Performance of a Novel Fertilizer-Drawn Forward Osmosis Aerobic Membrane Bioreactor (FDFO-MBR): Mitigating Salinity Build-Up by Integrating Microfiltration. *Water*. 9(1), 21.

Wang, X., Chang, V. W. C., Tang, C. Y., 2016. Osmotic membrane bioreactor (OMBR) technology for wastewater treatment and reclamation: Advances, challenges, and prospects for the future. *Journal of Membrane Science*. 504, 113-132.

Wang, Y.-K., Sheng, G.-P., Li, W.-W., Huang, Y.-X., Yu, Y.-Y., Zeng, R. J., Yu, H.-Q., 2011. Development of a Novel Bioelectrochemical Membrane Reactor for Wastewater Treatment. *Environmental Science & Technology*. 45(21), 9256-9261.

Wang, Z., Ma, J., Tang, C. Y., Kimura, K., Wang, Q., Han, X., 2014. Membrane cleaning in membrane bioreactors: A review. *Journal of Membrane Science*. 468(0), 276-307.

Wang, Z., Wu, Z., Mai, S., Yang, C., Wang, X., An, Y., Zhou, Z., 2008. Research and applications of membrane bioreactors in China: Progress and prospect. *Separation and Purification*

Technology. 62(2), 249-263.

Wanner, J., 1995. Activated Sludge: Bulking and Foaming Control. CRC Press, Boca Raton.

Weerasekara, N. A., Choo, K.-H., Lee, C.-H., 2014. Hybridization of physical cleaning and quorum quenching to minimize membrane biofouling and energy consumption in a membrane bioreactor. *Water Research*. 67(0), 1-10.

WWAP (United Nations World Water Assessment Programme). 2017. The United Nations World Water Development Report 2017. Wastewater: The Untapped Resource. Paris, UNESCO.

Xiao, K., Liang, S., Wang, X., Chen, C., Huang, X., 2019. Current state and challenges of full-scale membrane bioreactor applications: A critical review. *Bioresource Technology*. 271, 473-481.

Xu, M., Bernards, M., Hu, Z., 2014. Algae-facilitated chemical phosphorus removal during high-density Chlorella emersonii cultivation in a membrane bioreactor. *Bioresource Technology*. 153, 383-387.

Xu, M., Li, P., Tang, T., Hu, Z., 2015. Roles of SRT and HRT of an algal membrane bioreactor system with a tanks-in-series configuration for secondary wastewater effluent polishing. *Ecological Engineering*. 85, 257-264.

Yamato, N., Kimura, K., Miyoshi, T., Watanabe, Y., 2006. Difference in membrane fouling in membrane bioreactors (MBRs) caused by membrane polymer materials. *Journal of Membrane Science*. 280(1-2), 911-919.

Yoon, S.-H., Kim, H.-S., Lee, S., 2004. Incorporation of ultrasonic cell disintegration into a membrane bioreactor for zero sludge production. *Process Biochemistry*. 39(12), 1923-1929.

Yoshihiko, S., Takeshi, S., Akira, N., 2016. An innovative culture technique for microalgae using hollow fiber membranes. *ECI Digital Archives*.

Zhang, J., Chua, H. C., Zhou, J., Fane, A. G., 2006. Factors affecting the membrane performance in submerged membrane bioreactors. *Journal of Membrane Science*. 284(1-2), 54-66.

Zhang, M., Yao, L., Maleki, E., Liao, B.-Q., Lin, H., 2019. Membrane technologies for microalgal cultivation and dewatering: Recent progress and challenges. *Algal Research*. 44, 101686.

Zhang, Y., Zhang, M., Wang, F., Hong, H., Wang, A., Wang, J., Weng, X., Lin, H., 2014. Membrane fouling in a submerged membrane bioreactor: Effect of pH and its implications. *Bioresource Technology*. 152(0), 7-14.

Chapter 3 Simultaneous Removals of Nutrients and COD in a Novel Microalgal-Bacterial Membrane Photobioreactor (MB-MPBR): Effects of HRT and N/P ratio

Abstract: A microalgal-bacterial membrane photobioreactor (MB-MPBR) was developed for simultaneous COD and nutrients (N and P) removals from synthetic municipal wastewater in a single stage for a long-term operation over 350 days. The effects of HRT and N/P ratio on the biological performance were systematically evaluated for the first time. The results showed that a lower N/P ratio (3.9:1) and shorter HRT (2 d) promoted more biomass production, as compared to a high HRT (3 d) and a high N/P ratio (9.7:1). The highest biomass concentration (2.55 ± 0.14 g/L) and productivity (127.5 mg/L/d) were achieved at N/P ratio of 3.9:1 and HRT of 2 d due to the highest nitrogen and phosphorus loadings under such conditions. A COD and ammonia-N removal efficiency of over 96% and 99%, respectively, were achieved regardless of HRTs and N/P ratios. In the absence of nitrogen or phosphorus deficiency, shorter HRT (2 d) yielded a higher nitrogen and phosphorus uptake but lower removal efficiency. In addition, the imbalance N/P ratio (9.7:1) would decrease nitrogen or phosphorus removal. Overall, the results suggested that it was feasible to simultaneously achieve complete or high removal of COD, nitrogen, and phosphorous in MB-MPBR under the appropriate conditions. This study demonstrated for the first time that MB-MPBR is a promising technology that could achieve a high-quality effluent meeting the discharge standards of COD and nutrients in one single step.

Keywords: Microalgal-bacterial membrane photobioreactor; HRT; N/P ratio; Nutrients removal; Wastewater treatment

3.1 Introduction

As a promising technology, MBR has been extensively applied for wastewater treatment since the past decades because of its distinctive advantages (Cicek, 2003; Gander et al., 2000; Lin et al., 2012). However, typical bacterial-based MBR systems have low nutrients (N and P) removal and thus require additional processes to achieve high nutrients removal and satisfy wastewater discharge requirements. It involves extra equipment and instruments and thus leads to an increase in capital cost (Marbelia et al., 2014). Also, frequent membrane cleaning and replacement caused by membrane fouling will increase the maintenance and operation costs. Therefore, it is highly desirable to develop novel processes to achieve simultaneous COD and nutrients (N and P) removals in a single step.

In the recent decade, microalgae, which possess superior nutrient fixation capacity than bacteria, have attracted wide attention and been extensively used for nutrients removal from wastewaters (Gao et al., 2016a; Honda et al., 2017; Luo et al., 2017; Xu et al., 2015; Zhang et al., 2019). On the other hand, activated sludge has been widely used for COD/BOD removal from wastewater. By integrating the functions of microalgae and bacteria, the microalgae-bacteria consortia have a distinctive advantage of simultaneously removing organic matters and inorganic nutrients (N and P) from wastewaters with high efficiency (Alcántara et al., 2015; de Godos et al., 2011; Karya et al., 2013; Lee et al., 2015; Posadas et al., 2013). However, washout of free microalgae is a challenging drawback for this system. The application of membrane bioreactors can effectively avoid this problem. A microalgal-bacterial membrane photobioreactor (MB-MPBR) can not only effectively solve the washout problem but also improve the effluent quality and system stability. In an MB-MPBR, CO_2 produced by bacteria is used to support the growth of microalgae for inorganic nutrient removal and O_2 produced by microalgae is used for bacterial decomposition of organic compounds. This synergy reduces the energy demand of mechanical aerations for CO_2 and O_2 deliveries (Oswald, 1988; Sun et al., 2018a; Sun et al., 2018b; Sun et al., 2018c) and simplifies the process from multiple stages to a single stage. Moreover, MB-MPBR exhibited lower membrane fouling propensity than conventional MBR (C-MBR) due to the improved sludge properties after introducing microalgae (Sun et al., 2018a; Sun et al., 2018b; Sun et al., 2018c).

Like MBRs, the performance of MB-MPBRs depends on various factors, including influent

characteristics, nutrients loading rate, HRT, and SRT. Among these factors, HRT is a crucial factor affecting both pollutant removals and biomass productivity (Honda et al., 2017; Luo et al., 2018; Zhang et al., 2019). Longer HRT elevates foulant removal, but under the premise of high removal of pollutants, shorter HRT is recommended to reduce the footprint and save capital cost (Luo et al., 2017). HRT also significantly relates to nutrient loading rate. For wastewater containing a specific concentration of pollutants, shorter HRT induces more nutrients and then impacts the relative nutrient removal efficiency. N/P (nitrogen/phosphorus) ratio is another vital factor influencing nutrient removal efficiency because nitrogen and phosphorus are fixed at a relatively constant stoichiometric ratio (Beuckels et al., 2015; Choi & Lee, 2015; Lee et al., 2013). That is, the N/P ratio may be a key factor that ensures the quality of treated effluent from MB-MPBR system to meet the discharge requirements. Therefore, optimizing HRT and N/P ratio is essential to simultaneously remove inorganic nutrients (N and P) and organics in a single MB-MPBR and achieve superior effluent quality meeting the discharge standards. However, several current studies mainly focus on comparing the treatment and fouling performance between MB-MPBR and C-MBR. Furthermore, the nutrients (N and P) removal efficiencies of these studies were typically poor (Sun et al., 2018a; Sun et al., 2018b) and the proper values of HRT and N/P ratio were not optimized to achieve an effluent quality meeting discharge standard in a single step process.

In this study, long-term operation of an MB-MPBR over 350 days was conducted to study the impacts of HRT and N/P ratio on the biological performance of an MB-MPBR for synthetic municipal wastewater treatment. The biological performance with various parameters, including biomass production, biomass productivity, COD removal, nutrients (N and P) removal, and partial consortium properties, was determined and compared. It further demonstrated that MB-MPBR is a promising technology that can simultaneously remove nutrients (N and P) and COD and achieve a high effluent quality meets the discharge standards in one single step.

3.2 Material and methods

3.2.1 Microalgal inoculum preparation and activated sludge seed

A strain of microalgae *Chlorella Vulgaris* (CPCC 90) purchased from the Canadian Phycological Culture Centre (University of Waterloo, ON, Canada) was used as the microalgal inoculant. It was pre-cultivated in a modified Mineral Salt Medium (MSM) (Muñoz et al., 2005) under continuous aeration and light illumination at room temperature. The modified MSM medium

contained 3.82 g of NH_4Cl, 1.3251 g of K_2HPO_4, 0.6247 g of KH_2PO_4, 0.625 g of $MgSO_4 \cdot 7H_2O$, 0.1105 g of $CaCl_2 \cdot 2H_2O$, 0.1142 g of H_3BO_3, 0.0498 g of $FeSO_4 \cdot 7H_2O$, 0.0882 g of $ZnSO_4 \cdot 7H_2O$, 0.0144 g of $MnCl_2 \cdot 4H_2O$, 0.0118 g of $Na_2MoO_4 \cdot 2H_2O$, 0.0157 g of $CuSO_4 \cdot 5H_2O$, 0.004 g of $CoCl_2 \cdot 6H_2O$, and 0.64 g of EDTA disodium salt dehydrate per liter.

The activated sludge seed was from an activated sludge plant treating pulp and paper wastewater from a local pulp and paper mill.

3.2.2 Experimental set-up

The schematic of the lab-scale MB-MPBR set-up is shown in Figure 3-1. The reactor has a working volume of 10.35 L with an internal diameter of 19 cm and an effective height of 36.5 cm. The surface to volume ratio (S/V), which is defined as the ratio of the lighted surface area to working volume (Honda et al., 2012), was 23.8 m^{-1}. A polyvinylidene fluoride (PVDF) flat-sheet membrane module with an effective surface area of 0.03 m^2 (pore size 0.1 μm, SINAP Co. Ltd., Shanghai, China) was submerged in the reactor. At the bottom of the reactor, two tubes connected with mediate-bubble diffusers were installed directly below the membrane module to provide extra CO_2/O_2 for microalgal/bacterial growth and prevent membrane fouling by creating shear stress on the membrane surface. The air containing about 0.05% CO_2 was provided at an approximate airflow rate of 3.75 ± 0.42 L/min. A magnetic stirrer (Model 6795-611, Corning, USA) was loaded at the bottom of the reactor to provide a gentle mixing of the biomass to prevent the microalgal-bacterial settling. The reactor was continuously illuminated with LED light. Four LED lamps were placed outside the reactor (each side with two) to provide an approximate light intensity on the reactor surface of 8400 lux.

3.2.3 Reactor operation

A synthetic municipal wastewater with a medium strength was prepared as feed. The synthetic feed was prepared from glucose, NH_4Cl, KH_2PO_4 and trace elements, the average concentration of COD, TN and TP, as well as the corresponding N/P ratio for each phase, are displayed in Table 3-1. The trace elements in the feed included: 0.25 mg/L NaCl, 0.22 mg/L $MnCl_2 \cdot 4H_2O$, 0.39 mg/L $CuSO_2 \cdot 5H_2O$, 0.41 mg/L $CoCl_2 \cdot 6H_2O$, 0.44 mg/L $ZnSO_2 \cdot 7H_2O$, 1.26 mg/L $Na_2MoO_4 \cdot 2H_2O$, 2.49 mg/L $FeSO_4 \cdot 7H_2O$, 5.0 mg/L $CaCl_2$, 82 mg/L $MgSO_4 \cdot 7H_2O$ and 300 mg/L $NaHCO_3$. The feed was stored in a refrigerator at 4-5 ºC and delivered to the MB-MPBR system in a semi-continuous manner. A peristaltic pump controlled by a level sensor (LC40, Flowline Inc., USA) was used to

pump the feed into the reactor to supply nutrients and maintain a constant level in the reactor. The permeate was intermittently collected by a peristaltic pump (Model 77122-12, Masterflex®C/L®PWR, Cole-Parmer, USA) operating in the mode of 3-min-on and 2-min-off. The suspension temperature, pH, and dissolved oxygen (DO) in the MB-MPBR was maintained at a relatively constant level of 26.9 ± 0.9 ℃, 7.3 ± 0.6, and 7.3 ± 0.4 mg/L, respectively. The suspension pH was controlled by adjusting the pH of the feed using NaOH and HCl solution.

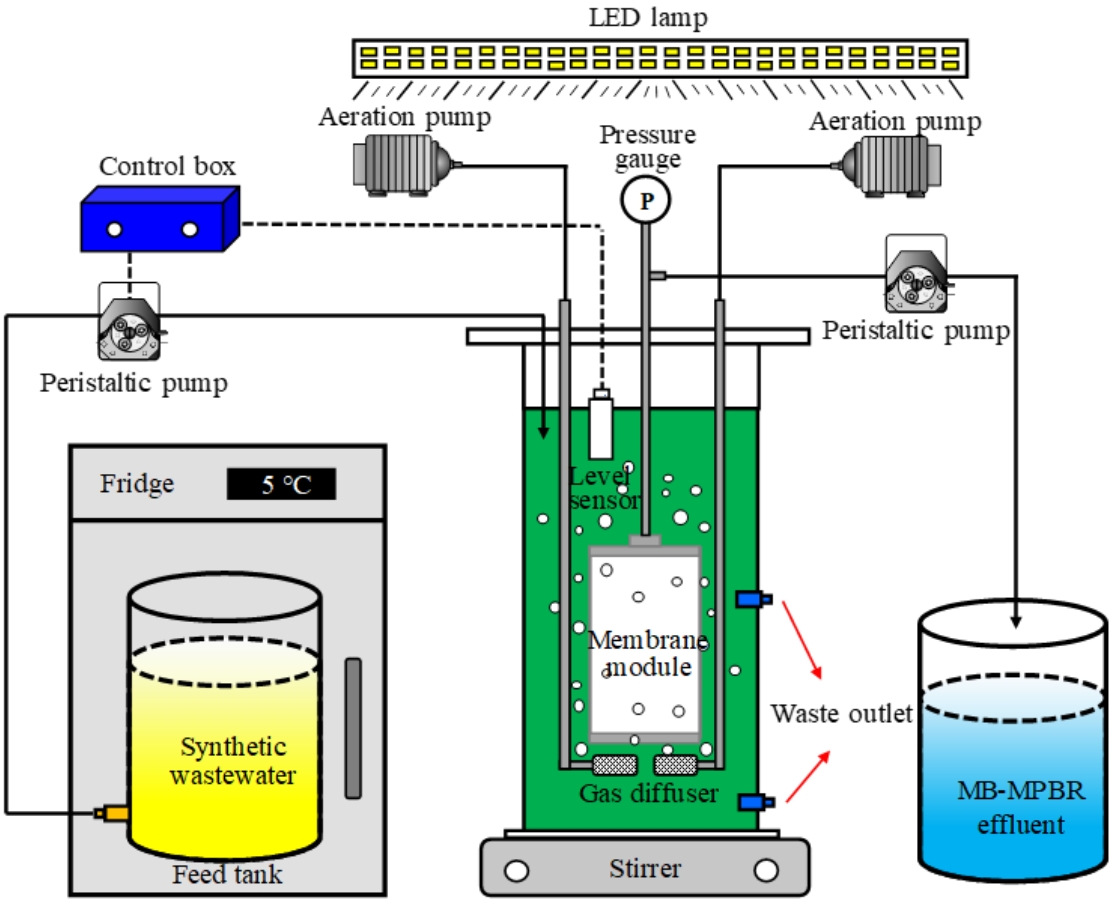

Figure 3-1 Experimental set-up of the submerged MB-MPBR system.

Table 3-1 Operational conditions of the MB-MPBR for each phase.

	Phase 1	Phase 2	Phase 3	Phase 4	Phase 5
Operating period (d)	1-63	64-127	128-200	201-267	268-351
Initial biomass concentration	0.6 g/L microalgae 3.0 g/L sludge	Following phase 1	Following phase 2	Following phase 3	Following phase 4
System SRT (d)	20	20	20	20	20
System HRT (d)	3.0 ± 0.1	2.0 ± 0.1	2.0 ± 0.0	3.0 ± 0.1	3.0 ± 0.1
Influent COD (mg/L)	440.3 ± 11.1	440.3 ± 11.1	440.3 ± 11.1	440.3 ± 11.1	440.3 ± 11.1
Influent TN (mg/L)	36.9 ± 2.2	36.9 ± 2.2	36.9 ± 2.2	36.9 ± 2.2	46.5 ± 1.9
Influent TP (mg/L)	3.8 ± 0.2	3.8 ± 0.2	9.5 ± 0.5	9.5 ± 0.5	9.5 ± 0.5
Influent N/P mass ratio	9.7:1	9.7:1	3.9:1	3.9:1	4.9:1
Average[1] MLSS (g/L)	1.67 ± 0.14	2.33 ± 0.20	2.55 ± 0.14	2.40 ± 0.07	2.17 ± 0.15
Average Biomass productivity (mg/L/d)	83.5	116.5	127.5	120.0	108.5
Average chlorophyll-a/MLSS (mg/g biomass)	7.83 ± 2.47	16.42 ± 1.10	25.74 ± 2.26	27.01 ± 1.42	32.58 ± 2.07

[1] Average was calculated from the data after day 20 until the end of the operation to exclude the start-up period for each phase. The data are expressed as mean ± standard deviation.

The pre-cultivated *Chlorella Vulgaris* and activated sludge were used as microalgal and bacterial inoculum, respectively. The inoculated ratio (microalgae/activated sludge) was 1:5, corresponding to initial microalgae and sludge concentrations of 0.6 g/L and 3.0 g/L, respectively. The reactor was operated for almost 350 days and divided into five phases by varying the HRT and N/P ratio of the system. Details about the operating conditions for each phase are listed in Table 3-1. Two HRTs (2 and 3 d) and three N/P mass ratios (9.7:1, 3.9:1, and 4.9:1) were tested in this study. The values of HRT and N/P ratio were controlled by adjusting the membrane flux and as well as TP and TN concentration in the feed. Within each phase, when the transmembrane pressure (TMP) of the MB-MPBR reached 30 kPa, only physical cleaning was conducted to remove the foulant layer and recover its permeability. At the end of each phase, the used membranes were replaced by new pieces of membranes.

3.2.4 Analytical methods

3.2.4.1 Chlorophyll-a extraction and analysis

Chlorophyll-a was extracted and analyzed following the processes as previously described (Nautiyal et al., 2014). A known volume of microalgal-bacterial suspension was centrifuged at 8000 × g for 10 min. The pellets were resuspended into a known volume of methanol and then kept in a water bath of 60 ℃ for 30 min. After that, the suspension was stood and cooled down at room temperature for downstream measurement. The chlorophyll-a content in the suspension was measured using a visible spectrophotometer (DR2800, Hach, Germany) at the wavelength of 750 nm, 665.2 nm and 652 nm, respectively. The concentration of chlorophyll-a can be calculated by substituting the absorbance values into the following equation:

$$\text{Chlorophyll-a (mg/L)} = 16.29(A^{665.2}-A^{750})-8.54(A^{652}-A^{750}) \quad (3\text{-}1)$$

where A^{750}, $A^{665.2}$, A^{652} represent the absorbance at 750, 665.2 and 652 nm, respectively (Nautiyal et al., 2014).

3.2.4.2 Particle size distribution (PSD)

The PSD of the mixture was measured by a Malvern Mastersizer 2000 instrument (Worcestershire, UK) with a detection range of 0.02-2000 μm. The scattered light is detected by a series of photosensitive detectors which convert the signal to a size distribution according to volume or number. Each sample was automatically measured in triplicate by the machine. This measurement was conducted 1-2 times per week.

3.2.4.3 Microscopic observation

The morphology of the original microalgae, original sludge, and microalgal- bacterial consortia was observed under an inverted optical microscope (Olympus IX51, Japan). The samples were firstly dropped on a slide and then dispersed by a cover slide. The prepared samples were placed on the stage of the microscope. At least 30 images were randomly taken by a digital camera connected with the microscope for each sample.

3.2.4.4 Other routine analysis

DO, pH and temperature of the suspension in the reactor were measured by a DO meter (Model 407510, Extech, USA), a pH meter (pH 700, Oakton, USA) and a thermometer, respectively. CO_2 concentration in the air around the MB-MPBR was determined by a gas chromatography instrument (Shimazu, Mondel GC-2014, Japan). The elemental compositions of C, H, N and S for biomass were analyzed by an elemental analyzer. Samples of feed and permeate were periodically collected from the system for water quality monitoring. The growth of biomass was monitored by the measurement of mixed liquor suspended solids (MLSS). MLSS, COD and NH_4^+-N were determined according to the standard methods (APHA, 2005). The TN and TP were measured with alkaline potassium persulfate digestion-UV spectrophotometric method and ammonium molybdate spectrophotometry (State Environmental Protection Administration of China, 2002), respectively. Duplicate measurements of MLSS, COD, TN and TP were conducted for each sample, and the average values were reported.

3.2.5 Calculation and statistical analysis

The average biomass productivity over the operation period was calculated according to the equation (Luo et al., 2018):

$$r_x = X \times Q_{waste}/V_{MB\text{-}MPBR} = X/SRT \quad (3\text{-}2)$$

where r_x is the productivity of the biomass (mg/L/d); X represents the average biomass concentration (equal to average MLSS in this study); Q_{waste} is the biomass wasting rate (L/d); $V_{MB\text{-}MPBR}$ is the working volume of the bioreactor (L).

The nutrient loading and removal rate of MSB-MPBR were estimated by the following equations (Gao et al., 2016b):

$$\text{Nutrient loading (mg/L/d)} = C_{inf} \times Q/V \quad (3\text{-}3)$$

$$\text{Removal rate (mg/L/d)} = (C_{inf} - C_{eff}) \times Q/V \quad (3\text{-}4)$$

where C_{inf} and C_{eff} are the concentration (mg/L) of TN, or TP in the feed and effluent, respectively; Q is the flow rate (L); V was the working volume (L) of the reactor.

An analysis of variance (ANOVA) was used to examine the statistically significant difference ($p < 0.05$) between phases. All the results satisfied with statistical analysis were expressed as mean ± standard deviation. The statistical analyses were carried out using the SPSS 17.0 software.

3.3 Results and discussion

3.3.1 Biomass production

When stable conditions were reached, the biomass concentration (represented by MLSS) maintained constant within each phase (Figure 3-2). The values of biomass concentration and productivity ranged from 1.67 - 2.55 g/L and 83.5 - 127.5 mg/L/d, respectively. On average, treatments with a higher HRT of 3 d yielded lower biomass concentration and productivity under the same N/P ratio (Phase 1 vs Phase 2 (N/P = 9.7:1) and Phase 3 vs Phase 4 (N/P = 3.9:1)) (Table 3-1) ($p < 0.05$). Similarly, a higher N/P ratio of 9.7:1 led to a lower biomass concentration and productivity when HRT was kept the same (Phase 1 vs Phase 4 (HRT = 3 d) and Phase 2 vs Phase 3 (HRT = 2 d)) (Table 3-1) ($p < 0.05$). It was clear that biomass yield and productivity in the MB-MPBR was highly dependent on HRT and N/P ratio. Decreased HRT (corresponding to an increased loading) can supply more nutrients and organics into the reactor and then promotes biomass production. Besides, the N/P ratio also played a vital role because microalgae and bacteria would assimilate nitrogen and phosphorus in specific stoichiometric proportion (Choi & Lee, 2015; Lee et al., 2015). In this study, the N/P ratio at Phases 1 and 2 (9.7:1) was much higher than the optimal ratio reported in the literature (Luo et al., 2017). Therefore, P deficiency might significantly limit the microalgal growth and biomass productivity. In comparison, the biomass productivity of this study is comparable or higher than that of the typical MPBRs (Gao et al., 2016a; Honda et al., 2017; Xu et al., 2015; Zhang et al., 2019), which could be attributed to the higher nutrients loading in this study.

Figure 3-2 also shows that the chlorophyll-a/MLSS content gradually increased from 5.09 mg/g biomass in Phase 1 (day 23) to 27.55 mg/g biomass in Phase 3 (day 196), kept relatively constant (27.01 ± 1.42 mg/g biomass) in Phase 4, and then reached the highest average value of 32.58 ± 2.07 mg/g biomass in Phase 5. This is reflected by the change of the biomass color with an increase of greener color (more microalgae) at the end of the experiment (Figure 3-3). It

suggests a higher microalgal content in the mixed liquor with experimental time. The effect of N/P ratio on chlorophyll-a/MLSS content kept consistent for different HRTs (Phase 1 vs Phase 4 (HRT = 3 d) and Phase 2 vs Phase 3 (HRT = 2 d)) while the impact of HRT was opposite for different N/P ratios (Phase 1 vs Phase 2 (N/P = 9.7:1) and Phase 3 vs Phase 4 (N/P = 3.9:1)) (Table 3-1). For comparison, the better growth of microalgae at N/P ratio of 3.9:1 should be ascribed to the elimination of P limitation after increasing the feed TP concentration. In Phases 1 and 2, P was deficient, a decreased HRT introduced more P into the MB-MPBR, and remarkably improved the growth of microalgae. After the N/P ratio was optimized, the chlorophyll-a/MLSS content in both phases (Phases 3 and 4) had no significantly different (ANOVA, $p > 0.05$), which indicated that the growth of microalgae and bacteria achieved balance in Phases 3 and 4 after stabilization. For long-term operation, optimizing HRT and N/P ratio is critical to balance the growth of microalgae and bacteria to maintain the MB-MPBR and improve the system performance.

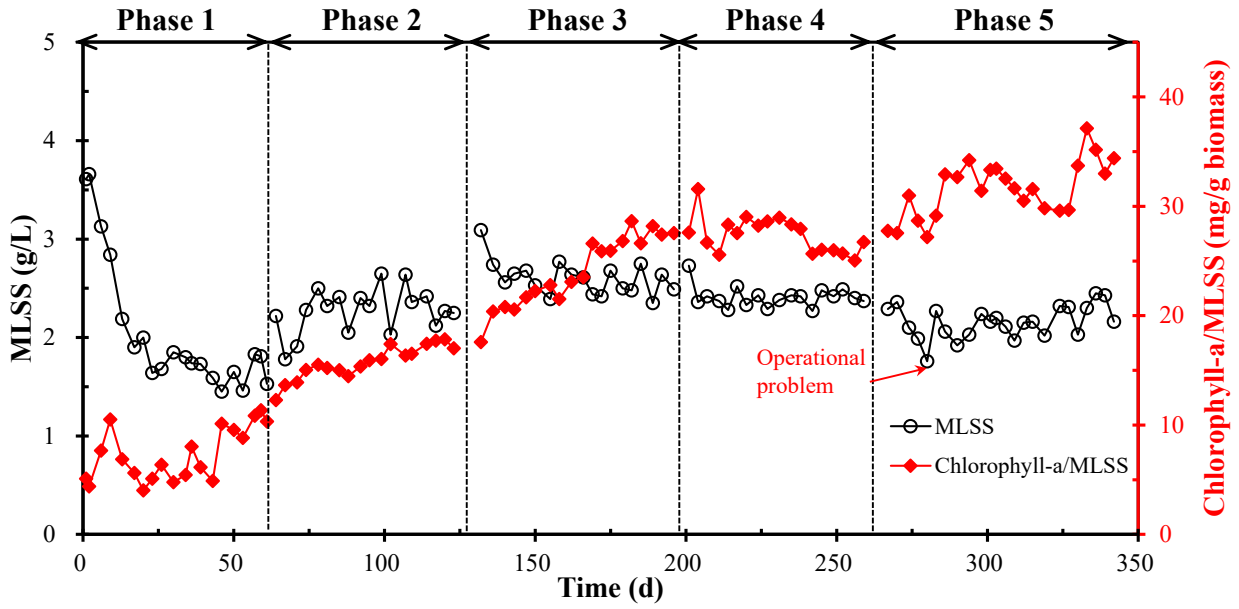

Figure 3-2 Variations of biomass concentration and chlorophyll-a/MLSS in the MB-MPBR under different HRTs and N/P ratios.

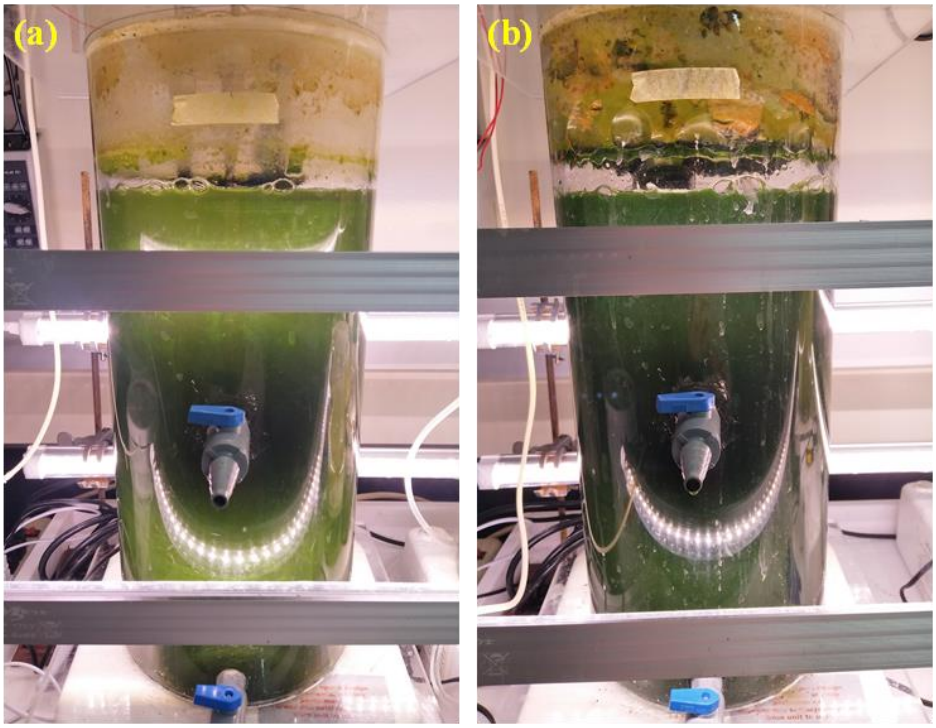

Figure 3-3 Optical images of the submerged MB-MPBR at (a) Phase 1 and (b) Phase 5.

3.3.2 Pollutants removal

Figure 3-4(a1-a2) displays the variation of TN removal efficiency and concentrations in influent and effluent as well as the average TN loading and removal rate. The influent TN concentration was maintained at a relatively constant level of 36.9 ± 2.2 mg/L for the first four phases and then increased to an average level of 46.5 ± 1.9 mg/L in Phase 5 (Figure 3-4(a1)). After stabilization, the effluent NH_4^+-N and TN concentration were less than 0.05 and 10 mg/L, respectively, in each phase (Table 3-2). As shown in Figure 3-4(a2), shorter HRT (higher TN loading) yielded higher TN removal rate and lower removal efficiency (Phase 1 vs Phase 2 (N/P = 9.7:1) and Phase 3 vs Phase 4 (N/P = 3.9:1)). It is consistent with the results reported in previous studies (Gao et al., 2018; Honda et al., 2017; Luo et al., 2018). Under the same TN loading, both the TN removal rate and removal efficiency were comparable between Phases 2 and 3 ($p > 0.05$), but significantly different between Phases 1 and 4 ($p < 0.05$) (Figure 3-4(a2)). It suggests that the impacts of N/P ratio on the removal rate and removal efficiency remarkably depended on the degree of P deficiency. The inhibitory effect from P deficiency for nitrogen removal would be more severely under lower loading because the increased loading can offset the inhibitory effect of the imbalanced N/P ratio (Phase 1 vs Phase 2). In this study, the highest TN removal efficiency of over

99% was achieved in Phase 4. A further increase of TN loading at Phase 5 did not improve the TN removal (Figure 3-4(a2)), implied that nitrogen was not a limiting factor in Phase 4.

Figure 3-4(b1-b2) shows the influent TP concentration varied in a low range of 3.49-4.15 mg/L (average 3.8 ± 0.2 mg/L) at the first two phases and a high range of 8.92-10.73 mg/L (average 9.5 ± 0.5 mg/L) over the next three phases. The effluent TP concentration in the stabilized stage almost reached zero at Phases 1 and 2, corresponding to the removal efficiency of above 99%. After increased the influent TP concentration to 9.5 ± 0.5 mg/L, an effluent TP concentration of 5.18 ± 0.37, 3.14 ± 0.27, and 3.63 ± 0.46 mg/L was achieved for Phases 3, 4, and 5, respectively. The corresponding removal efficiency was 45.44 ± 3.94%, 66.90 ± 2.82%, and 61.78 ± 4.85% for Phases 3, 4, and 5, respectively. As shown in Figure 3-4(b2), the impact of HRT on TP removal differed between the two N/P ratios. In the case of P deficiency (N/P = 9.7:1), TP removal efficiency always reached the highest level of over 99%, decreased HRT only led to an increased removal rate (Phase 1 vs Phase 2) (Figure 3-4(b2)). In the opposite case (N/P = 3.9:1), TP removal rate kept at the highest level, and the decreased HRT reduced the removal efficiency (Phase 3 vs Phase 4) (Figure 3-4(b2)). Besides, the performance of phosphorus removal worsened after increase the influent TN concentration at Phase 5. The above results suggested that under a specific condition, there was a threshold for phosphorus removal and above which the increase of nutrient loading could no longer enhance the phosphorus removal rate. It is because, above the threshold, other factors (such as lighting, carbon dioxide and SRT) might replace nutrients as the limiting factors (Luo et al., 2018; Zhang et al., 2019).

Figure 3-4(c1-c2) shows the influent COD concentration kept at a constant value of 440.3 ± 11.1 mg/L over the whole study period. The effluent COD concentration maintained constant (14.55 ± 7.69 mg/L) throughout the five phases despite the different HRTs and N/P ratios (Figure 3-4(c1)). Correspondingly, a constant COD removal efficiency of 96.55 ± 1.65%, was achieved. The high removal efficiency indicated that almost all the COD in the feed were effectively removed regardless of HRT and N/P ratio. It is reasonable because the applied organic loading rate (146.06-218.87 mg/L/d) (Figure 3-4(c2)) was far lower than that in typical MBR systems (Lin et al., 2013; Ozgun et al., 2013). The effluent in some phases completely meets the EU discharge requirements (Phases 1 and 2) (Table 3-2). Therefore, it can be speculated that the MB-MPBR has a promising potential to achieve superior effluent quality meeting the discharge standard in a single system under optimized operating conditions.

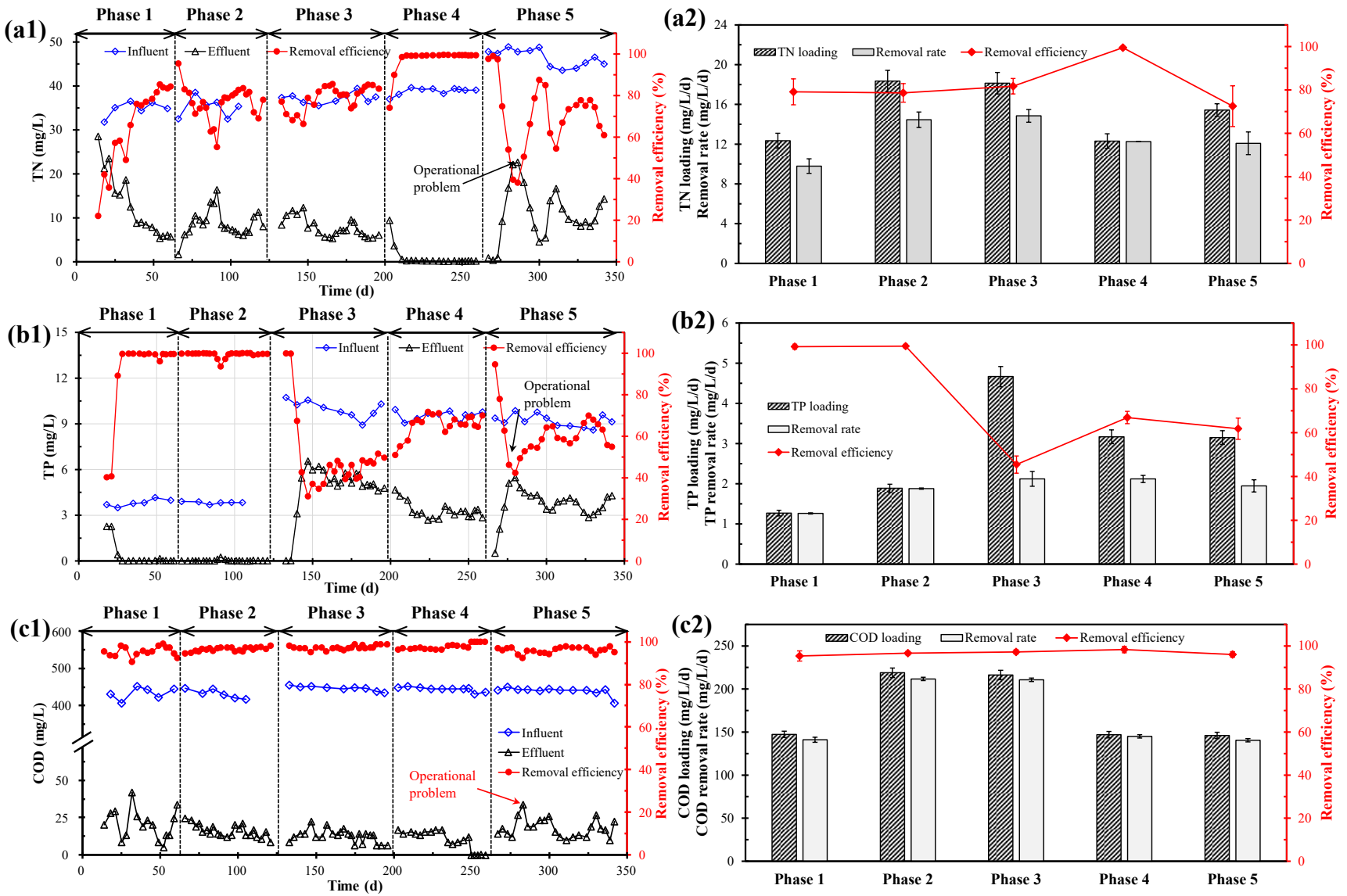

Figure 3-4 Effects of HRT and N/P ratio on the biological performance of the MB-MPBR: (a) TN; (b) TP, and (c) COD.

Table 3-2 Comparison of COD and nutrients removal in different types of membrane-related bioreactors.

	HRT (h)	SRT (d)	Effluent COD (mg/L)	Effluent NH_4-N (mg/L)	Effluent TN		Effluent TP		References
					Concentration (mg/L)	Removal efficiency (%)	Concentration (mg/L)	Removal efficiency (%)	
Discharge standards of EU	N/A[6]	N/A	125	< 1	10-15	N/A	1-2	N/A	(Kraume et al., 2005)
MB-MPBR[1]	72	20	15.45 ± 9.44	< 0.05	0.19-10.06	72.5-99.5	0.03-3.63	61.8-99.2	This study[7]
MB-MPBR	48	20	13.32 ± 4.09	< 0.05	6.69-7.82	78.6-81.7	0.02-5.18	45.4-99.5	This study
MB-MPBR	8	15	18.3 ± 1.9	1.7 ± 0.3	27.9 ± 0.9	30.2	3.1 ± 0.7	23.7	(Sun et al., 2018a)
MPBR[2]	48	21.1	N/A	N/A	1.76-3.82	81.4	0.01-0.14	90.8	(Gao et al., 2018)
MPBR	24	18	3.06	N/A	9.02	36	1.73	31	(Luo et al., 2018)
MABR[3]	12	N/A	< 50	< 3	< 40	~ 55	< 4.5	> 59	(Sun et al., 2015)
MABR	24	N/A	< 100	~ 15	< 20	~ 88.7	N/A	N/A	(Lin et al., 2015)
Post-denitrification + MBR[4]	38	20	20.1 ± 14.8	N/A	24.6 ± 3.6	72.9 ± 6.1	N/A	N/A	(Gómez-Silván et al., 2013)
A_1-A_2-O-A_2-MBR[5]	33-38	27-37	3-36	0.17-8.27	3.02-13.10	N/A	0.03-0.67	N/A	(Shen et al., 2012)

[1] MB-MPBR: microalgal-bacterial membrane photobioreactor

[2] MPBR: membrane photobioreactor

[3] MABR: membrane aerated biofilm reactor

[4] MBR: membrane bioreactor

[5] A_1: anaerobic, A_2: anoxic, O: oxic (aerobic)

[6] N/A: not available

[7] Presented values are the average of the stabilized stage after day 20 for each phase

Table 3-3 Elemental compositions of C, H, N and S for inoculated sludge and microalgal-bacterial flocs.

	Sludge seed	Microalgal-bacterial flocs				
		Phase 1	Phase 2	Phase 3	Phase 4	Phase 5
C (%)	47.12 ± 0.20	47.00 ± 0.44	49.18 ± 0.51	50.20 ± 1.08	49.89 ± 0.96	50.32 ± 0.49
H (%)	6.26 ± 0.07	7.20 ± 0.23	7.87 ± 0.14	8.24 ± 0.31	8.05 ± 0.47	8.21 ± 0.19
S (%)	1.02 ± 0.07	0.95 ± 0.18	1.47 ± 0.12	1.00 ± 0.03	1.01 ± 0.05	0.84 ± 0.04
N (%)	4.47 ± 0.04	7.05 ± 0.70	7.42 ± 0.23	8.77 ± 0.11	9.00 ± 0.13	8.78 ± 0.41

Note: Sample number n = 3 and 4 for sludge and microalgal-bacterial flocs, respectively. The sludge seed was from an activated sludge plant treating pulp and paper wastewater from a local pulp and paper mill. The data are expressed as mean ± standard deviation.

3.3.3 Particle size distribution and microscopic morphology of biological flocs

Figure 3-5(a) shows the particle size of the two inoculums had a similar unimodal shape but distributed in different range. In comparison, the microalgal-sludge flocs had a broader size distribution ranging from 1 μm to 1000 μm and the profiles varied from phase to phase (Figure 3-5(b)). As shown in Figure 3-5(b), only the flocs from Phase 1 distributed in perfect unimodal shape and the sharp primary peak located at the range of 30-200 μm. Phase 2 had two weak secondary peaks with a size range of 1-20 μm and 300-1000 μm as compared with Phase 1. The other three phases exhibited similar PSD profiles and the position of the sharp primary peak transferred to the range of 2-30 μm.

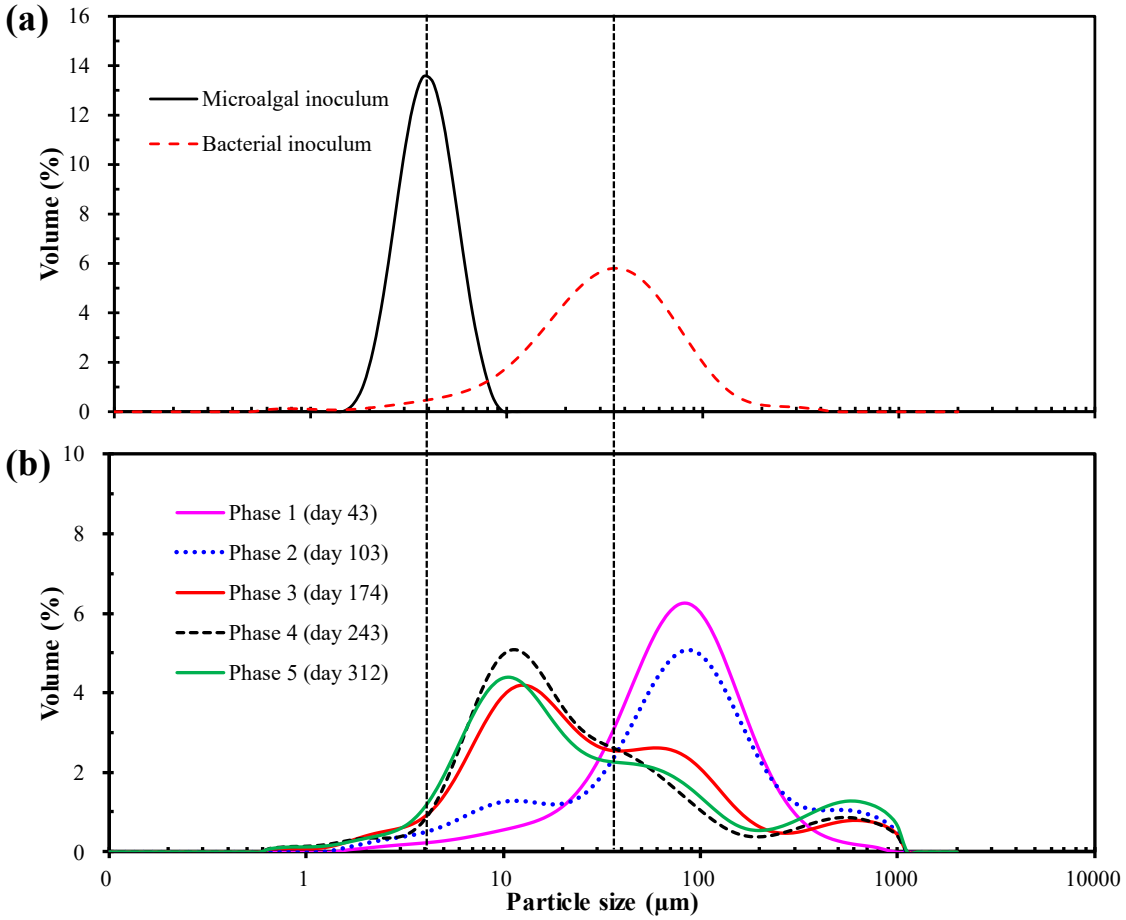

Figure 3-5 Particle size distributions of (a) microalgal and bacterial inoculum and (b) microalgal-bacterial flocs in the MB-MPBR under different HRTs and N/P ratios.

The microscopic observation further proved the variation of the biological particle size (Figure 3-6). Before inoculation, *Chlorella Vulgaris* cells individually existed in the culture (Figure 3-6(a)) and activated sludge contained filamentous bacteria (Figure 3-6(b)). After inoculation, microalgae and bacteria coexisted overall the operational period. In Phase 1, small *Chlorella Vulgaris* cells embedded into bacteria flocs and formed good microalgal-sludge symbiotic with a few filamentous bacteria (Figure 3-6(c)). In Phase 2, filamentous bacteria multiplied, and some *Scenedesmus* cells appeared at the end of this phase (Figure 3-6(d)). In the following three phases, the density of filamentous bacteria sharply decreased, and *Scenedesmus* dominated in the microalgae ecosystem Figure 3-6(e-g).

The results of particle size distribution and microscopic morphology jointly demonstrated that HRT and N/P ratio critically impact the characteristics of microalgal-bacterial interactions. After mixing, the microalgae and bacteria cooperated and compared with each other. These interactions varied with HRT and N/P ratio. From Phase 1 to Phase 2, the sudden increase of organic loading rate (from 147.33 to 218.87 mg/L/d) changed the balance between the microalgal and bacterial populations. The filamentous bacteria made full use of the carbon resources and rapidly multiplied, and the *Scenedesmus* also grasped on the chance and started to compete with the *Chlorella Vulgaris*. These result in the formation of two secondary peaks in Phase 2 (Figure 3-5(b)). In Phase 3, P-supplement further enhanced the competitiveness of *Scenedesmus*. Finally, filamentous bacteria notably decreased, and *Scenedesmus* dominated the system, which led to the increase of more small particles (individual *Scenedesmus* cells) and the shift of primary sharp peak Figure 3-5(b). In the following two phases, reduced organic loading rate limited the growth of filamentous bacteria more severely, and the status of *Scenedesmus* further solidified. The variation of the biological communities revealed that the ecological structure in a microalgal-bacterial MPBR is adjustable. Besides, the evolution of the microalgal communities suggested that *Scenedesmus* had stronger competitiveness than *Chlorella Vulgaris* under phosphorus-rich conditions. It does not agree with the results reported by previous research conducted in batch tubular reactors (with *Scenedesmus* sp. and *Chlorella* sp.) for anaerobic digestion treatment (Marcilhac et al., 2015). This may be due to the different operational mode and *Chlorella* species used in that study.

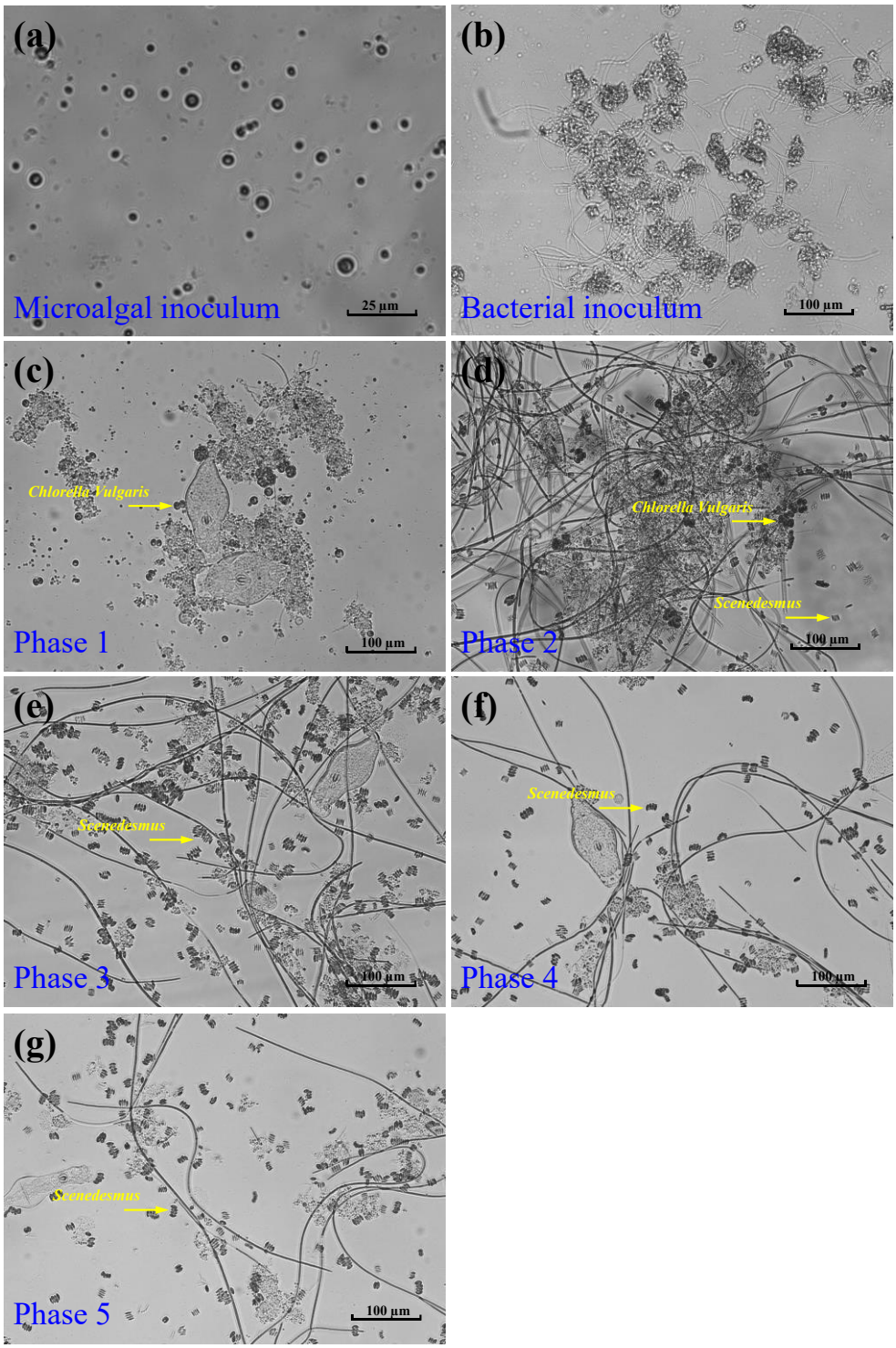

Figure 3-6 Microscope images showing micromorphology of (a) microalgae inoculum, (b) bacterial inoculum, and microbial flocs in the MB-MPBR at (c) Phase 1 (day 52), (d) Phase 2 (day 107), (e) Phase 3 (day 187), (f) Phase 4 (day 249), (g) Phase 5 (day 320).

3.3.4 Evaluation of MB-MPBR for wastewater treatment

This study showed that MB-MPBR is a promising technology for wastewater treatment and can achieve effluent quality meets the EU discharge standards in a single step. In this study, the effluent COD concentration maintained at 14.55 ± 7.69 mg/L regardless of the variation of HRT and N/P ratio. The effluent NH_4^+-N and TN concentration were less than 0.05 and 10 mg/L, respectively overall the experimental period, while the highest TN removal efficiency of > 99% was obtained at Phase 4. The effluent TP concentration reached almost zero (corresponding to the removal efficiency of > 99%) in Phases 1 and 2. Overall, complete removal of TN and TP was not achieved at the same phase in this study. Nevertheless, the effluent quality of Phases 1 and 2 meets the requirements of the EU discharge standards for COD (125 mg/L), NH_4^+-N (< 1 mg/L), TN (10-15 mg/L) and TP (1-2 mg/L) (Table 3-2). It suggested that HRT and N/P ratio had significant impacts on the biological performance of MB-MPBR, which was attributed to the different nutrient loading rates resulted from the various combinations of HRT and N/P ratio. As for MB-MPBR, there exists a nutrient removal threshold above which a further increase of nutrient loading cannot further improve the biomass production and nutrients uptake but will dramatically reduce the removal efficiency. Therefore, optimizing the N/P ratio and HRT to control the nutrient loading is the key to achieve complete nitrogen and phosphorus removal in MB-MPBR.

Regarding the simultaneous removal of COD and nutrients (N and P) in a single system, MB-MPBR is competitive to other membrane-related processes (Table 3-2). In typical membrane photobioreactor (MPBR), the microalgae can only use nutrients (N and P) for their growth, and thus MPBR mainly used to treat secondary sewage in which organic matters have been mostly removed (Zhang et al., 2019). As for membrane aerated biofilm reactor (MABR) and other integrated MBR processes, although the removal efficiency of nitrogen was significantly enhanced, phosphorus removal was generally still low. In comparison, MB-MPBR is more competitive because it can simultaneously remove COD and nutrients (N and P) in a single step. Table 3-3 shows the nitrogen proportion of biomass in Phases 1, 2, 3, 4 and 5 increased by 57.7%, 66.0%, 96.2%, 101.3% and 96.4% respectively compared to the inoculated pure sludge. As the nutrients

in this study mainly removed by microalgal assimilation, the higher nitrogen proportion in microalgal-bacterial consortium demonstrated the better nitrogen assimilation ability of the microalgae than that of the activated sludge. Furthermore, lower nitrogen proportion was observed in the first two phases (Table 3-3), which can be ascribed to the P deficiency resulted from the inappropriate N/P ratio. Therefore, an appropriate N/P ratio is critical to the excellent removal of nutrients in MB-MPBR.

As displayed in Table 3-2, the HRT value in MB-MPBR is longer than that in other membrane-related systems, which is a distinctive drawback for this technology. Undeniably, as a new technology, MB-MPBR is still in its very early stage of research and development and should overcome lots of challenges before realizing engineering applications. However, MB-MPBR takes considerable advantage of simultaneous removal of carbon, nitrogen and phosphorus from wastewater and meeting discharge standards in a single system. Moreover, by optimizing other factors (such as light penetration and CO_2 supply), the HRT can also be shortened. Therefore, MB-MPBR is promising for wastewater treatment and requires more research to improve processing performance. Further studies can focus on the optimization of process conditions and wastewater characteristics to reduce the HRT to the comparable level of HRT of other technologies for municipal wastewater treatment.

3.4 Conclusions

This study showed that HRT and N/P ratio significantly affected the biological performance of MB-MPBR. The underlying reason was the different nutrient loading rate resulted from the various combinations of HRT and N/P ratio. A lower N/P ratio (3.9:1) and HRT (2 d) promoted the biomass yield. A COD and ammonia-N removal efficiency of over 96% and 99% respectively was achieved under all tested conditions, regardless of N/P ratio and HRT. The TN and TP removal varied under different conditions, but a low level of TN (< 10 mg/L) and TP (< 1 mg/L) was achieved under the appropriate conditions and met the discharge standards of effluent in a single stage. Overall, MB-MPBR is a promising technology to achieve a high-quality effluent meets discharge standards in a single system. Further studies should focus on the optimization of process

conditions, such as reducing HRT, to make it more competitive as compared to current technologies in the commercial market.

3.5 References

Alcántara, C., Domínguez, J. M., García, D., Blanco, S., Pérez, R., García-Encina, P. A., Muñoz, R., 2015. Evaluation of wastewater treatment in a novel anoxic–aerobic algal–bacterial photobioreactor with biomass recycling through carbon and nitrogen mass balances. *Bioresource Technology*. 191, 173-186.

APHA. 2005. *Standard Methods for the Examination of Water and Wastewater*. *twentieth ed*. American Public Health Association, American Water Works Association, Water Environmental Federation, Washington, USA.

Beuckels, A., Smolders, E., Muylaert, K., 2015. Nitrogen availability influences phosphorus removal in microalgae-based wastewater treatment. *Water Research*. 77, 98-106.

Choi, H. J., Lee, S. M., 2015. Effect of the N/P ratio on biomass productivity and nutrient removal from municipal wastewater. *Bioprocess and Biosystems Engineering*. 38(4), 761-766.

Cicek, N., 2003. A review of membrane bioreactors and their potential application in the treatment of agricultural wastewater. *Canadian Biosystems Engineering*. 45(6), 37-49.

de Godos, I., Guzman, H. O., Soto, R., García-Encina, P. A., Becares, E., Muñoz, R., Vargas, V. A., 2011. Coagulation/flocculation-based removal of algal–bacterial biomass from piggery wastewater treatment. *Bioresource Technology*. 102(2), 923-927.

Gómez-Silván, C., Arévalo, J., Pérez, J., González-López, J., Rodelas, B., 2013. Linking hydrolytic activities to variables influencing a submerged membrane bioreactor (MBR) treating urban wastewater under real operating conditions. *Water Research*. 47(1), 66-78.

Gander, M., Jefferson, B., Judd, S., 2000. Aerobic MBRs for domestic wastewater treatment: a review with cost considerations. *Separation and Purification Technology*. 18(2), 119-130.

Gao, F., Li, C., Yang, Z.-H., Zeng, G.-M., Feng, L.-J., Liu, J.-z., Liu, M., Cai, H.-w., 2016a. Continuous microalgae cultivation in aquaculture wastewater by a membrane photobioreactor for biomass production and nutrients removal. *Ecological Engineering*. 92, 55-61.

Gao, F., Li, C., Yang, Z.-H., Zeng, G.-M., Mu, J., Liu, M., Cui, W., 2016b. Removal of nutrients, organic matter, and metal from domestic secondary effluent through microalgae cultivation in a membrane photobioreactor. *Journal of Chemical Technology and Biotechnology*. 91(10), 2717-2719.

Gao, F., Peng, Y.-Y., Li, C., Cui, W., Yang, Z.-H., Zeng, G.-M., 2018. Coupled nutrient removal from secondary effluent and algal biomass production in membrane photobioreactor (MPBR): Effect of HRT and long-term operation. *Chemical Engineering Journal*. 335, 169-175.

Honda, R., Boonnorat, J., Chiemchaisri, C., Chiemchaisri, W., Yamamoto, K., 2012. Carbon dioxide capture and nutrients removal utilizing treated sewage by concentrated microalgae cultivation in a membrane photobioreactor. *Bioresource Technology*. 125, 59-64.

Honda, R., Teraoka, Y., Noguchi, M., Yang, S., 2017. Optimization of Hydraulic Retention Time and Biomass Concentration in Microalgae Biomass Production from Treated Sewage with a Membrane Photobioreactor. *Journal of Water and Environment Technology*. 15(1), 1-11.

Karya, N. G. A. I., van der Steen, N. P., Lens, P. N. L., 2013. Photo-oxygenation to support nitrification in an algal–bacterial consortium treating artificial wastewater. *Bioresource Technology*. 134, 244-250.

Kraume, M., Bracklow, U., Vocks, M., Drews, A., 2005. Nutrients removal in MBRs for municipal wastewater treatment. *Water Science and Technology*. 51(6-7), 391-402.

Lee, C. S., Lee, S.-A., Ko, S.-R., Oh, H.-M., Ahn, C.-Y., 2015. Effects of photoperiod on nutrient removal, biomass production, and algal-bacterial population dynamics in lab-scale photobioreactors treating municipal wastewater. *Water Research*. 68, 680-691.

Lee, S.-H., Ahn, C.-Y., Jo, B.-H., Lee, S.-A., Park, J.-Y., An, K.-G., Oh, H.-M., 2013. Increased microalgae growth and nutrient removal using balanced N:P ratio in wastewater. *Journal of microbiology and biotechnology*. 23(1), 92-98.

Lin, H., Gao, W., Meng, F., Liao, B.-Q., Leung, K.-T., Zhao, L., Chen, J., Hong, H., 2012. Membrane bioreactors for industrial wastewater treatment: a critical review. *Critical Reviews in Environmental Science and Technology*. 42(7), 677-740.

Lin, H., Peng, W., Zhang, M., Chen, J., Hong, H., Zhang, Y., 2013. A review on anaerobic membrane bioreactors: Applications, membrane fouling and future perspectives. *Desalination*. 314, 169-188.

Lin, J., Zhang, P., Yin, J., Zhao, X., Li, J., 2015. Nitrogen removal performances of a polyvinylidene fluoride membrane-aerated biofilm reactor. *International Biodeterioration & Biodegradation*. 102, 49-55.

Luo, Y., Le-Clech, P., Henderson, R. K., 2018. Assessment of membrane photobioreactor (MPBR) performance parameters and operating conditions. *Water Research*. 138, 169-180.

Luo, Y., Le-Clech, P., Henderson, R. K., 2017. Simultaneous microalgae cultivation and wastewater treatment in submerged membrane photobioreactors: A review. *Algal Research*. 24, 425-437.

Marbelia, L., Bilad, M. R., Passaris, I., Discart, V., Vandamme, D., Beuckels, A., Muylaert, K., Vankelecom, I. F. J., 2014. Membrane photobioreactors for integrated microalgae cultivation and nutrient remediation of membrane bioreactors effluent. *Bioresource Technology*. 163, 228-235.

Marcilhac, C., Sialve, B., Pourcher, A.-M., Ziebal, C., Bernet, N., Béline, F., 2015. Control of nitrogen behaviour by phosphate concentration during microalgal-bacterial cultivation using digestate. *Bioresource Technology*. 175, 224-230.

Muñoz, R., Jacinto, M., Guieysse, B., Mattiasson, B., 2005. Combined carbon and nitrogen removal from acetonitrile using algal–bacterial bioreactors. *Applied Microbiology and Biotechnology*. 67(5), 699-707.

Nautiyal, P., Subramanian, K. A., Dastidar, M. G., 2014. Production and characterization of biodiesel from algae. *Fuel Processing Technology*. 120, 79-88.

Oswald, W. J. 1988. Micro-algae and waste-water treatment. in: *Micro-algal Biotechnology*, (Eds.) Borowitska, M. A., Borowitzka, L. J., Cambridge, pp. 305-328.

Ozgun, H., Dereli, R. K., Ersahin, M. E., Kinaci, C., Spanjers, H., van Lier, J. B., 2013. A review of anaerobic membrane bioreactors for municipal wastewater treatment: Integration options,

limitations and expectations. *Separation and Purification Technology*. 118(0), 89-104.

Posadas, E., García-Encina, P.-A., Soltau, A., Domínguez, A., Díaz, I., Muñoz, R., 2013. Carbon and nutrient removal from centrates and domestic wastewater using algal–bacterial biofilm bioreactors. *Bioresource Technology*. 139, 50-58.

Shen, Y.-x., Xiao, K., Liang, P., Sun, J.-y., Sai, S.-j., Huang, X., 2012. Characterization of soluble microbial products in 10 large-scale membrane bioreactors for municipal wastewater treatment in China. *Journal of Membrane Science*. 415-416, 336-345.

State Environmental Protection Administration of China, 2002. Monitoring and analysis methods of water and wastewater (4th edition). China Environmental Science Press, Beijing.

Sun, L., Tian, Y., Zhang, J., Cui, H., Zuo, W., Li, J., 2018a. A novel symbiotic system combining algae and sludge membrane bioreactor technology for wastewater treatment and membrane fouling mitigation: Performance and mechanism. *Chemical Engineering Journal*. 344, 246-253.

Sun, L., Tian, Y., Zhang, J., Li, H., Tang, C., Li, J., 2018b. Wastewater treatment and membrane fouling with algal-activated sludge culture in a novel membrane bioreactor: Influence of inoculation ratios. *Chemical Engineering Journal*. 343, 455-459.

Sun, L., Tian, Y., Zhang, J., Li, L., Zhang, J., Li, J., 2018c. A novel membrane bioreactor inoculated with symbiotic sludge bacteria and algae: Performance and microbial community analysis. *Bioresource Technology*. 251, 311-319.

Sun, L., Wang, Z., Wei, X., Li, P., Zhang, H., Li, M., Li, B., Wang, S., 2015. Enhanced biological nitrogen and phosphorus removal using sequencing batch membrane-aerated biofilm reactor. *Chemical Engineering Science*. 135, 559-565.

Xu, M., Li, P., Tang, T., Hu, Z., 2015. Roles of SRT and HRT of an algal membrane bioreactor system with a tanks-in-series configuration for secondary wastewater effluent polishing. *Ecological Engineering*. 85, 257-264.

Zhang, M., Yao, L., Maleki, E., Liao, B.-Q., Lin, H., 2019. Membrane technologies for microalgal cultivation and dewatering: Recent progress and challenges. *Algal Research*. 44, 101686.

Chapter 4 Influences of N/P Ratio on the Properties of Microalgal-Bacterial Consortium and Their Role in Membrane Fouling for a Microalgal-Bacterial Membrane Photobioreactor (MB-MPBR)

Abstract: The effect of N/P ratio on the properties of microalgal-bacterial consortium and their role in membrane fouling was evaluated for the first time in a novel microalgal-bacterial membrane photobioreactor (MB-MPBR). Membrane performance was worsened with a decrease of N/P ratio from 9.7:1 to 3.9:1. X-ray photoelectron spectroscopy (XPS) showed a significantly lower total C and higher total N at N/P ratio of 3.9:1 than that of 9.7:1. Particle size distribution (PSD) analysis and microscope observation showed that the microalgal-bacterial suspension at N/P ratio of 3.9:1 had a smaller particle size and more free microalgae. No significant differences in the total SMPs was observed between the two N/P ratios, and a significant difference for EPSs was only found under P-limitation conditions. In addition, the different fouling performance under the N/P ratios of 3.9:1 and 4.9:1 was attributed to the significant difference in SMP content. The dominant fouling mechanism was cake layer formation. The above results suggested that the particle size, micromorphology, and surface composition of the microalgal-bacterial consortium played the primary role in controlling membrane fouling and cake layer formation. It was mainly controlled by the growth balance of microalgae and bacteria. Accordingly, optimizing the operating conditions to balance the microalgae and bacteria growth at an appropriate ratio is the key for membrane fouling control in MB-MPBR.

Keywords: Microalgal-bacterial membrane photobioreactor; Characterization; Membrane fouling; N/P ratio

4.1 Introduction

By exerting the function of microalgae and bacteria, the microalgal-bacterial consortium has a distinctive advantage of simultaneously removing organics and nutrients. Its application for wastewater treatment has been well concerned in recent decades (Alcántara et al., 2015; Gutzeit et al., 2005; Lee et al., 2015; Posadas et al., 2013; Tang et al., 2010). However, conventional microalgal-bacterial reactors face the problems of low efficiencies and washout of free microalgae (Marbelia et al., 2014; Zhang et al., 2019). Integration of membrane separation with the microalgal-bacterial process can effectively solve the problem of washout. Moreover, compared to the typical MBR process, MB-MPBR offers several advantages of improved nutrient removal efficiency, lower aeration energy consumption, and reduced membrane fouling (Liu et al., 2017; Sun et al., 2018a; Sun et al., 2018c). Nevertheless, membrane fouling is inevitable in any membrane-related process, which would impede the further development and widespread application of MB-MPBR.

The formation of membrane fouling is complicated, resulting from the undesirable accumulation of various foulants on the membrane surface (Aslam et al., 2017; Chen et al., 2020; Wang et al., 2014). Like traditional MBR, due to the heterogeneous nature of the suspended mixture, membrane fouling in MB-MPBR is inevitable and affected by numerous factors (Erkan et al., 2016; Li et al., 2019; Zhang et al., 2015). In general, all the influencing factors can be allocated into four groups, including membrane properties, feed characteristics, operation conditions and biomass characteristics (Meng et al., 2009). Among the four groups of factors, biomass characteristics are the critical influencing factors since the sludge mixture directly interacts with the membrane surface. Other factors, such as organic strength, SRT, and aeration would indirectly impact membrane fouling by changing the biomass characteristics (Huang et al., 2011; Xue et al., 2015). N/P ratio is one of the most critical factors. It is because the N/P ratio can influence the balance of microalgae and bacteria and the physiological properties of microalgal-bacterial consortium in MB-MPBR. The N/P ratio may also control the amount of SMPs and EPSs that can affect fouling performance (Kim et al., 2014; Kim & Dempsey, 2013; Lin et al., 2014; Teng et al., 2019). Furthermore, the effects of N/P ratio on fouling performance may change under different HRT due to the different loading rate.

Considerable studies have demonstrated the effect of N/P ratios on microalgae or bacteria in

pure microalgal or bacterial systems for wastewater treatment. In conventional bacterial wastewater treatment processes, it was reported that N/P ratios influenced not only nutrient removal efficiency but also sludge properties (Dilek Sanin et al., 2006; Durmaz & Sanin, 2003; Fu et al., 2009; Meng et al., 2008). Similarly, in traditional microalgal photobioreactors, N/P ratio is a critical factor controlling microalgal growth, nutrient removal efficiency as well as lipid productivity (Choi & Lee, 2015; Lee et al., 2013). Besides, N/P ratio controlled the membrane fouling in an MBR system by changing the EPS and SMP composition in the sludge (Hao et al., 2016). As mentioned above, current studies have mainly paid attention to the effects of N/P ratio in pure microalgal or bacterial systems. The concept of MB-MPBR has just received attention in recent years (Sun et al., 2018a; Sun et al., 2018b; Sun et al., 2018c; Yang et al., 2018), but no in-depth study of membrane fouling in MB-MPBR has been conducted. To our knowledge, none of studies has investigated the impact of N/P ratio on membrane fouling in MB-MPBR. On the other hand, N/P ratio is critically important to the balance of microalgae and bacteria as well as the consortium properties. As overgrowth of microalgae in MB-MPBR would lead to severe membrane fouling (Sun et al., 2018b), optimizing the N/P ratio is significantly essential to exert the advantages of MB-MPBR fully.

Therefore, the main purpose of this study was to comprehensively compare the physic-chemical properties of microalgal-bacterial consortium and its membrane fouling propensity under different operating conditions (HRTs and N/P ratios). Long-term operation of an MB-MPBR over 350 days was conducted to treat synthetic municipal wastewater and divided into five phases according to the variation of N/P ratios and HRTs. The treatment performance of the MB-MPBR, including biomass production, biomass productivity, COD removal, and nutrient (N and P) removal, were compared and reported in Chapter 3. Experimental characterizations, including TMP, filtration resistance composition, SMP, EPS, XPS, FTIR, PSD, and microscopic observation, were determined. This study strengthened our fundamental knowledge of membrane fouling in an MB-MPBR and can guide the design, operation, development, and application of MB-MPBR for wastewater treatment.

4.2 Material and methods

4.2.1 MB-MPBR set-up and operation

A lab-scale submerged microalgal-bacterial membrane photobioreactor (MB-MPBR) was

operated to treat synthetic municipal wastewater in this study. The schematic of the set-up is shown in Figure 3-1. The basic parameters regarding the membrane module (purchased from SINAP Co. Ltd., Shanghai, China) and operating conditions are listed in Table 4-1. The pre-cultivated *Chlorella vulgaris* and activated sludge were inoculated at a ratio of 1:5 (0.6 and 3.0 g/L for microalgae and activated sludge respectively). The activated sludge seed was collected from an activated sludge plant at a local pulp and paper mill. The reactor was operated for almost 350 days and divided into five phases by varying the HRT and N/P ratio of the system. Detailed information about the operating process and feed composition can refer to Chapter 3. Within each phase, physical cleaning was conducted to remove the foulant layer to recover the membrane permeability when the transmembrane pressure (TMP) reached 30 kPa. At the end of each phase, the permeability of the used membrane after physical cleaning and chemical cleaning was measured to determine the composition of each filtration resistance. Moreover, new pieces of membrane were used to replace the used membrane for a new phase.

Table 4-1 Specifications of the membrane module and operational parameters of the lab-scale MB-MPBR system in this study.

	Value
Module specification	
Total membrane surface area	0.03 m^2
Membrane materials	Polyvinylidene fluoride (PVDF)
Membrane type	Flat sheet
Mean membrane pore size	0.1 μm
Operational parameter	
Working volume	10.34 L
Temperature	26.9 ± 0.9 ℃
pH	7.3 ± 0.6
Aeration rate	3.75 ± 0.42 L/min
Illumination intensity	8400 lux

4.2.2 Evaluation of membrane filtration resistance

Darcy's law was applied to calculate the filtration resistance using the following formula (Lin et al., 2009):

$$R = \frac{\Delta P}{J\mu} \tag{4-1}$$

$$R_t = R_m + R_p + R_c \tag{4-2}$$

where, R is the filtration resistance; R_t, R_m, R_p, and R_c represents the total filtration resistance, virgin membrane filtration resistance, pore-clogging filtration resistance, and cake layer filtration resistance, respectively; ΔP is the trans-membrane pressure difference; J signifies the permeate flux; μ is the permeate dynamic viscosity.

The value of each resistance was determined according to the procedure as follows: R_t was calculated from the data at the end of the operation. R_m was measured by the permeability test of the virgin membrane with tap water. The total resistance of R_m and R_p can be obtained by measuring the permeability of the fouled membrane after physical cleaning, then the value of R_p and R_c can be successively calculated.

4.2.3 Analytical methods for microalgal-bacterial consortium characterization

4.2.3.1 SMP and EPS extraction and measurement

SMP was harvested by centrifuging microalgal-bacterial mixture at 4,000 × g for 10 min, following the filtration of the supernatant through 0.45 μm filter paper.

EPS was extracted using the cation exchange resin (CER) (Dowex™ Marathon™ C, Na^+ form, Sigma-Aldrich, Bellefonte, PA) method (Frølund et al., 1996). The microalgal-bacterial suspension containing 0.25 g biomass was centrifuged (IEC MultiRF, Thermo IEC, USA; Eppendorf Centrifuge 5430, Germany) at 4,000 × g for 10 min and then washed using buffer solution. The pellets were resuspended into the buffer solution after another cnetrifugation at 10,000 × g for 10 min and then transferred into an extraction beaker containing 20 g clean CER (80 g/g MLSS). The beaker was put in an ice-water bath and stirred for 2 h. The supernatant obtained after centrifugation (18,700 × g for 20 min) was regarded as bound EPS (Lin et al., 2009). The composition of the buffer solution includes 2 mM Na_3PO_4, 4 mM NaH_2PO_4, 9 mM NaCl and 1 mM KCl at pH 7.0 (Frølund et al., 1996).

Both the total SMP and bound EPS were normalized as the sum of protein and carbohydrates. The contents of protein and carbohydrates were determined colorimetrically according to Lowry's method and Gaudy's method, respectively (Gaudy, 1962; Lowry et al., 1951).

4.2.3.2 Particle size distribution (PSD) and microscopic observation

The PSD of the mixed liquor was determined by a Malvern Mastersizer 2000 instrument (Worcestershire, UK) 1-2 times per week. Each sample was automatically measured in triplicate.

An inverted optical microscope (Olympus IX51, Japan) was applied for the micromorphology observation of the microalgal-bacterial consortia. For each sample, at least 30 images were randomly taken by a digital camera connected with the microscope.

4.2.3.3 XPS analysis

The elemental composition of C, O, and N on the microalgal-bacterial surface was determined by an XPS spectrometer (AXIS Supra+, Kratos Analytical Ltd., UK) using Al-K X-rays as the excitation source. Prior to the measurement, the microalgal-bacterial suspensions were firstly filtered with 0.45 μm filter paper, then moved into a freezer dryer (Labconco Freezone 12, USA) and kept at -35 ℃ for more than one week. A low-resolution survey spectrum and high-resolution spectra for C, N, and O regions were taken for each sample. Data analysis was conducted with the software (ESCApe) provided with the equipment.

4.2.3.4 FTIR measurement

A Tenthesor 37 FTIR spectrometer (Bruker Optics Inc., Billerica, MA, USA) was applied to measure the functional groups of the microalgal-bacterial samples. Before FTIR analysis, the microalgal-bacterial flocs from each phase were collected and put into crucibles, following by at least 48 h heating in an oven at 105 ℃ to dry the samples. Thereafter, the dried microalgal-bacterial powder would be used for FTIR measurement.

4.2.3.5 Other measurements

A gas chromatography instrument (Shimazu, Mondel GC-2014, Japan) was used to determine the CO_2 concentration in the air around the MB-MPBR. The measurements of MLSS, COD, NH^{4+}-N, TN, and TP followed the methods applied in Chapter 3.

4.2.4 Statistical analysis

Statistical analysis was conducted by using SPSS 17.0 software. The statistically significant difference ($p < 0.05$) was examined by the analysis of variance (ANOVA) for the SMP and EPS concentration between different operating conditions. The difference in surface chemical composition content was analyzed through the student t-test.

4.3 Results and Discussion

4.3.1 Overall performance

Despite the varied N/P ratio and HRT, COD concentration in the effluent maintained at 14.55 ± 7.69 mg/L, corresponding to a constant removal efficiency of 96.55 ± 1.65% (Chapter 3). Unlike COD, the removal efficiency of TN and TP was significantly affected by the variation of N/P ratio and HRT. Throughout the experimental period, the NH_4^+-N and TN concentration in the effluent were less than 0.05 and 10 mg/L, respectively, while > 99% of TN removal efficiency (almost zero TN concentration in effluent) was only obtained in Phase 4 (Chapter 3). The effluent TP concentration collected in Phases 1 and 2 reached almost zero and met the requirement of the discharge standards (Chapter 3). These results showed that MB-MPBR is a promising technology to achieve high-quality effluent in a single system under optimized operational conditions. Apart from biological performance, membrane fouling is equally important for the MB-MPBR system, which is exactly the subject of this study.

4.3.2 Comparison of fouling behavior

Figure 4-1 presents the variations of TMP and flux for the MB-MPBR under different operating conditions. Under the same flux, TMP is proportional to filtration resistance and is a visual indicator directly monitoring the membrane filtration resistance. As illustrated in Figure 4-1, under the same N/P ratio (Phases 1 and 2 (9.7:1), Phases 3 and 4 (3.9:1)), lower HRT of 2 d (Phases 2 and 3) resulted in a more severe membrane fouling (Phase 2 vs Phase 1; Phase 3 vs Phase 4). It is because the higher flux at the short HRT (2 days) led to more foulants transferred to the membrane surface and pores and thus caused more rapid membrane fouling. Also, under the same HRT (Phase 1 and Phase 4 (HRT = 3 days); Phases 2 and 3 (HRT = 2 days)), N/P ratio of 3.9:1 led to a more rapidly membrane fouling as compared to the higher N/P ratio of 9.7:1 (Phase 4 vs Phase 1; Phase 3 vs Phase 2). As compared to Phase 4, an increase in feed TN concentration (corresponding to a higher N/P ratio of 4.9:1) caused a higher membrane fouling rate in Phase 5. The above results suggested that different N/P ratios have great impacts on membrane fouling in the MB-MPBR, which might be ascribed to the variation of biomass properties.

Table 4-2 shows the compositions of the membrane filtration resistances under different operating conditions. As displayed in Table 4-2, cake layer resistance accounted for the highest proportion of the total resistance, indicating that the predominant fouling mechanism was cake

layer formation. It is further verified by the visual observation of the cake layer formed on the surface of membrane at the end of each cycle of filtration operation, as shown in Figure 4-2. In comparison, the membrane surface in Phase 1 was partially covered with cake layer, which was attributed to the large size of the constituting particles and the different scouring force at the different area on the membrane surface. The above phenomenon was considered as the main reason for the lower R_m in Phase 1.

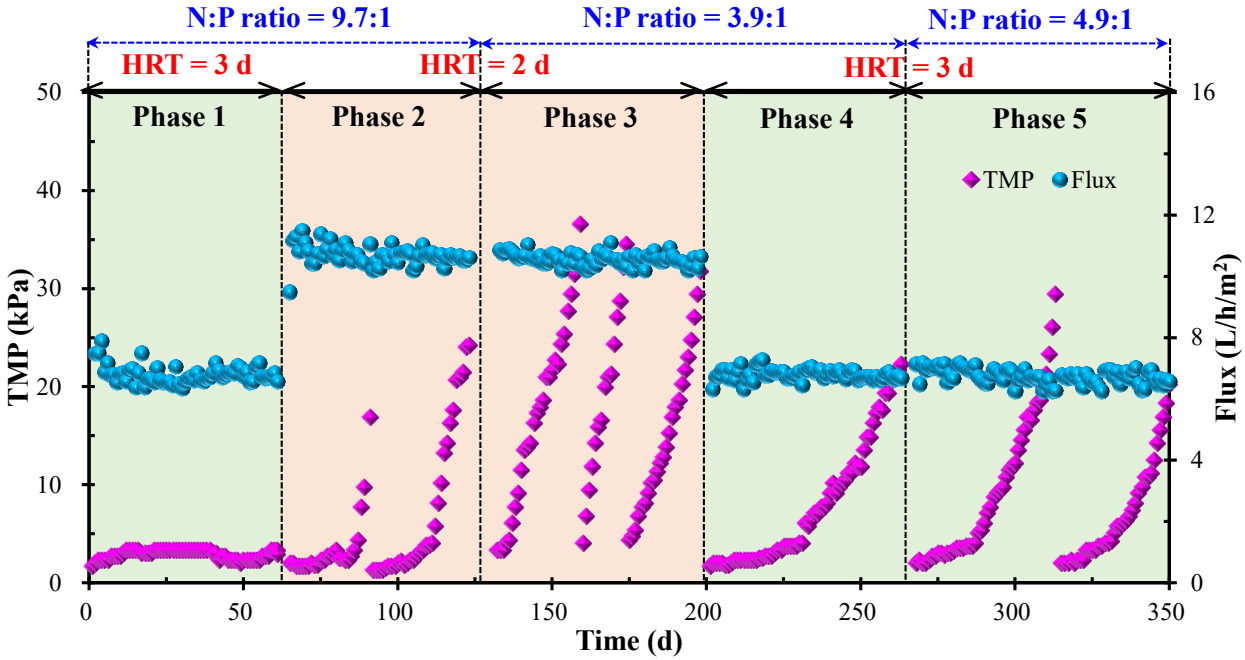

Figure 4-1 Variations of TMP and flux for the MB-MPBR.

Table 4-2 Compositions of membrane filtration resistances under different operating conditions.

	R_m ($\times 10^{12}$ m^{-1})	R_p ($\times 10^{12}$ m^{-1})	R_c ($\times 10^{12}$ m^{-1})	R_t ($\times 10^{12}$ m^{-1})
Phase 1	0.463 (25.13%)[a]	0.392 (21.29%)[a]	0.987 (53.59%)[a]	1.842 (100%)[a]
Phase 2	0.486 (5.95%)[a]	0.025 (0.31%)[a]	7.659 (93.74%)[a]	8.171 (100%)[a]
Phase 3	0.512 (4.53%)[a]	1.274 (11.27%)[a]	9.521 (84.20%)[a]	11.308 (100%)[a]
Phase 4	0.517 (4.32%)[a]	0.035 (0.29%)[a]	11.397 (95.39%)[a]	11.949 (100%)[a]
Phase 5	0.510 (4.75%)[a]	0.045 (0.42%)[a]	10.171 (94.83%)[a]	10.725 (100%)[a]

[a] Percentage of the total resistance R_t shown in parentheses.

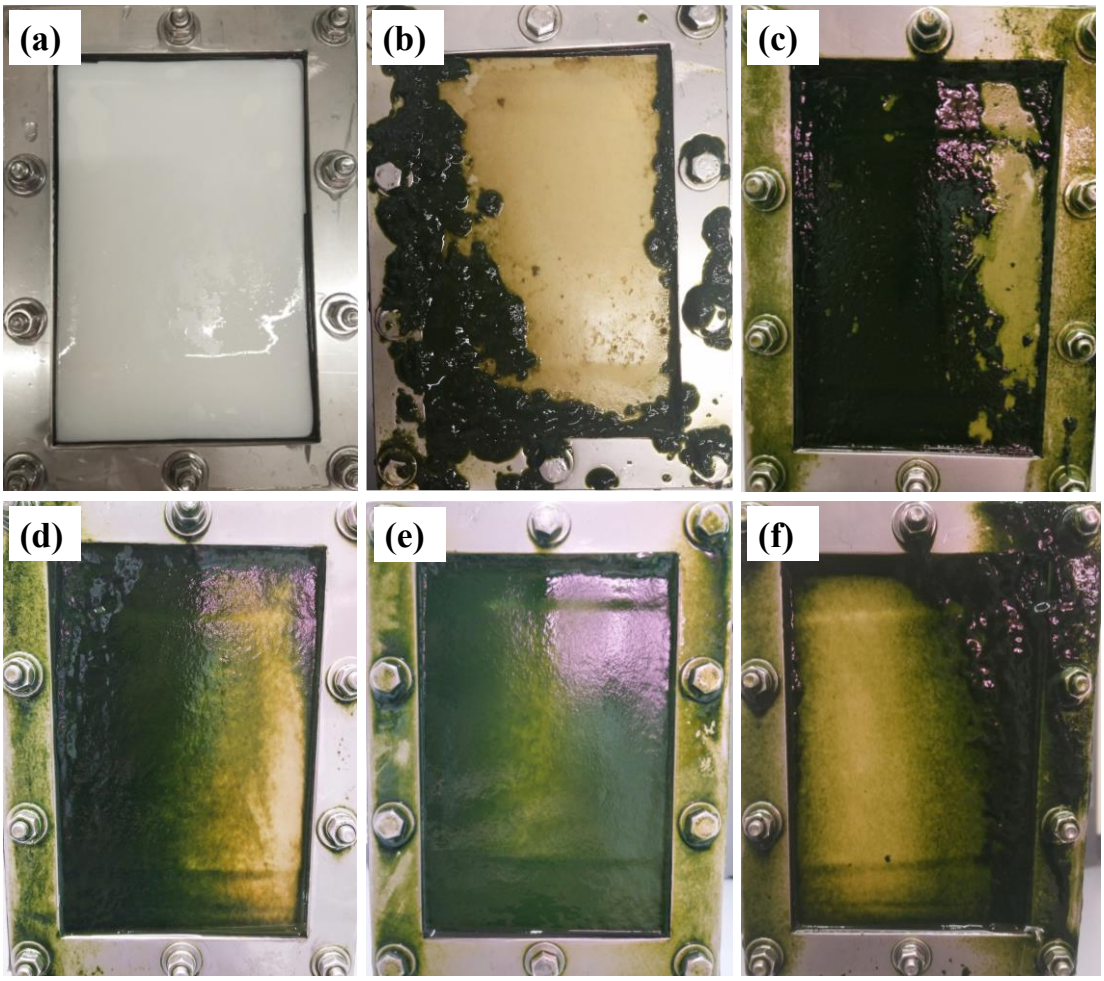

Figure 4-2 Optical images of the (a) virgin membrane and fouled membrane at (b) Phase 1 (HRT = 3 d, N/P ratio = 9.7:1), (c) Phase 2 (HRT = 2 d, N/P ratio = 9.7:1), (d) Phase 3 (HRT = 2 d, N/P ratio = 3.9:1), (e) Phase 4 (HRT = 3 d, N/P ratio = 3.9:1), and (f) Phase 5 (HRT = 3 d, N/P ratio = 4.9:1).

4.3.3 Characterization of the microalgal-bacterial consortium

4.3.3.1 Comparison of SMP

Figure 4-3 presents the comparison of SMP values measured under different operational conditions. According to the principle of single variation, the comparison of the five phases can be allocated into three groups (the same HRT in each comparison) (Phase 2 vs Phase 3, Phase 1 vs Phase 4, and Phase 4 vs Phase 5). Under the same HRT of 2 d and influent TN concentration of 36.9 ± 2.2 mg/L (Phase 2 vs Phase 3), the amount of carbohydrate, protein and total SMP was comparable ($p > 0.05$) between the two different N/P ratios. However, with the fixed influent TN concentration, when HRT increased to 3 d (Phase 1 vs Phase 4), the total SMP and soluble

carbohydrate and protein concentration at N/P ratio of 3.9:1 was significantly lower than that of N/P ratio of 9.7:1 ($p < 0.05$), which was opposite to the trend of TMP variation. As SMP is generally defined as the biopolymers released by the biomass, the high value of SMP in Phase 1 indicated that serious P-limitation (influent P = 3.8 ± 0.2 mg/L; no detectable P in permeate) boosted the decomposition of microalgal-bacterial consortium. The decrease of SMP in Phase 2, on the other hand, showed that an increase in nutrient loading rate via HRT decrease could offset the negative impact of P-limitation. In general, SMP was considered playing a critical role in membrane fouling, and higher content of SMP corresponded to a higher filtration resistance (Lee et al., 2003; Meng et al., 2006b; Teng et al., 2020). However, this is not the case for this study. Based on the above results, therefore, it can be concluded that the difference in SMP concentration was not the cause of the different fouling behavior between Phase 1 and Phase 4 and between Phase 2 and Phase 3 as shown in Figure 4-1. However, for the comparison of Phases 4 and 5 (HRT = 3 d, influent TP = 9.5 ± 0.5 mg/L), both the soluble carbohydrate and total SMP content significantly increased ($p < 0.05$) after the increase of N/P ratio by increasing the influent TN concentration. The same variation trend as TMP revealed that SMP might be one reason for the faster TMP increase in Phase 5. These results suggest that the role of SMP might change and depend on the relative importance of sludge properties, such as particle size, the composition and quantity of bound EPS and SMP, zeta potential and hydrophobicity etc. SMP is responsible for the gel layer formation on membrane surface and/or pores. However, as shown in Figure 4-2, the dominant fouling mechanism was cake layer rather than gel layer formation. This could at least partially be attributed to the low concentration of total SMPs (4-15 mg/L) in the mixed liquor. It was clear that the mass ratio of microalgae to sludge continuously increased from Phase 1 to Phase 5 (Chapter 3). This would lead to the change of mixed liquor properties. The role of other sludge properties would be explored in later sections.

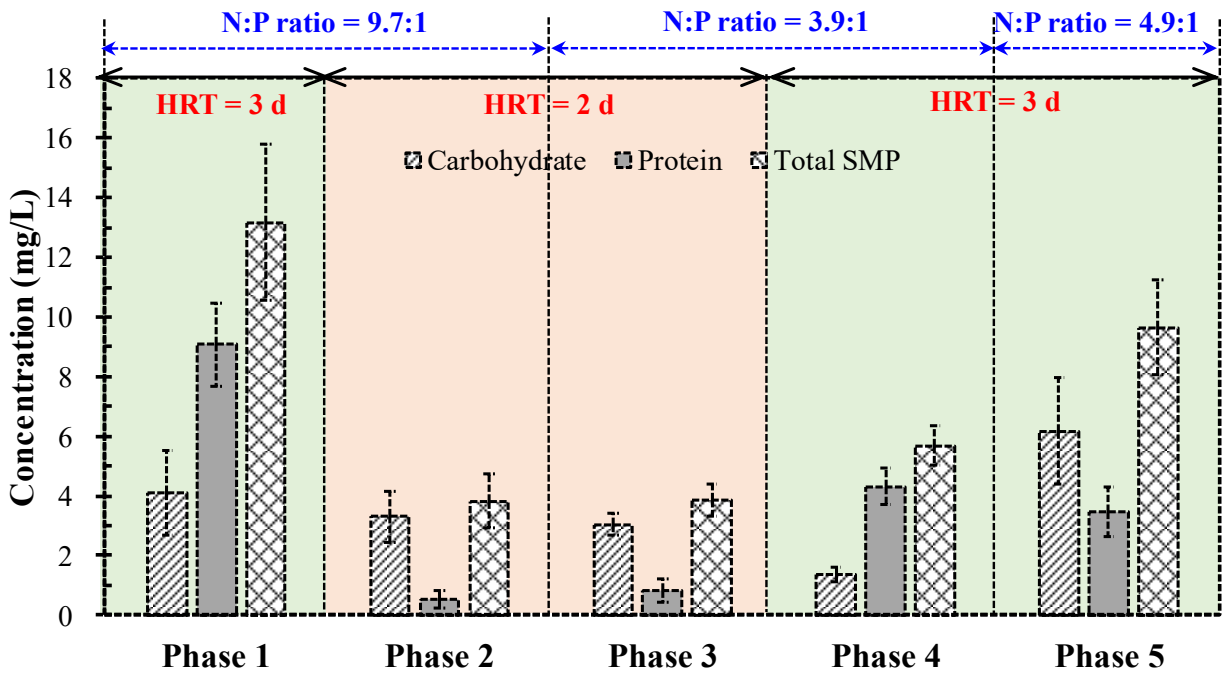

Figure 4-3 Comparison of SMP under different conditions.

4.3.3.2 Comparison of EPS

Figure 4-4 compares the bound EPS values of the microalgal-bacterial consortium under different conditions. The total EPS were 20.79 ± 4.40, 37.08 ± 7.23, 36.01 ± 2.35, 34.26 ± 4.28, and 32.86 ± 5.47 mg/g MLSS for Phases 1, 2, 3, 4, and 5, respectively. ANOVA data showed that the differences in total EPS, carbohydrate and protein between Phases 1 and 4 were statistically significant ($p < 0.05$), while not significant between Phase 2 and Phase 3, and Phase 4 and Phase 5 ($p > 0.05$). As shown in Figure 4-4, the protein contents were much higher than that of carbohydrates, which agrees with the results reported in previous literature (Ding et al., 2015; Lin et al., 2011; Xuan et al., 2010). In general, a higher EPS content corresponds to a higher membrane fouling rate (Lin et al., 2014; Meng & Yang, 2007). In this study, the EPS contents in Phases 2 to 5 were comparable, indicating EPS was not the reason for the different fouling performance of these four phases. However, for the comparison of Phases 1 and 4, the TMP increase rate in Phase 4 was significantly higher than that of Phase 1, which might be due to the much higher EPS content in Phase 4. According to the current investigation, N/P ratio had a notable impact on the concentration of bound EPS under the condition of insufficient nutrient loading, and the more quickly increase in TMP can be partially explained by the higher content of EPS in the biomass. Nevertheless, when the nutrient loading was sufficient, other properties rather than the total EPS

content might be a vital contributor to the difference in TMP variation.

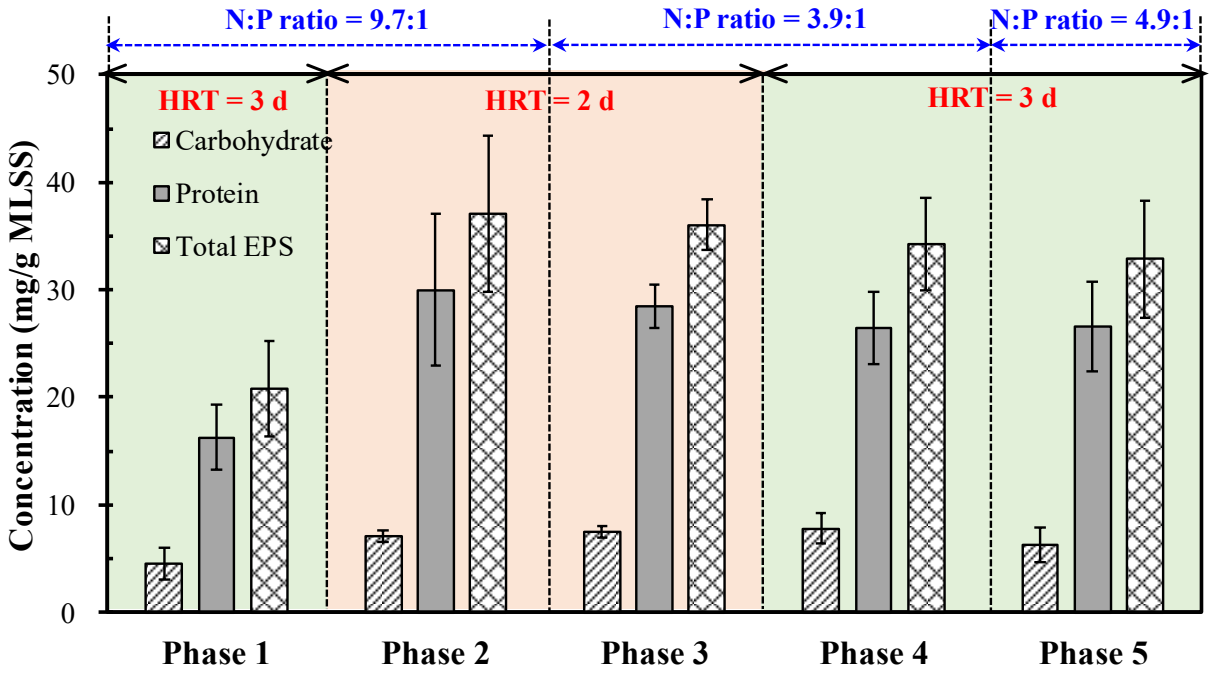

Figure 4-4 Comparison of bound EPS of the microalgal-bacterial consortium under different conditions.

4.3.3.3 XPS analysis

The measurement of the surface chemical composition was conducted through XPS analysis for the microalgal-bacterial consortium under different operating conditions. The whole XPS spectra in the energy range of 0-1200 eV showed that the major elements on the biomass surface were C, O, and N (Figure 4-5(a)). According to Figure 4-5(b-c), the C, O, and N peaks could be resolved into four, three, and two different bonds, respectively. The peaks at the binding energy of 284.8, 286.3, 288.0, and 289.0 eV are ascribed to C-(C, H), C-(O, N), C=O or C-O-C, and O=C-OH bond, respectively (Hao et al., 2016; Lin et al., 2011). The C-(O, N) bond (286.3 eV) may stem from amide, amine, alcohol, and ether, while the sources of C=O or C-O-C bond (288.0 eV) include acetal, hemiacetal, ester, carboxylate, carbonyl, and amide (Hao et al., 2016). The O peaks (O1s, O1sA, and O1sB) were attributed to three bonds (Hao et al., 2016; Lin et al., 2011): C-OH from hydroxide and C-O-C from hemiacetal at a binding energy of 530.7 eV; O=C in aldehyde, ketone, and amide at a binding energy of 531.4 eV; and O-C=O in ester, carboxylate, and acid anhydride at a binding energy of 534.0 eV. The N peaks could be decomposed into two different bonds of N-C and N-H at the binding energy of 400.1 and 402.1 eV, respectively (Hao et al., 2016; Lin et al.,

2011).

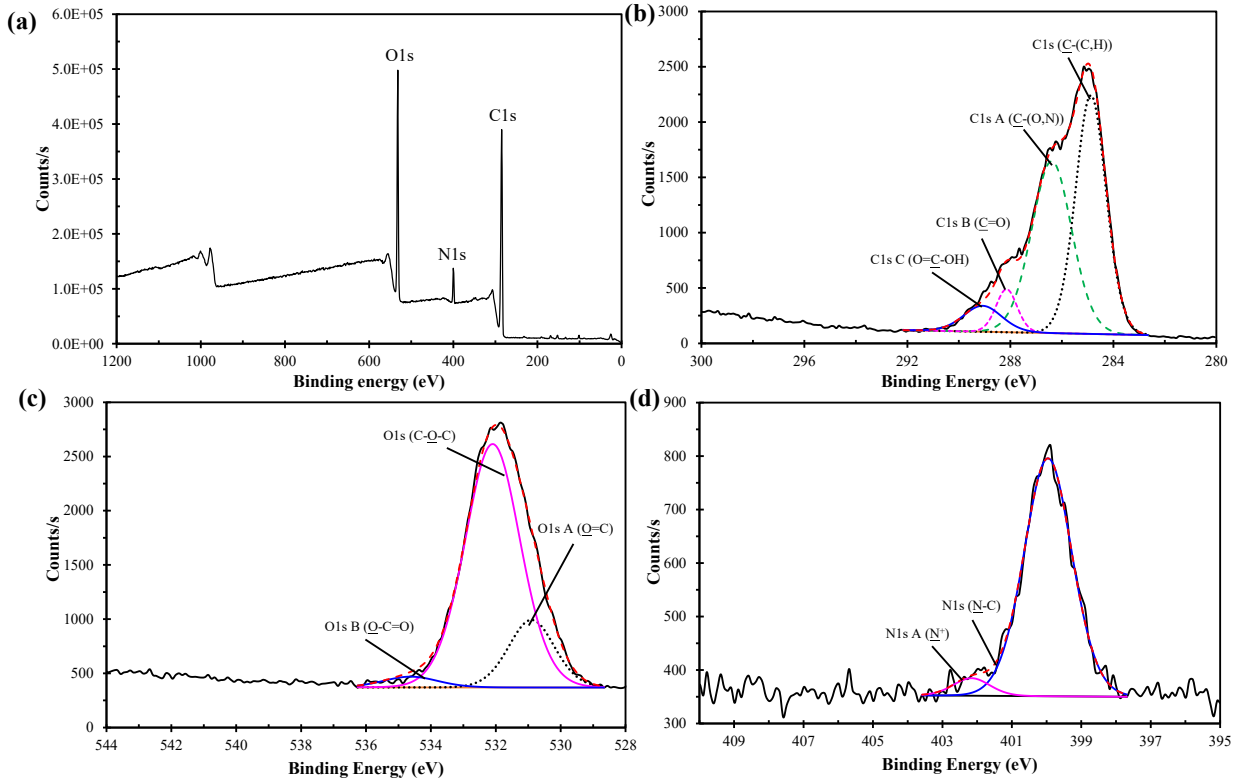

Figure 4-5 XPS spectra of microalgal-bacterial consortium, (a) whole spectra, (b) C1s spectra, (c) O1s spectra, and (d) N1s spectra.

Table 4-3 presents the concentrations of element C, N and O on microalgal-bacterial consortium surface under different operating conditions. The quantity of total C, O, and N was significantly different between the microalgal-bacterial samples of Phases 2 and 3 (Student t-test, $p < 0.05$). A significant difference in the quantity of C and N was found between the microalgal-bacterial samples of Phases 1 and 4 (Student t-test, $p < 0.05$). The quantity of O=C, C-O-C, and O-C=O were significantly different between Phases 1 and 4 (Student t-test, $p < 0.05$) although the total O was not significantly different (Student t-test, $p > 0.05$). Overall, N/P ratio of 3.9:1 resulted in a lower total C and higher total N as compared to that of N/P ratio of 9.7:1, which might be attributed to the increased proportion of microalgae in the consortium. Unlike the above two groups of comparison, no significant difference was observed between the quantity of total C, O, and N in the biomass samples of Phases 4 and 5 (Student t-test, $p > 0.05$). A careful examination of the changes in total C and total N of the surface of sludge indicates that a decrease in total C and an increase in total N of sludge surface composition correlated to an increase in membrane

fouling rate (Phase 1 vs Phase 4; Phase 2 vs Phase 3). This might suggest the importance of surface composition (i. e., bound EPS composition) of sludge in controlling membrane fouling.

4.3.3.4 FTIR analysis

The FTIR spectra of the microalgal-bacterial consortium are displayed in Figure 4-6. The broadband detected in the range of 3600-3200 cm^{-1} represented the symmetric stretching of O-H and N-H (Kumar et al., 2019). The two bands at ~1630 cm^{-1} and ~1530 cm^{-1} were attributed to the C=O stretching and N-H bending of amides I and amides II, respectively, indicating the presence of proteins (Lin et al., 2009). The peak of 1380 cm^{-1} associated with C-O stretching of COO- groups (Dean et al., 2010). The band at ~1224 cm^{-1} corresponded to P=O bonds associated with polysaccharides and nucleic acids (Mayers et al., 2013). The bands at 1030 cm^{-1} illustrated the presence of carbohydrate (C-O) and polysaccharides (Kumar et al., 2019). The peak of 2926 cm^{-1} in the latter three phases was attributed to fatty acid components (Kumar et al., 2019). Fatty acid is a critical component of microalgae, the presence of FTIR peak at 2926 cm^{-1} suggested that a great number of microalgae at Phases 3 to 5. As compared to traditional MBR, the addition of microalgae can alleviate membrane fouling, while a too high proportion of microalgae would, in turn, lead to severer membrane fouling (Sun et al., 2018b). Accordingly, the higher membrane fouling rate under lower N/P ratio of 3.9:1 might be due to the overgrowth of microalgae.

Table 4-3 Surface composition of the microalgae-sludge consortium determined by XPS: average atom fraction (%) excluding hydrogen.

Element component	**Phase 1** HRT = 3 d N/P = 9.7:1	**Phase 2** HRT = 2 d N/P = 9.7:1	**Phase 3** HRT = 2 d N/P = 3.9:1	**Phase 4** HRT = 3 d N/P = 3.9:1	**Phase 5** HRT = 3 d N/P = 4.9:1	Significant difference[1]		
						Phase 2 and Phase 3	Phase 1 and Phase 4	Phase 4 and Phase 5
Total C	70.84 ± 1.17	71.19 ± 0.72	68.70 ± 1.51	68.26 ± 0.57	69.02 ± 1.52	Y (0.008)	Y (0.002)	N (0.291)
C-(C,H)	33.56 ± 2.12	35.03 ± 1.48	30.37 ± 2.40	29.33 ± 1.26	32.05 ± 1.98	Y (0.004)	Y (0.002)	Y (0.018)
C-(O,N)	26.94 ± 2.48	23.39 ± 1.72	26.73 ± 1.71	26.49 ± 0.55	25.23 ± 1.24	Y (0.010)	N (0.682)	Y (0.046)
C=O	5.72 ± 1.87	11.07 ± 1.21	8.46 ± 1.42	8.11 ± 0.94	7.48 ± 0.31	Y (0.010)	Y (0.019)	N (0.149)
O=C-OH	4.59 ± 0.73	1.70 ± 0.38	3.13 ± 0.89	4.33 ± 0.60	4.27 ± 0.44	Y (0.009)	N (0.504)	N (0.842)
Total O	22.84 ± 0.88	20.56 ± 0.69	22.30 ± 1.60	22.69 ± 1.20	22.67 ± 1.66	Y (0.046)	N (0.812)	N (0.978)
O=C	3.67 ± 0.43	6.44 ± 0.37	7.60 ± 0.40	7.13 ± 0.19	5.35 ± 0.39	Y (0.001)	Y (0.000)	Y (0.000)
C-OH and C-O-C	18.73 ± 0.75	13.74 ± 0.54	14.50 ± 1.55	15.45 ± 1.04	16.59 ± 1.69	N (0.302)	Y (0.000)	N (0.093)
O-C=O	0.44 ± 0.18	0.37 ± 0.08	0.20 ± 0.11	0.11 ± 0.06	0.36 ± 0.08	Y (0.015)	Y (0.002)	Y (0.000)
Total N	5.28 ± 0.48	7.19 ± 0.26	8.09 ± 0.25	8.16 ± 1.28	7.11 ± 0.97	Y (0.000)	Y (0.000)	N (0.143)
N-C	4.93 ± 0.44	6.63 ± 0.21	7.50 ± 0.24	7.85 ± 1.24	6.51 ± 0.88	Y (0.000)	Y (0.000)	N (0.056)
N^+	0.36 ± 0.07	0.56 ± 0.12	0.59 ± 0.14	0.30 ± 0.04	0.60 ± 0.09	N (0.718)	N (0.136)	Y (0.000)

[1] sig. value is shown in parentheses. Sample number n = 5 for Phase 2 and 6 for the rest four phases.

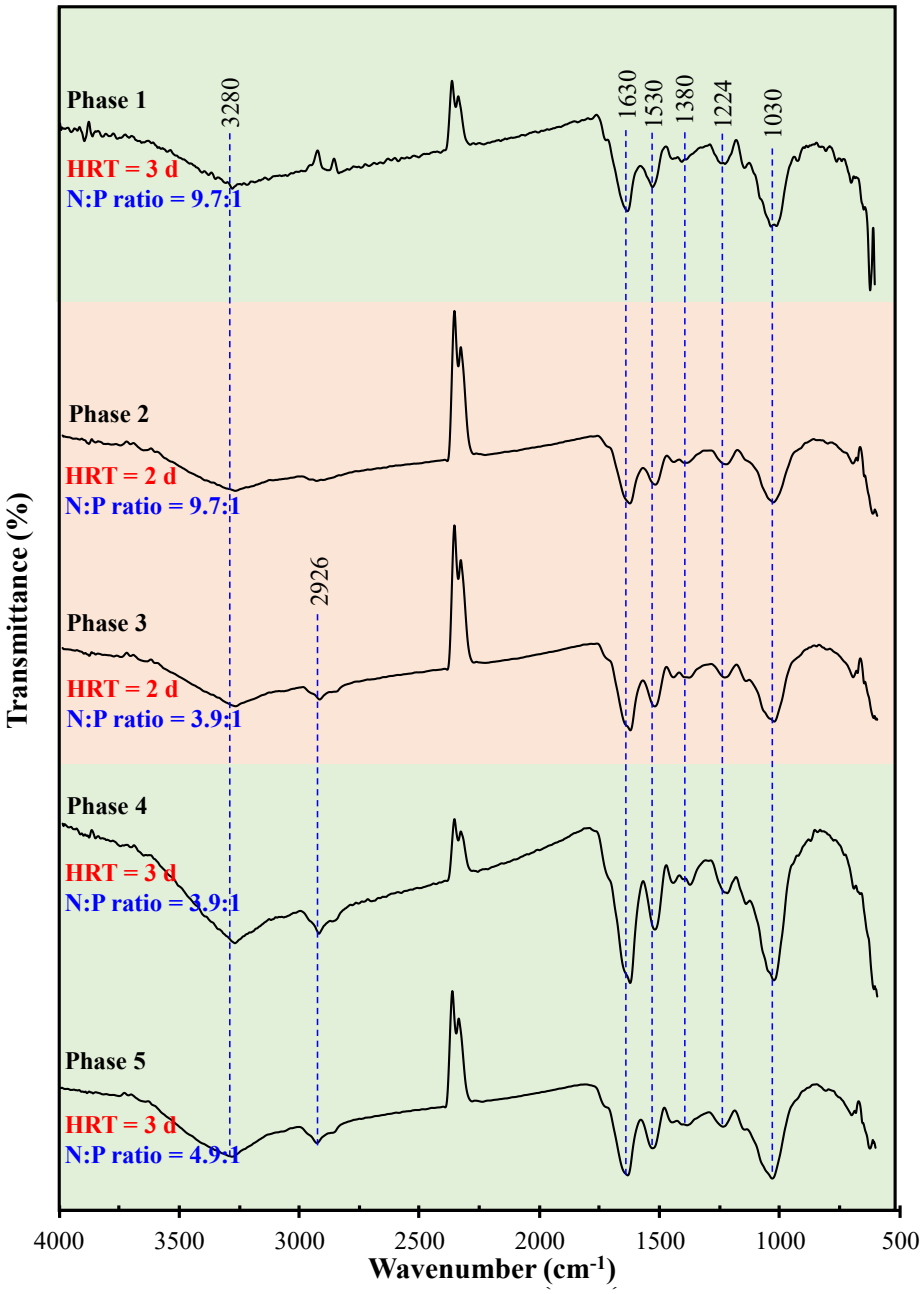

Figure 4-6 FTIR spectra of microalgal-bacterial consortium for the MB-MPBR under different operating conditions.

4.3.3.5 Floc size and morphology analysis

Figure 4-7 shows the microalgal-bacterial flocs distributed in a wide range of 1-1000 μm and the profiles varied from phase to phase. In comparison, only the flocs from Phase 1 had a perfect unimodal shape and the sharp primary peak located at the range of 20-200 μm. Excluding the sharp primary peak, Phase 2 had another two weak secondary peaks as compared with Phase 1. Phase 3

had three peaks and the sharp primary peak transferred to the range of 2-30 μm. The rest two phases exhibited very close PSD profiles and had the same position of the sharp primary peak as Phase 3. The difference in floc size was further demonstrated by microscopic observation. As shown in Figure 4-8, microalgae and bacteria coexisted overall the operational period. At Phase 1, small *Chlorella Vulgaris* cells embedded into bacteria flocs and formed good microalgae-sludge symbiotic with a few filamentous bacteria (Figure 4-8(a)). At Phase 2, filamentous bacteria multiplied and reunited into large flocs, and some *Scenedesmus* cells appeared at the end of this phase (Figure 4-8(b)). In the following three phases, the density of filamentous bacteria sharply decreased. *Scenedesmus* replaced *Chlorella Vulgaris*, dominated in the microalgae ecosystem, and mainly distributed in free status (Figure 4-8(c-e)).

In membrane related system, particle size is an important characteristic parameter affecting the filterability of biomass and formation of membrane fouling (Shen et al., 2015; Wang et al., 2008). As reported in previous literature, sludge flocs with larger particle size generally had lower fouling potential because they had lower adhesive ability and can produce lower cake layer resistance and higher membrane filterability (Cao et al., 2015; Shen et al., 2015; Wang et al., 2008). Moreover, micromorphology and filamentous bacteria also play a vital role in membrane fouling (Meng et al., 2006a; Wang et al., 2010). In this study, under the condition of same HRT and influent TN concentration, the microalgal-bacterial flocs from Phases 1 and 2 had a much higher fraction of large particles than that from the Phases 4 and 3, respectively. These results indicated more small particles generated under the lower N/P ratio of 3.9:1, which might be ascribed to the rapid reproduction of microalgae under P-rich condition (Figure 4-8(c-d)). The variation trend of particle size coincided with that of TMP, suggesting that floc size is the vital reason contributed to the TMP variation of Phases 1 to 4. However, as for Phases 4 and 5, both the PSD and morphology of the flocs were similar, indicating that the different fouling performance in Phases 4 and 5 should not be ascribed to the PSD.

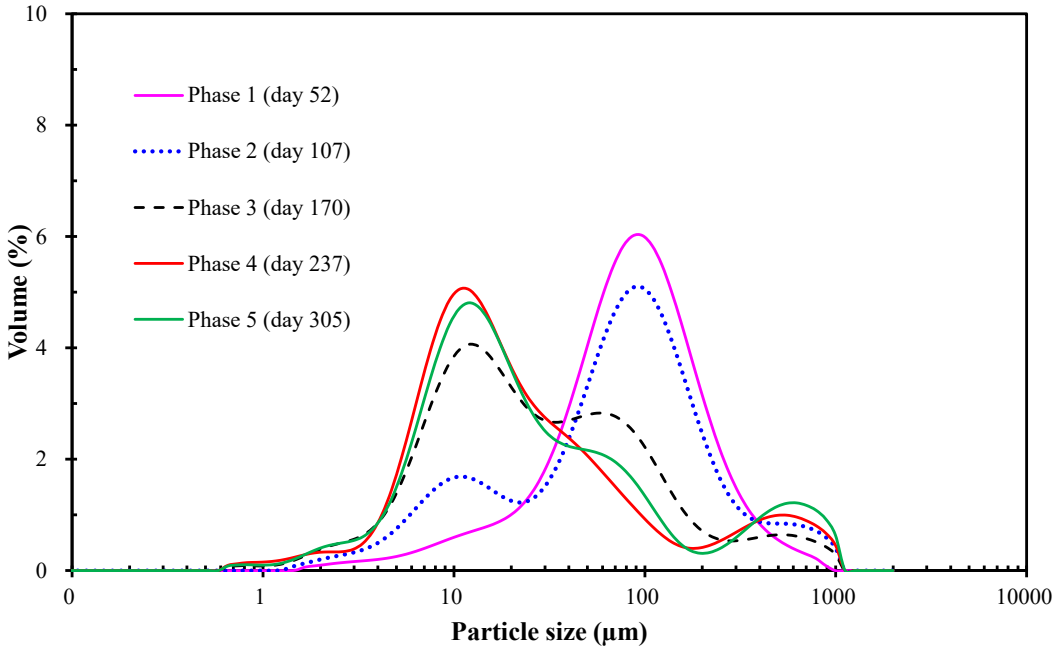

Figure 4-7 Particle size distribution of microalgal-bacterial suspended liquor for different phases.

4.3.4 Combined influence of N/P ratios and HRT on the properties of microalgal-bacterial consortium and its implication for membrane fouling control

The experimental results indicated that N/P ratio and nutrients loading rates had a significant impact on membrane fouling in MB-MPBR by regulating the growth balance of microalgae and bacteria. According to this study, under the same HRT and influent TN concentration, a lower N/P ratio of 3.9:1 (Phases 4 and 3) caused more serious membrane fouling than that of 9.7:1 (Phases 1 and 2). In the third group of comparison, an increase in N/P ratio (4.9:1) by increasing influent TN concentration led to an increase in membrane fouling rate (Figure 4-1). It is apparent that the difference in fouling performance resulted from the variation of microalgal-bacterial consortium properties caused by the different N/P ratios and nutrients loading rates. Interestingly, the main contributors to membrane fouling in the three comparison groups are different. It suggested that the final effect of N/P ratio on the membrane fouling relied on other influencing factors.

For the comparison of Phases 1 and 4, the microalgal-bacterial flocs from Phase 1 had less EPS (signified in mass) and larger floc size. However, the content of SMP at Phase 1 was much higher than that of Phase 4. In general, larger floc size and lower content of EPS correspond to lower membrane fouling (Lin et al., 2014; Meng & Yang, 2007). On the contrary, higher content

of SMP would cause higher filtration resistance (Lee et al., 2003; Teng et al., 2020). It worth noting that although Phase 1 had more SMP, the effect strength was far weaker than that of EPS and PSD. Therefore, the more quickly TMP increase in Phase 4 can be attributed to the smaller PSD and higher EPS content and changes in the surface composition of the sludge. As for the comparison between Phases 2 and 3, although the particle size of the biomass from Phase 3 was smaller than that of Phase 2, the concentration of SMP and EPS was comparable in the two phases. That is, differences in floc size and surface composition of sludge were the critical contributors to the difference in TMP variation. In the case of Phases 4 and 5, the biomass from Phase 5 had similar EPS content, surface composition of sludge, and PSD but higher membrane fouling rate as compared to that of Phase 4, which was mainly attributed to the higher content of SMP.

The above findings could give some implications for MB-MPBR development and its membrane fouling control. So far, several studies have demonstrated the positive effect of microalgae addition in MBR for biological performance and membrane fouling mitigation (Sun et al., 2018a; Sun et al., 2018c). However, the deteriorated membrane performance was also reported due to the too high microalgae/bacteria inoculation ratio (Sun et al., 2018b). In this study, serious P-limitation in Phase 1 inhibited the growth of microalgae, most of the small size microalgae embedded into bacteria and coexisted in the form of large flocs (Figure 4-8(a)). At Phase 2, due to the decrease in HRT, organic, and nutrient loading rate increased, which changed the balance between the microalgae and bacteria. As a result, filamentous bacterial rapidly multiplied, more microalgae flocs formed, and large particles were also formed using filamentous bacteria as a backbone with microalgae attached on Also, the *Scenedesmus* appeared and started to compete with the *Chlorella Vulgaris* (Figure 4-8(b)). In the following three phases, nutrients (both N and P) were sufficient, and *Scenedesmus* dominated the system (Figure 4-8(c-e)). Due to the low density of bacteria, the small size microalgae mainly distributed in a free status, easily attached to the membrane surface, and formed a dense cake layer. As discussed above, it can be speculated that there exists an optimized ratio for microalgae and bacteria, under such a status, microalgae and bacteria cooperate, aggregate into large particles, and possess the lowest fouling propensity. In opposite, the unbalanced ratio would lead to overgrowth of microalgae or bacteria and severer membrane fouling. Therefore, to exert the advantages of MB-MPBR fully, optimized conditions should be applied to control the balance of microalgae and bacteria and kept them at an appropriate ratio. This study strengthened our knowledge of membrane fouling in MB-MPBR and can guide

the design, operation, development, and application of MB-MPBR for wastewater treatment.

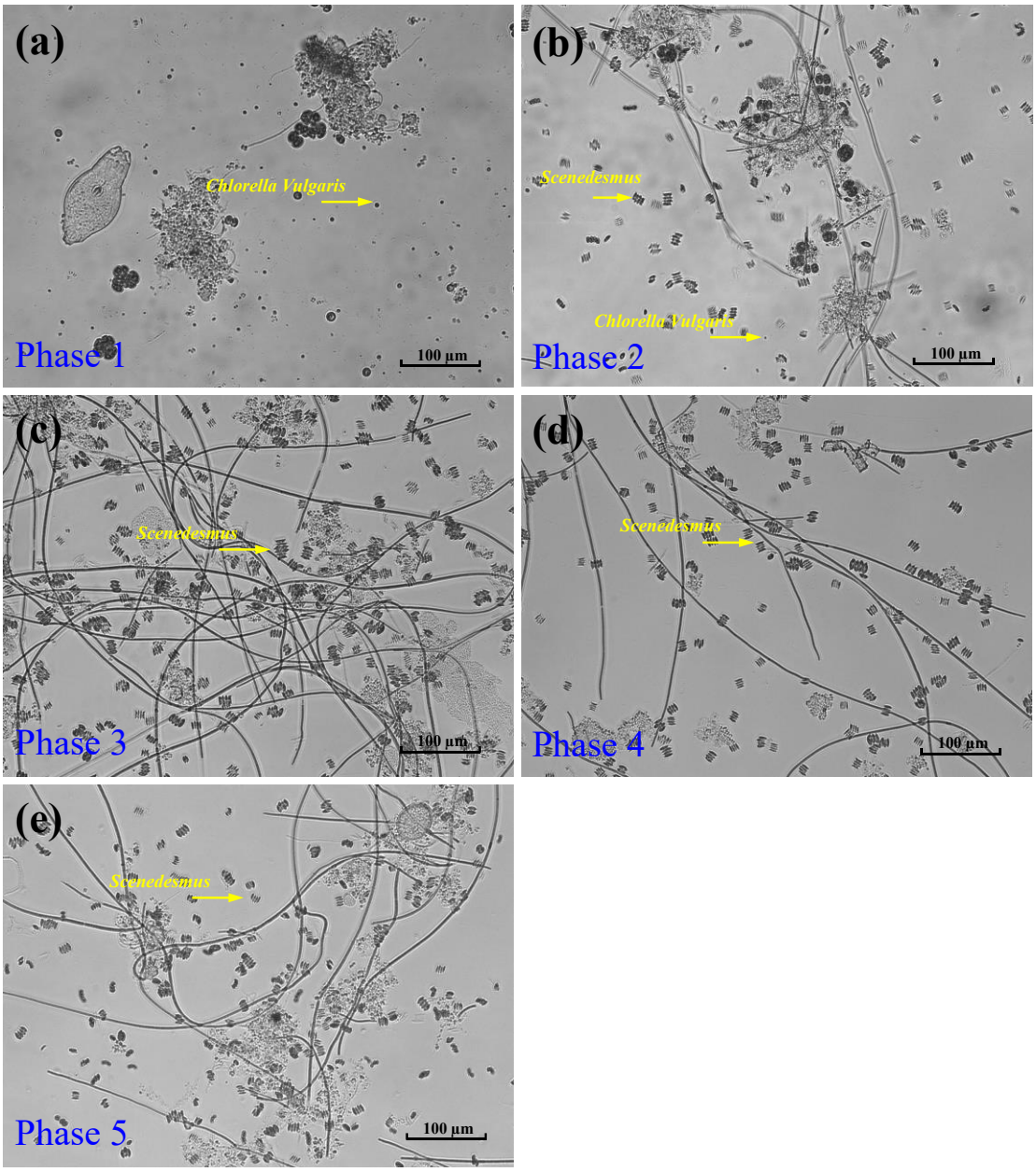

Figure 4-8 Microscopic morphology of microalgal-bacterial flocs at (a) Phase 1 (day 52), (b) Phase 2 (day 107), (c) Phase 3 (day 187), (d) Phase 4 (day 237), and (e) Phase 5 (day 312).

4.4 Conclusions

In MB-MPBR, N/P ratio significantly affected membrane performance by controlling the growth balance of microalgae and bacteria and their biological properties. A lower N/P ratio of 3.9:1 led to a more quickly TMP increase under the same HRT and influent TN concentration.

Characterization results showed that smaller particle size and changes in surface composition (i.e., bound EPS composition) under the lower N/P ratio were the primary contributors to the faster increase in membrane fouling. The dominant fouling mechanism was cake layer formation. XPS, FTIR, and microscopic analysis demonstrated that the underlying reason for the decreased floc size was attributed to the strengthened competitiveness and overgrowth of microalgae at P-rich conditions. In brief, optimizing the operating conditions, such as appropriate nutrients loading rate and COD/N/P ratio, to balance the microalgae and bacteria growth at an appropriate ratio is the key for membrane fouling control in MB-MPBRs.

4.5 References

Alcántara, C., Domínguez, J. M., García, D., Blanco, S., Pérez, R., García-Encina, P. A., Muñoz, R., 2015. Evaluation of wastewater treatment in a novel anoxic–aerobic algal–bacterial photobioreactor with biomass recycling through carbon and nitrogen mass balances. *Bioresource Technology*. 191, 173-186.

Aslam, M., Charfi, A., Lesage, G., Heran, M., Kim, J., 2017. Membrane bioreactors for wastewater treatment: A review of mechanical cleaning by scouring agents to control membrane fouling. *Chemical Engineering Journal*. 307, 897-913.

Cao, T. A., Van De Staey, G., Smets, I. Y., 2015. Integrating activated sludge floc size information in MBR fouling modeling. *Water Science and Technology*. 71(7), 1073-1080.

Chen, Y., Shen, L., Li, R., Xu, X., Hong, H., Lin, H., Chen, J., 2020. Quantification of interfacial energies associated with membrane fouling in a membrane bioreactor by using BP and GRNN artificial neural networks. *Journal of Colloid and Interface Science*. 565, 1-10.

Choi, H. J., Lee, S. M., 2015. Effect of the N/P ratio on biomass productivity and nutrient removal from municipal wastewater. *Bioprocess and Biosystems Engineering*. 38(4), 761-766.

Dean, A. P., Sigee, D. C., Estrada, B., Pittman, J. K., 2010. Using FTIR spectroscopy for rapid determination of lipid accumulation in response to nitrogen limitation in freshwater microalgae. *Bioresource Technology*. 101(12), 4499-4507.

Dilek Sanin, F., Vatansever, A., Turtin, I., Kara, F., Durmaz, B., Sesay, M. L., 2006. Operational Conditions of Activated Sludge: Influence on Flocculation and Dewaterability. *Drying Technology*. 24(10), 1297-1306.

Ding, Y., Tian, Y., Li, Z., Zuo, W., Zhang, J., 2015. A comprehensive study into fouling properties of extracellular polymeric substance (EPS) extracted from bulk sludge and cake sludge in a

mesophilic anaerobic membrane bioreactor. *Bioresource Technology*. 192(0), 105-114.

Durmaz, B., Sanin, F. D., 2003. Effect of carbon to nitrogen ratio on the physical and chemical properties of activated sludge. *Environmental Technology*. 24(11), 1331-1340.

Erkan, H. S., Engin, G. O., Ince, M., Bayramoglu, M. R., 2016. Effect of carbon to nitrogen ratio of feed wastewater and sludge retention time on activated sludge in a submerged membrane bioreactor. *Environmental Science and Pollution Research*. 23(11), 10742-10752.

Frølund, B., Palmgren, R., Keiding, K., Nielsen, P. H., 1996. Extraction of extracellular polymers from activated sludge using a cation exchange resin. *Water Research*. 30(8), 1749-1758.

Fu, Z., Yang, F., Zhou, F., Xue, Y., 2009. Control of COD/N ratio for nutrient removal in a modified membrane bioreactor (MBR) treating high strength wastewater. *Bioresource Technology*. 100(1), 136-41.

Gaudy, A. F., 1962. Colorimetric determination of protein and carbohydrate. *Industrial water & wastes*. 7, 17-22.

Gutzeit, G., Lorch, D., Weber, A., Engels, M., Neis, U., 2005. Bioflocculent algal–bacterial biomass improves low-cost wastewater treatment. *Water Science and Technology*. 52(12), 9-18.

Hao, L., Liss, S. N., Liao, B. Q., 2016. Influence of COD:N ratio on sludge properties and their role in membrane fouling of a submerged membrane bioreactor. *Water Research*. 89, 132-141.

Huang, Z., Ong, S. L., Ng, H. Y., 2011. Submerged anaerobic membrane bioreactor for low-strength wastewater treatment: effect of HRT and SRT on treatment performance and membrane fouling. *Water Research*. 45(2), 705-13.

Kim, B.-C., Nam, D.-H., Na, J.-H., Kang, K.-H., 2014. Analysis of extracellular polymeric substance (EPS) release in anaerobic sludge holding tank and its effects on membrane fouling in a membrane bioreactor (MBR). *Water Science and Technology*. 70(1), 82-88.

Kim, H.-C., Dempsey, B. A., 2013. Membrane fouling due to alginate, SMP, EfOM, humic acid, and NOM. *Journal of Membrane Science*. 428(0), 190-197.

Kumar, S. S., Basu, S., Gupta, S., Sharma, J., Bishnoi, N. R., 2019. Bioelectricity generation using sulphate-reducing bacteria as anodic and microalgae as cathodic biocatalysts. *Biofuels*. 10(1), 81-86.

Lee, C. S., Lee, S.-A., Ko, S.-R., Oh, H.-M., Ahn, C.-Y., 2015. Effects of photoperiod on nutrient removal, biomass production, and algal-bacterial population dynamics in lab-scale

photobioreactors treating municipal wastewater. *Water Research*. 68, 680-691.

Lee, S.-H., Ahn, C.-Y., Jo, B.-H., Lee, S.-A., Park, J.-Y., An, K.-G., Oh, H.-M., 2013. Increased microalgae growth and nutrient removal using balanced N:P ratio in wastewater. *Journal of microbiology and biotechnology*. 23(1), 92-98.

Lee, W., Kang, S., Shin, H., 2003. Sludge characteristics and their contribution to microfiltration in submerged membrane bioreactors. *Journal of Membrane Science*. 216(1-2), 217-227.

Li, R., Lou, Y., Xu, Y., Ma, G., Liao, B.-Q., Shen, L., Lin, H., 2019. Effects of surface morphology on alginate adhesion: Molecular insights into membrane fouling based on XDLVO and DFT analysis. *Chemosphere*. 233, 373-380.

Lin, H., Liao, B.-Q., Chen, J., Gao, W., Wang, L., Wang, F., Lu, X., 2011. New insights into membrane fouling in a submerged anaerobic membrane bioreactor based on characterization of cake sludge and bulk sludge. *Bioresource Technology*. 102(3), 2373-2379.

Lin, H., Zhang, M., Wang, F., Meng, F., Liao, B.-Q., Hong, H., Chen, J., Gao, W., 2014. A critical review of extracellular polymeric substances (EPSs) in membrane bioreactors: Characteristics, roles in membrane fouling and control strategies. *Journal of Membrane Science*. 460(0), 110-125.

Lin, H. J., Xie, K., Mahendran, B., Bagley, D. M., Leung, K. T., Liss, S. N., Liao, B. Q., 2009. Sludge properties and their effects on membrane fouling in submerged anaerobic membrane bioreactors (SAnMBRs). *Water Research*. 43(15), 3827-3837.

Liu, J., Wu, Y., Wu, C., Muylaert, K., Vyverman, W., Yu, H.-Q., Muñoz, R., Rittmann, B., 2017. Advanced nutrient removal from surface water by a consortium of attached microalgae and bacteria: A review. *Bioresource Technology*. 241, 1127-1137.

Lowry, O. H., Rosebrough, N. J., Farr, A. L., Randall, R. J., 1951. Protein measurement with the folin phenol reagent. *Journal of Biological Chemistry*. 193, 265-275.

Marbelia, L., Bilad, M. R., Passaris, I., Discart, V., Vandamme, D., Beuckels, A., Muylaert, K., Vankelecom, I. F. J., 2014. Membrane photobioreactors for integrated microalgae cultivation and nutrient remediation of membrane bioreactors effluent. *Bioresource Technology*. 163, 228-235.

Mayers, J. J., Flynn, K. J., Shields, R. J., 2013. Rapid determination of bulk microalgal biochemical composition by Fourier-Transform Infrared spectroscopy. *Bioresource Technology*. 148, 215-220.

Meng, F., Chae, S.-R., Drews, A., Kraume, M., Shin, H.-S., Yang, F., 2009. Recent advances in membrane bioreactors (MBRs): Membrane fouling and membrane material. *Water Research*. 43(6), 1489-1512.

Meng, F., Yang, F., 2007. Fouling mechanisms of deflocculated sludge, normal sludge, and bulking sludge in membrane bioreactor. *Journal of Membrane Science*. 305(1-2), 48-56.

Meng, F., Zhang, H., Yang, F., Li, Y., Xiao, J., Zhang, X., 2006a. Effect of filamentous bacteria on membrane fouling in submerged membrane bioreactor. *Journal of Membrane Science*. 272(1-2), 161-168.

Meng, F., Zhang, H., Yang, F., Zhang, S., Li, Y., Zhang, X., 2006b. Identification of activated sludge properties affecting membrane fouling in submerged membrane bioreactors. *Separation and Purification Technology*. 51(1), 95-103.

Meng, Q. J., Yang, F. L., Liu, L. F., Meng, F. G., 2008. Effects of COD/N ratio and DO concentration on simultaneous nitrification and denitrification in an airlift internal circulation membrane bioreactor. *Journal of Environmental Sciences-China*. 20(8), 933-939.

Posadas, E., García-Encina, P.-A., Soltau, A., Domínguez, A., Díaz, I., Muñoz, R., 2013. Carbon and nutrient removal from centrates and domestic wastewater using algal–bacterial biofilm bioreactors. *Bioresource Technology*. 139, 50-58.

Shen, L.-g., Lei, Q., Chen, J.-R., Hong, H.-C., He, Y.-M., Lin, H.-J., 2015. Membrane fouling in a submerged membrane bioreactor: Impacts of floc size. *Chemical Engineering Journal*. 269(0), 328-334.

Sun, L., Tian, Y., Zhang, J., Cui, H., Zuo, W., Li, J., 2018a. A novel symbiotic system combining algae and sludge membrane bioreactor technology for wastewater treatment and membrane fouling mitigation: Performance and mechanism. *Chemical Engineering Journal*. 344, 246-253.

Sun, L., Tian, Y., Zhang, J., Li, H., Tang, C., Li, J., 2018b. Wastewater treatment and membrane fouling with algal-activated sludge culture in a novel membrane bioreactor: Influence of inoculation ratios. *Chemical Engineering Journal*. 343, 455-459.

Sun, L., Tian, Y., Zhang, J., Li, L., Zhang, J., Li, J., 2018c. A novel membrane bioreactor inoculated with symbiotic sludge bacteria and algae: Performance and microbial community analysis. *Bioresource Technology*. 251, 311-319.

Tang, X., He, L. Y., Tao, X. Q., Dang, Z., Guo, C. L., Lu, G. N., Yi, X. Y., 2010. Construction of

an artificial microalgal-bacterial consortium that efficiently degrades crude oil. *Journal of Hazardous Materials*. 181(1), 1158-1162.

Teng, J., Shen, L., Xu, Y., Chen, Y., Wu, X.-L., He, Y., Chen, J., Lin, H., 2020. Effects of molecular weight distribution of soluble microbial products (SMPs) on membrane fouling in a membrane bioreactor (MBR): Novel mechanistic insights. *Chemosphere*. 248, 126013.

Teng, J., Zhang, M., Leung, K.-T., Chen, J., Hong, H., Lin, H., Liao, B.-Q., 2019. A unified thermodynamic mechanism underlying fouling behaviors of soluble microbial products (SMPs) in a membrane bioreactor. *Water Research*. 149, 477-487.

Wang, J., Guan, J., Santiwong, S. R., Waite, T. D., 2008. Characterization of floc size and structure under different monomer and polymer coagulants on microfiltration membrane fouling. *Journal of Membrane Science*. 321(2), 132-138.

Wang, Z., Ma, J., Tang, C. Y., Kimura, K., Wang, Q., Han, X., 2014. Membrane cleaning in membrane bioreactors: A review. *Journal of Membrane Science*. 468(0), 276-307.

Wang, Z., Wang, P., Wang, Q., Wu, Z., Zhou, Q., Yang, D., 2010. Effective control of membrane fouling by filamentous bacteria in a submerged membrane bioreactor. *Chemical Engineering Journal*. 158(3), 608-615.

Xuan, W., Bin, Z., Zhiqiang, S., Zhigang, Q., Zhaoli, C., Min, J., Junwen, L., Jingfeng, W., 2010. The EPS characteristics of sludge in an aerobic granule membrane bioreactor. *Bioresource Technology*. 101(21), 8046-8050.

Xue, W., Tobino, T., Nakajima, F., Yamamoto, K., 2015. Seawater-driven forward osmosis for enriching nitrogen and phosphorous in treated municipal wastewater: Effect of membrane properties and feed solution chemistry. *Water Research*. 69, 120-130.

Yang, J., Gou, Y., Fang, F., Guo, J., Ma, H., Wei, X., Shahmoradi, B., 2018. Impacts of sludge retention time on the performance of an algal-bacterial bioreactor. *Chemical Engineering Journal*. 343, 37-43.

Zhang, M., Liao, B.-q., Zhou, X., He, Y., Hong, H., Lin, H., Chen, J., 2015. Effects of hydrophilicity/hydrophobicity of membrane on membrane fouling in a submerged membrane bioreactor. *Bioresource Technology*. 175(0), 59-67.

Zhang, M., Yao, L., Maleki, E., Liao, B.-Q., Lin, H., 2019. Membrane technologies for microalgal cultivation and dewatering: Recent progress and challenges. *Algal Research*. 44, 101686.

Chapter 5 Effects of Solids Retention Time on the Biological Performance of a Novel Microalgal-Bacterial Membrane Photobioreactor (MB-MPBR)

Abstract: The feasibility of using microalgal-bacterial membrane photobioreactor (MB-MPBR) to treat industrial anaerobic digestion effluent was studied at three solids retention time (SRT) for almost 300 days. The biological performance and consortium characteristics were investigated under three SRTs of 10, 20, and 30 d. The results showed that the longer SRT corresponded to higher biomass concentration, whereas the growth status of microalgae nonlinearly correlated to SRT. The removal of COD (90%-94%) did not change much at different SRTs. However, the nutrients (N and P) removals were significantly affected by SRT, which were mainly caused by the different MLSS levels resulted from the variation of SRT. The removal of TN relied on microalgae growth since the nitrogen in the wastewater was mainly removed through microalgae assimilation. TP was removed through both microalgae assimilation and biomass adsorption. The increased TP removal efficiency with increasing SRT was mainly attributed to the enhanced surface-adsorption under higher biomass concentration. SRT significantly influenced the PSD and microscopic morphology of microalgal-bacterial consortium. In addition, high nutrients concentrations negatively impacted the microalgae growth and nutrients removals, and thus influent dilution or a longer HRT is required to achieve effluent quality meets the discharge standards. In summary, intermediate SRT was the optimal selection for reliable operation of MB-MPBRs.

Keywords: Microalgal-bacterial membrane photobioreactor, Solids retention time, Nutrients removal, Anaerobic digestion effluent

5.1 Introduction

Anaerobic membrane bioreactor (AnMBR) has been extensively used to treat high organic strength industrial wastewater like malting wastewater because of its distinctive advantages of low sludge production, small footprint, and biogas generation (Huang et al., 2011; Lin et al., 2013). However, the anaerobic sludge digestion effluent or other high strength wastewater with enriched nutrients (such as malting wastewater) typically contained high concentrations of COD, nitrogen, and phosphorus (Chen et al., 2018; Marcilhac et al., 2015; Praveen et al., 2018). Inappropriate disposal of such sewage would cause serious environmental problems such as eutrophication and ecosystem deterioration (Marcilhac et al., 2015; Xie et al., 2018). As a renewable biomass feedstock, microalgae have attracted wide attention and been increasingly used for nutrients recovery from wastewater because of the excellent nutrient fixation capacity (Honda et al., 2017; Luo et al., 2017; Xu et al., 2015). Nevertheless, in typical microalgae-based processes, most of the microalgae can only assimilate nutrients for their growth. The high concentration of COD in the anaerobic digestion effluent cannot be effectively removed. On the contrary, it would inhibit the microalgae growth and nutrients removal. Therefore, more attempts are required to develop a feasible and efficient way to treat anaerobic digestion effluent.

Combining the functions of microalgae and bacteria, the microalgal-bacterial consortium seems a promising technology for the treatment of anaerobic digestion effluent. It can simultaneously remove COD and nutrients from the wastewater with high efficiency (Alcántara et al., 2015; Karya et al., 2013; Lee et al., 2015). However, washout of free microalgae is a huge issue faced in traditional algal-bacterial systems, which leads to the deterioration of permeate quality and system stability (Sun et al., 2018a). Recently, a new concept of integrating microalgal-bacterial consortium within an MBR setup called microalgal-bacterial membrane photobioreactor (MB-MPBR) has been proposed to solve the problem of washout and improve the performance of MBR (Sun et al., 2018a; Sun et al., 2018c; Yang et al., 2018). In the MB-MPBR, the energy demand of mechanical aeration was reduced because CO_2 and O_2 released by bacteria and microalgae respectively can be used by each other for nutrients uptake and organics decomposition, respectively (Oswald, 1988). In addition, a mitigated membrane fouling was observed in MB-MPBR than conventional MBR because of the improved sludge properties after the introduction of microalgae (Sun et al., 2018a; Sun et al., 2018b; Sun et al., 2018c).

SRT is a key operating parameter that controls the process performance in MB-MPBR. It crucially affects the biomass properties and pollutant removal efficiencies (Choi et al., 2008; Han et al., 2005). A long SRT is often considered as an advantage for traditional MBR because it can maintain high biomass concentration and reduce sludge production and thus can save the cost for the sludge handling and disposal (Ouyang & Liu, 2009). Unlike MBR system, membrane photobioreactor (MPBR) tends to be operated with moderate SRT to simultaneously avoid self-shading and obtain high nutrients removal (Zhang et al., 2019). That is, the preferred SRT for activated sludge (bacteria) and microalgae is different. In MB-MPBR, microalgae and bacteria coexist. They are cooperative and competitive (Liu et al., 2017). Microalgae can maintain the growth of bacteria by providing organic carbon, and the consumption of O_2 and the release of CO_2 by bacteria will reduce the oxygen tension of photosynthesis and increase the concentration of CO_2, respectively, thereby promoting the growth of microalgae (Liu et al., 2017). On the other hand, some microalgae metabolites present the effect of sterilization or inhibition of bacterial quorum sensing, and some substances secreted by bacteria may affect the transcription of photosynthesis-related genes or have algaecide effects (Liu et al., 2017). In addition, the excessive growth of bacteria would also enhance the photo-inhibition effect of microalgae, thereby limiting the growth of microalgae. Therefore, the impact of SRT on MB-MPBR would be more complicated than that in MBR and MPBR. SRT may exert its effect through not only the total biomass concentration but also the growth status between microalgae and bacteria. However, the recent few studies regarding MB-MPBR mainly focused on the comparison of treatment and fouling performance between MBR and MB-MPBR (Sun et al., 2018a; Sun et al., 2018c). To date, impacts of SRT on the biological performance of MB-MPBR for the treatment of anaerobic digestion effluent could hardly be found in the literature.

Accordingly, the long-term operation of the MB-MPBR to treat industrial anaerobic digestion effluent with high strength of COD and nutrients was conducted under three SRTs of 10, 20, and 30 d. The operational performance of biomass concentration, COD removal and nutrients removal were determined and compared. In addition, the biological properties of the particle size distribution (PSD) and micromorphology of the consortium were analyzed.

5.2 Material and methods

5.2.1 Microalgal pre-cultivation, activated sludge seed, and synthetic wastewater

The microalgae culture, *Chlorella Vulgaris* (CPCC 90), was purchased from Canadian Physiological Culture Centre and pre-cultivated in a modified Mineral Salt Medium (MSM) in this study (Muñoz et al., 2005). The microalgae were grown under continuous aeration and light illumination at room temperature. The composition of the modified MSM medium can refer to Chapter 3.

The activated sludge seed was from an activated sludge plant treating pulp and paper wastewater from a local pulp and paper mill.

A synthetic wastewater with high strength of nutrients and organics, simulating secondary effluent from a lab-scale anaerobic MBR for malting wastewater treatment, was used as feed in this study (Table 5-1). The feed contained 1106.17 ± 20.05 mg/L COD, 136.72 ± 8.17 mg/L total nitrogen (TN), and 24.63 ± 1.13 mg/L total phosphorus (TP).

5.2.2 Experimental setup and operation

The diagram of the MB-MPBR is displayed in Figure 5-1. The effective working volume was 9.64 L (internal diameter: 19 cm; effective height: 34 cm) and the surface to volume ratio (S/V) of 24.0 m^{-1}. A flat sheet membrane module (0.03 m^2) was used for liquid/solids separation. All the membranes used throughout the experimental period were made of PVDF materials and had an average pore size of 0.1 μm (SINAP Co. Ltd., Shanghai, China). The air (0.05% CO_2) with a flow rate of 3.39 ± 0.16 L/min was supplied through two stainless steel tubes connected with mediate bubble diffusers to provide mixing and prevent the foulants adhesion on the membrane surface. In addition, a magnetic stirrer (Model 6795-611, Corning, USA) was loaded at the reactor bottom to prevent biomass settling by providing gentle mixing. Continuous illumination was provided by four LED lamps placed outside of the reactor. The light intensity on the reactor surface was approximately 8400 lux.

Table 5-1 Chemical compositions of the synthetic anaerobically treated malting secondary wastewater.

Reagent	Concentration (mg/L)
Glucose	1000
NH_4Cl	573.2
$NaH_2PO_4 \cdot H_2O$,	111.3
KCl	152.8
NaCl	461.5
$MgSO_4 \cdot 7H_2O$	98.4
$CaCl_2$	87.4
$AlCl_3 \cdot 6H_2O$	5.8
$NiCl_2 \cdot 6H_2O$	0.364
$K_2Cr_2O_7$	0.023
$MnCl_2 \cdot 4H_2O$	0.540
$FeCl_3 \cdot 6H_2O$	0.155
$CuSO_4 \cdot 5H_2O$	0.098
$CoCl_2 \cdot 6H_2O$	0.089

The pre-cultivated *Chlorella vulgaris* and activated sludge were used as microalgal and bacterial inoculum, respectively. The initial concentration of microalgae and sludge was 1.02 and 3.06 g/L, respectively, corresponding to an inoculated ratio (microalgae/activated sludge) of 1:3. A refrigerator was used for storing the synthetic wastewater at 4-5 ℃, and the influent was automatically pumped into the reactor by a feeding pump controlled by a level sensor (LC40, Flowline Inc., USA). A peristaltic pump (Model 77122-14, Masterflex®C/L®PWR, Cole-Parmer, USA) operating in the mode of 3-min-on and 2-min-off was used to obtain the permeate. The flux of the membrane was controlled by adjusting the pump speed, and calibration was made daily. The MB-MPBR was continuously operated for 300 days and divided into four phases. Details about the operating conditions for each phase are listed in Table 5-2. At the end of each phase, the used membranes were replaced by new pieces of membrane to keep the same initial membrane conditions.

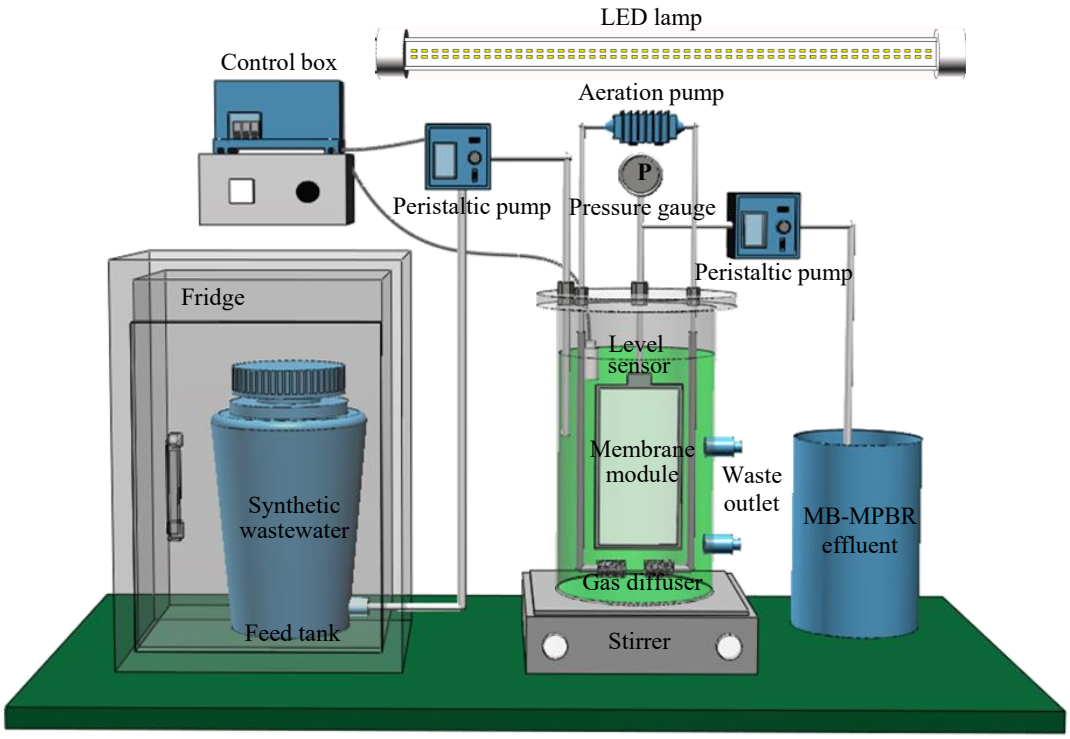

Figure 5-1 Experimental setup of the submerged MB-MPBR.

5.2.3 Analytical methods

5.2.3.1 Chlorophyll-a extraction and analysis

Chlorophyll-a was extracted and analyzed according to the processes previously reported (Nautiyal et al., 2014). The microalgal-bacterial pellets after 10 min centrifugation at 8000×g were resuspended into a known volume of methanol and then put in a water bath at 60 ℃ for 30 min. After cooled down to room temperature, the supernatant was collected for downstream determination. A visible spectrophotometer (DR2800, Hach, Germany) was used for the measurement of the chlorophyll-a content in the biomass. The concentration of chlorophyll-a can be calculated using the equation as follows (Nautiyal et al., 2014):

$$\text{Chlorophyll-a (mg/L)} = 16.29(A^{665.2}-A^{750})-8.54(A^{652}-A^{750}) \quad (5\text{-}1)$$

where A^{750}, $A^{665.2}$, A^{652} represent the absorbance at 750, 665.2 and 652 nm, respectively.

Table 5-2 Operational parameters and biological performance of the lab-scale MB-MPBR under different operating conditions.

	Phase 1	Phase 2	Phase 3	Phase 4
System HRT (d)	2.8 ± 0.2	2.8 ± 0.2	2.8 ± 0.2	5.8 ± 0.3
System SRT (d)	10	20	30	20
Temperature (℃)	26.7 ± 0.4	28.2 ± 0.9	27.8 ± 0.9	26.5 ± 0.5
Mixed liquor pH	6.8 ± 0.8	7.1 ± 0.2	7.2 ± 0.2	7.3 ± 0.2
MLSS (g/L)	1.34 ± 0.32	2.25 ± 0.18	3.40 ± 0.15	0.87 ± 0.10
Chlorophyll-a/MLSS (mg/g biomass)	1.48 ± 0.19	2.19 ± 0.40	1.07 ± 0.34	1.43 ± 0.68
Chlorophyll-a concentration (mg/L)	2.00 ± 0.70	4.89 ± 0.59	3.24 ± 0.95	1.22 ± 0.54
Influent COD (mg/L)	1124.49 ± 10.19	1103.78 ± 25.81	1104.30 ± 13.83	1100.23 ± 19.86
Effluent COD (mg/L)	71.32 ± 7.44	79.61 ± 19.26	111.82 ± 6.37	73.85 ± 14.45
COD removal efficiency (%)	93.66 ± 0.66	92.79 ± 1.74	89.87 ± 0.58	93.29 ± 1.31
Influent TN (mg/L)	130.40 ± 4.74	132.18 ± 5.59	141.81 ± 7.04	139.19 ± 8.84
Effluent TN (mg/L)	106.86 ± 12.99	106.72 ± 6.06	121.10 ± 2.52	121.12 ± 7.30
TN removal efficiency (%)	18.05 ± 9.96	19.26 ± 4.58	14.60 ± 1.78	12.98 ± 5.25
Influent TP (mg/L)	25.08 ± 0.46	24.80 ± 1.03	24.35 ± 1.03	24.49 ± 1.54
Effluent TP (mg/L)	17.96 ±1.80	12.81 ± 1.47	10.97 ± 1.06	18.52 ± 2.87
TP removal efficiency (%)	28.38 ± 7.16	48.36 ± 5.91	54.95 ± 4.36	24.38 ± 11.71

Note: The average values of MLSS, chlorophyll-a concentration, and effluent pollutants (COD, TN, and TP) concentration, as well as the removal efficiency, were calculated from the data of last two weeks for each phase. The data are expressed as mean ± standard deviation.

5.2.3.2 Particle size distribution (PSD) and morphology analysis

A Malvern Mastersizer 2000 instrument (Worcestershire, UK) with a detection range of 0.02-2000 μm was used for PSD measurement of the mixed liquor. Each sample was automatically measured in triplicate by the machine. This measurement was conducted 1-2 times per week.

An inverted optical microscope (Olympus IX51, Japan) was applied to observe the micromorphology of the original microalgae, original sludge, and microalgae-bacterial consortia.

For each sample, more than 30 images were randomly captured by a digital camera connected with the microscope.

5.2.3.3 Other routine analysis

The measurement of pH and temperature for the suspension was conducted with a pH meter (pH 700, Oakton, USA) and a thermometer, respectively. A gas chromatography instrument (Shimazu, Mondel GC-2014, Japan) was applied to determine the CO_2 concentration in the air. Samples of feed and permeate were periodically collected for water quality monitoring. MLSS and COD was determined using standard methods (APHA, 2005). The TN and TP were measured with alkaline potassium persulfate digestion UV spectrophotometric method and ammonium molybdate spectrophotometry (State Environmental Protection Administration of China, 2002), respectively. For each sample, average values of two determinations were reported.

5.2.3.4 Calculation

The nutrients (N and P) removal rates of MB-MPBR were estimated by the following equation (Gao et al., 2016b):

$$\text{Removal rate (mg/L/d)} = (C_{inf} - C_{eff}) \times Q/V \quad (5\text{-}2)$$

where C_{inf} and C_{eff} are the concentration (mg/L) of TN or TP in the feed and effluent, respectively; Q is the flow rate (L); V was the working volume (L) of the reactor.

5.3 Results and discussion

5.3.1 Effects of SRT on biomass production

The variation of biomass concentration (represented by MLSS) in the MB-MPBR was displayed in Figure 5-2. At SRT of 10 d, the reactor started with an initial MLSS of 3.90 g/L and continuously reduced to 1.01 g/L at the end of Phase 1. The continuous decline of MLSS suggested that the amount of the microalgal-bacterial biomass produced in the MB-MPBR was less than that in the waste. It should be noted that the SRT adjustment was conducted on day 68 to avoid the collapse of the system. If the operation time of Phase 1 prolonged, the average biomass concentration at the steady state of 10 d SRT was expected equal to or less than 1.01 g/L. After the increase of SRT from 10 to 20 d at Phase 2, MLSS decline stopped and gradually increased to 2.24 g/L on day 100. Afterwards, the average MLSS maintained at 2.27 ± 0.11 g/L. At Phase 3, a further increase in SRT (from 20 d to 30 d) resulted in a further rise of MLSS and eventually maintained at 3.41 ± 0.12 g/L when stable state reached. According to the above results, it can be concluded

that SRT had a significant impact on biomass concentration in MB-MPBR. The longer SRT corresponded to a higher biomass concentration (Table 5-2).

Figure 5-2 also demonstrates the variations of chlorophyll-a/MLSS and total chlorophyll-a concentration in the MB-MPBR under different SRTs. The chlorophyll-a/MLSS content represents the relative life status between microalgae and activated sludge while chlorophyll-a concentration signifies the total amount of microalgae in the MB-MPBR. As shown in Figure 5-2, the content of chlorophyll-a/MLSS slightly fluctuated in the initial 20 days due to the operational problem of overflow occurred on day 8, maintained at constant (3.48 ± 0.26 mg/g biomass) from day 24 to 52, and then rapidly decreased to 1.37 mg/g biomass on day 67. With the increase of SRT from 10 d to 20 d at Phase 2, the chlorophyll-a/MLSS content remarkably increased in the initial period, reached the highest value of 8.88 mg/g biomass on day 93, and then continuously decreased to 1.70 mg/g biomass until the end of Phase 2. Unlike the variation trend at SRT of 20 d, the chlorophyll-a/MLSS content kept stable (2.10 ± 0.34 mg/g biomass) in the initial 45 days and then gradually decreased to 0.63 mg/g biomass at the end of Phase 3 with SRT of 30 d. Except for Phase 1, the variation trend of chlorophyll-a was consistent with that of the chlorophyll-a/MLSS. At Phase 1 with SRT of 10 d, the chlorophyll-a concentration slowly decreased before day 52 and then sharply decreased to an extremely low value of 1.39 mg/L on day 67. As summarized in Table 5-2, the highest value of chlorophyll-a/MLSS and chlorophyll-a concentration was achieved at SRT of 20 d.

Unlike MLSS, the growth status of microalgae nonlinearly correlated to SRT. The impact of SRT on microalgae growth in MB-MPBR closely related to the total biomass concentration. A wide range of MLSS variation under different SRTs may induce the initiation of other influencing factors. As shown in Figure 5-2, before day 52, although chlorophyll-a concentration continuously decreased, the chlorophyll-a/MLSS content kept at constant because of the simultaneous decrease in MLSS, indicating the balanced growth of microalgae and bacteria before day 52. However, a sharp decline in chlorophyll-a/MLSS content, chlorophyll-a concentration, and MLSS were observed after day 52, which was attributed to the too low microalgal biomass concentration retained in the reactor. Many studies have demonstrated that excessive concentration of ammonia nitrogen would inhibit the growth of microalgae (Cai et al., 2013; Chen et al., 2018; Park et al., 2010; Praveen et al., 2018). In this study, the ammonia nitrogen concentration in the influent exceeded the inhibition saturation. Before day 52, the biomass concentration was above the

threshold, and hence the microalgae could tolerate the inhibition and maintained a stable chlorophyll-a/MLSS value. Nevertheless, a further decline in biomass concentration below the threshold significantly weakened the tolerance capability of microalgae to ammonia nitrogen inhibition. As a result, the growth of microalgae remarkably impeded, and eventually led to the striking decrease of chlorophyll-a/MLSS content, total chlorophyll-a concentration, and MLSS. After increased the SRT to 20 d at Phase 2, more microalgae retained in the reactor, the growth of microalgae recovered and the chlorophyll-a/MLSS content and chlorophyll-a concentration gradually increased and reached their highest value of 8.88 mg/g biomass and 16.08 mg/L, respectively. However, a further increase in MLSS led to the reduction of chlorophyll-a/MLSS content and chlorophyll-a concentration due to the enhanced self-shading effect at a high biomass concentration (Honda et al., 2017; Van Thuan et al., 2018). The inhibitory effect was more severe at SRT of 30 d at Phase 3 because of the higher biomass concentration. Among the three SRTs studied, SRT of 20 d was considered as the best SRT. However, the growth status of microalgae did not reach a steady balance at SRT of 20 d, suggesting that 20 d was not the optimal SRT for the MB-MPBR. For a given MB-MPBR, there existed a critical biomass concentration where the growth of microalgae and bacteria can reach a balance and maintain stability during long-term operation. The SRT value which can maintain the critical biomass concentration was regarded as the optimal SRT for MB-MPBR system. The optimal SRT should be in the range of 10-20 d according to the results of this study.

The operation of the last phase was to investigate the recovery ability of microalgal-bacterial symbiosis after imbalanced growth. In this phase, after adjusted the SRT and HRT from 30 to 20 d and 2.8 ± 0.2 to 5.8 ± 0.3 d, respectively, the MLSS gradually decreased and finally maintained at 0.88 ± 0.09 g/L. The values of chlorophyll-a/MLSS and chlorophyll-a concentration maintained at 0.34 ± 0.09 mg/g biomass and 0.55 ± 0.22 mg/L respectively, only about 8.72% and 4.35% of the initial value, respectively. Until the end of Phase 4, both the chlorophyll-a/MLSS and chlorophyll-a concentration restarted increase. These results suggested that the unbalanced growth of microalgae and bacteria under unfavorable operating conditions can be restored but required several weeks or even several months. In practical operation, such a situation should be avoided.

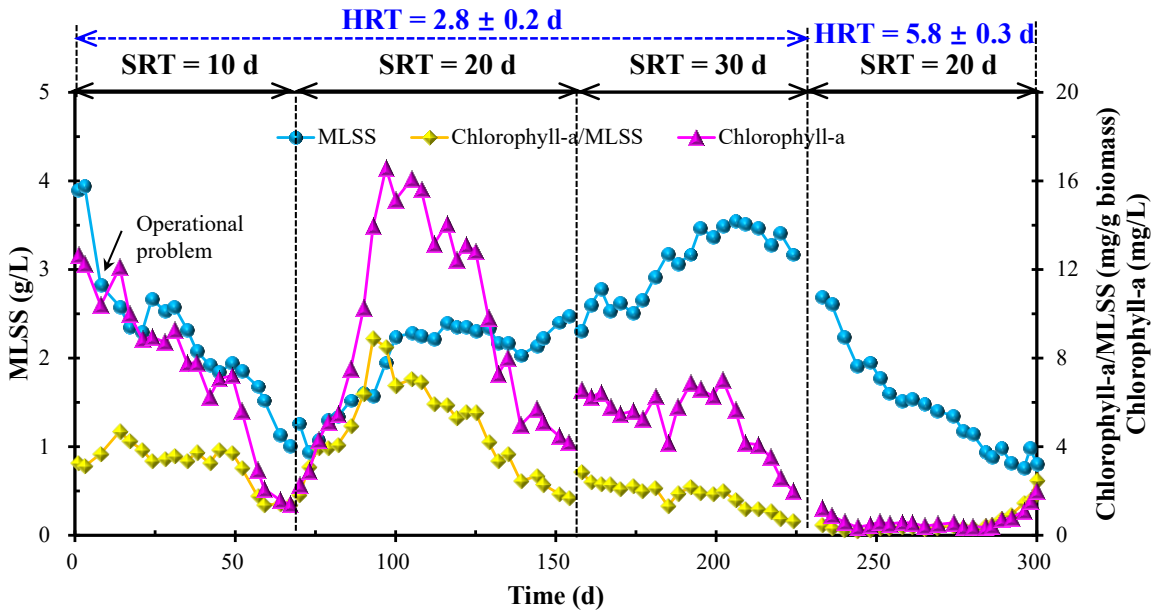

Figure 5-2 Variations of biomass concentration, chlorophyll-a/MLSS, and chlorophyll-a concentration in the MB-MPBR under different SRTs.

5.3.2 Effects of SRT on COD, TN, and TP removal

Figure 5-3 displays the removal efficiencies of COD, TN, and TP as well as their concentration in influent and effluent under different SRTs. As shown in Figure 5-3(a), the influent COD concentration maintained at constant throughout the entire study period. Overall, a good COD removal efficiency of about 90% was observed at all three SRTs (Table 5-2). However, it must be noted that with the increase in SRT, a lower COD removal rate was found during the steady period (Table 5-2), although the impact of SRT was not significant. It is reasonable because the applied organic loading rate in this study was in the range of 396.17-403.60 mg/L/d, which was much lower than that in typical MBR systems (Lin et al., 2013; Ozgun et al., 2013).

As shown in Figure 5-3, the influent TN concentration maintained at a relatively constant value of 136.79 ± 8.20 mg/L. The effluent TN concentration continuously increased in at SRT of 10 d. At SRTs of 20 d and 30 d, it fluctuated significantly in the initial periods and then stabilized at an average value of 106.72 ± 6.06 and 121.10 ± 2.52 mg/L, respectively. The average TN removal efficiency at the last two weeks was 18.05 ± 9.96, 19.26 ± 4.58, and 14.60 ± 1.78 mg/L for Phases 1, 2, and 3, respectively. The lowest TN removal efficiency was observed at an SRT of 30 d, which might be attributed to the deteriorated status of microalgae growth (Figure 5-2) (reduced microalgae and increased bacteria levels). In comparison, it was found the variation trend

of TN removal efficiency was consistent with that of the chlorophyll-a concentration, indicated that nitrogen in the wastewater was mainly removed through microalgae assimilation. Similar results were also reported in previous studies (Gao et al., 2016; Praveen & Loh, 2019; Xu et al., 2015). Therefore, as for MB-MPBR system, there existed a critical SRT above which the increase in SRT would weaken microalgae growth and nitrogen removal due to the decrease in light accessibility. That is, too short or too long SRT is not conducive to the healthy growth of microalgae and the effective removal of nitrogen in MB-MPBR. A moderate SRT value in the range of 10-20 d should be the optimal SRT for MB-MBPR system.

Figure 5-3(c) demonstrates the variation of TP removal efficiency and concentrations in influent and effluent under different SRTs. The influent TP concentration varied in the range of 22.12-27.67 mg/L (average 24.63 ± 1.13 mg/L) throughout the experimental period. The effluent TP concentration first rose then fluctuated significantly at SRT of 10 d, while maintained relatively constant at SRTs of 20 and 30 d. Based on the data of last two weeks, the average TP concentration in the effluent was calculated to be 17.96 ±1.80, 12.81 ± 1.47, and 10.97 ± 1.06 mg/L for SRTs of 10, 20, and 30, respectively. The corresponded removal efficiency was 28.38 ± 7.16%, 48.36 ± 5.91%, and 54.95 ± 4.36% for SRTs of 10, 20, and 30, respectively. Unlike TN, the TP removal enhanced with the prolonged SRT. Moreover, the variation trend of TP removal efficiency was inconsistent with that of the chlorophyll-a concentration. It suggested that except for microalgae assimilation, other pathways also contributed to the removal of TP in the studied MB-MPBR. Some previous studies reported that precipitation and surface-adsorption are another two mechanisms for phosphorus removal (Beuckels et al., 2015; Derakhshan et al., 2018; Xu et al., 2014; Xu et al., 2015). As shown in Table 5-2, the mixture suspension pH kept around 7.0 over the experimental period. Therefore, phosphorus precipitation should not be the main contributor to the improved phosphorus removal because it generally occurs at the alkaline condition. From Fig. 5-3c and Fig. 5-2, the variation trend of effluent TP concentration was opposite to that of the MLSS, indicating that the enhanced phosphorus removal should be resulted from the phosphorus adsorption by biomass.

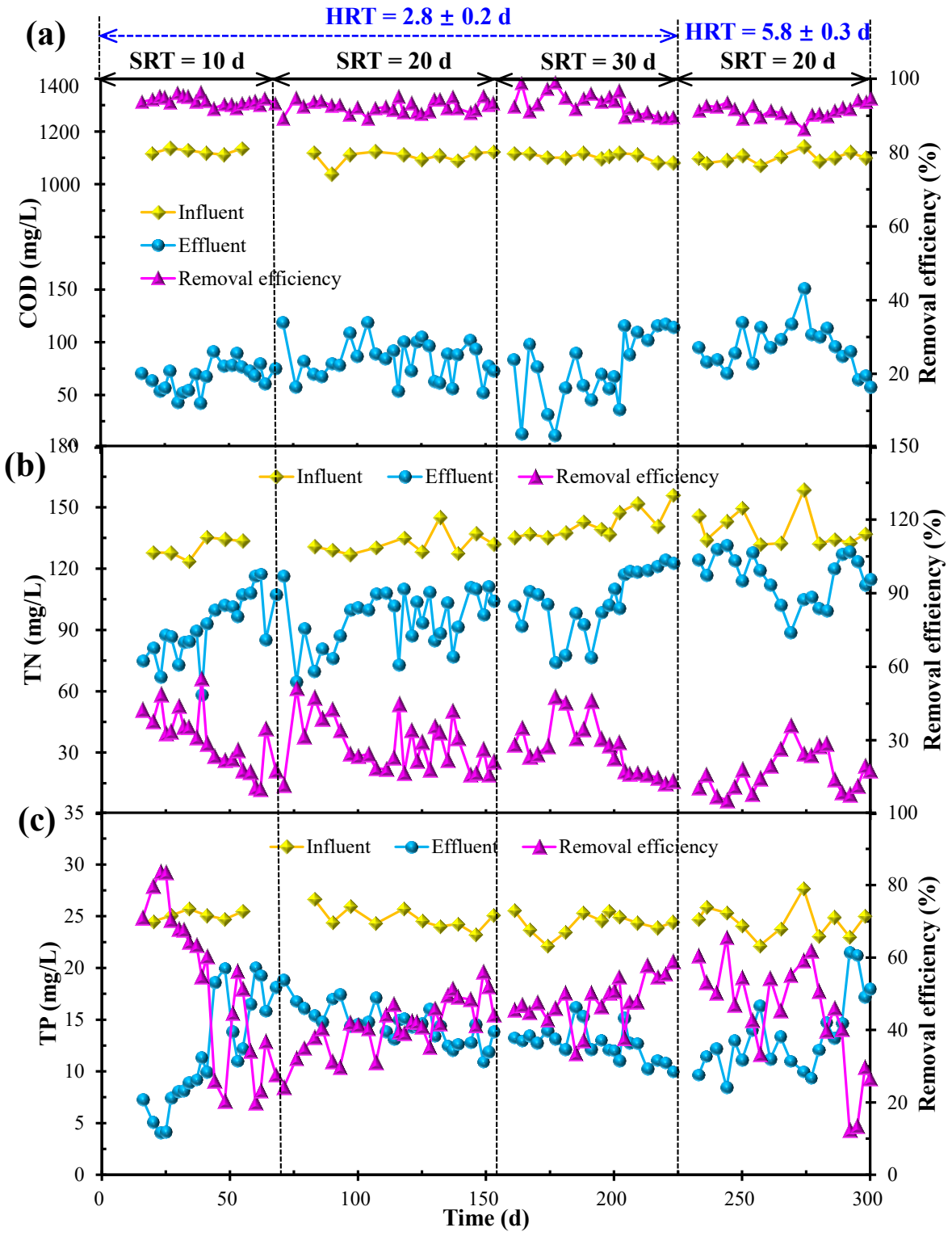

Figure 5-3 Effects of SRT on the biological performance of the MB-MPBR: (a) COD; (b) TN, and (c) TP.

Figure 5-3 also shows pollutants removal performance in Phase 4. As shown in Figure 5-3, the effluent COD, TN, and TP fluctuated throughout the whole phase. The average concentration of COD, TN, and TP in the effluent during the last two weeks was calculated to be 73.85 ± 14.45, 121.12 ± 7.30, and 18.52 ± 2.87 mg/L, respectively (Table 5-2). As compared to the other three phases, the COD removal efficiency at Phase 4 was comparable while TN and TP removal efficiency was much lower. This result indicated that prolonged HRT at Phase 4 did not improve the nutrients removal performance, which was ascribed to the severe imbalance in microalgal and bacterial growth. In other words, the insufficient growth of microalgae led to the low removal efficiency of TN and TP. In addition, the reduction in biomass concentration due to the shortened SRT resulted in a decrease of phosphorus content removed through adsorption. Therefore, optimization of the operating conditions should be conducted before the occurrence of the imbalanced growth of microalgae and bacteria to maintain the stable operation and improve the treatment performance of the MB-MPBR.

The above results showed that SRT had little impact on COD removal, a relative lower COD removal efficiency was achieved under longer SRT. However, the nutrients (N and P) removal was significantly affected by SRT, which was mainly caused by the different MLSS resulted from the variation of SRT. The prosperous growth of microalgae benefited the improvement of nitrogen removal since the nitrogen in the wastewater was mainly removed through microalgae assimilation (Gao et al., 2016; Praveen & Loh, 2019; Xu et al., 2015). Therefore, a medium SRT, which can maintain the healthy and balanced growth of microalgae and bacteria, was considered as the optimal SRT for the achievement of excellent nitrogen removal. Unlike TN, the TP removal efficiency increased with the increase in SRT. That is, the amount of phosphorus removed increased with the rise in biomass concentration. As a result, it can be speculated that surface-adsorption played a vital role in phosphorus removal in this study.

Apparently, MB-MPBR can simultaneously remove COD and nutrients (N and P) from the anaerobically treated malting secondary wastewater. Nevertheless, the obtained effluent did not meet the discharge standards, which was ascribed to the too high concentration of COD, TN, and TP in the influent. According to Equation 5-2, the removal rate of TN was calculated to be 8.45 ± 4.66, 9.14 ± 2.17, and 7.43 ± 0.90 mg/L/d at SRTs of 10, 20, and 30 d, respectively. Correspondingly, the TP removal rate was computed to be 2.55 ± 0.64, 4.30 ± 0.53, and 4.80 ± 0.38 mg/L/d, respectively. In comparison, the removal rate of TN was comparable or lower than

that of the MPBR (Derakhshan et al., 2019; Honda et al., 2017; Praveen & Loh, 2019; Xu et al., 2015), suggesting the negative impact of high nitrogen concentration on microalgae growth and nitrogen removal. Moreover, although the removal efficiency of TP was low, the calculated removal rate was higher than that in the MPBR systems (Derakhshan et al., 2019; Honda et al., 2017; Praveen & Loh, 2019; Xu et al., 2015), demonstrating the critical role of surface-adsorption for phosphorus removal. In brief, The MB-MPBR is a promising technology to treat anaerobically treated malting secondary wastewater. However, it is necessary to prolong the HRT or dilute the feed to achieve effluent quality meets the discharge standards.

5.3.3 Effects of SRT on biological properties of the microalgal-bacterial consortium

Figure 5-4 presents the PSD of the microalgal-bacterial suspensions under different SRTs. As shown in Figure 5-4, the PSD of the four microalgal-bacterial liquors had a similar unimodal shape but different proportion distributions. At SRT of 10 d, the suspended flocs distributed as a sharp peak mainly ranging from 20 to 110 μm. With the increase of SRT from 10 to 20 d, the proportion of the flocs in the range of 20-110 and 110-1000 μm significantly decreased and increased, respectively. A further increase in SRT to 30 d led to a rise in the proportion of small flocs. At Phase 4, the percentage of the small flocs in the range of 5-60 μm further increased. The microscopic observation further demonstrated the variation of the biological floc size for the suspension displayed in Figure 5-5. Apparently, microalgae and bacteria coexisted throughout the operating period. *Chlorella Vulgaris* cells dispersed in the suspension or adhered to the surface of the bacterial flocs at SRT of 10 d, and almost no filamentous bacteria were observed (Figure 5-5(a)). At SRT of 20 d, filamentous bacteria multiplied, more *Chlorella Vulgaris* cells stuck to bacterial flocs and formed microalgal-bacterial symbiotic with larger size (Figure 5-5(b)). At SRT of 30 d, the density of filamentous bacteria and microalgae increased and decreased, respectively (Figure 5-5(c)). Many filamentous fragments were also observed in this phase, which may attribute to the decomposition of filamentous bacterial aggregates (Figure 5-5(c)). In the last phase, filamentous bacteria dominated in the ecosystem, the density of microalgae sharply decreased, and tiny cells were observed (Figure 5-5(d)).

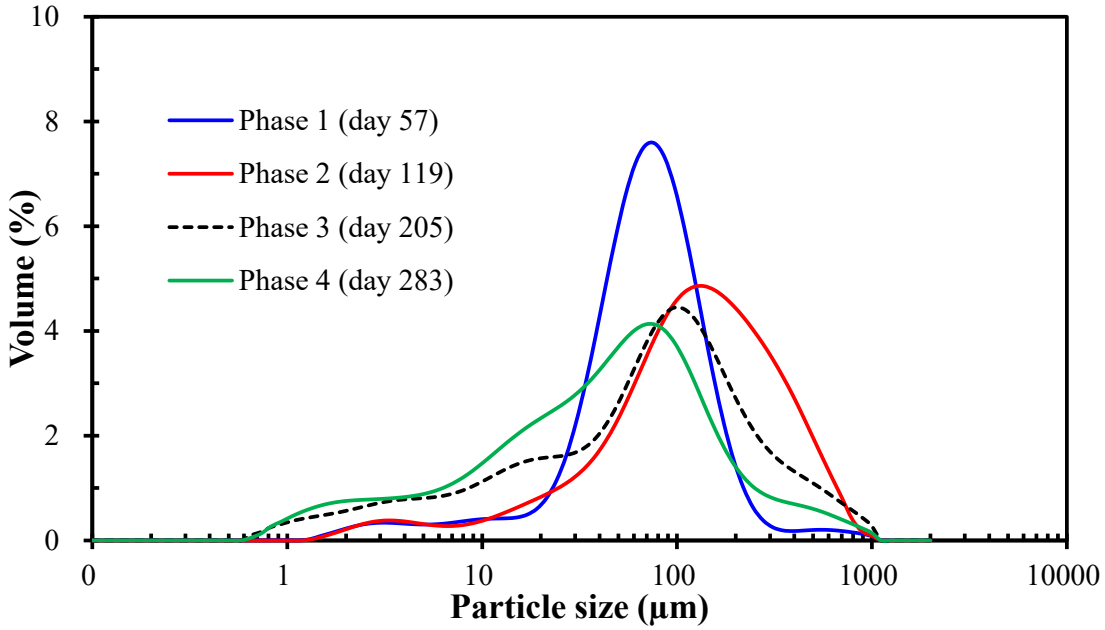

Figure 5-4 Particle size distributions of microalgal-bacterial consortia in the MB-MPBR under different SRTs (SRT = 10, 20, 30, and 20 for Phases 1, 2, 3, and 4, respectively; HRT = 2.8 ± 0.2 d for Phases 1 to 3 and 5.8 ± 0.3 d for Phase 4).

The results of particle size distribution and microscopic morphology jointly demonstrated the critical effect of SRT on the characteristics of microalgal-bacterial interaction. After mixing, the microalgae and bacteria in the MB-MPBR cooperated and competed. Such an interaction varied with SRT due to the variation of biomass concentration and biological community. At SRT of 10 d, the floc-forming bacteria and *Chlorella Vulgaris* dominated in the system. After SRT increased from 10 to 20 d, filamentous bacteria prevailed, and the network structure promoted the attachment of *Chlorella Vulgaris* cells and the formation of large flocs. At SRT of 30 d, a further increase in biomass concentration enhanced the light shading effect. As a result, the competitiveness of microalgae reduced, and more filamentous bacteria accumulated in the reactor. Nevertheless, the increased density of filamentous bacteria also strengthened the intra-species competition, resulting in the death and lysis of some filamentous bacteria. It is a reasonable explanation for the filamentous fragments and the increased proportion of small size particles observed at Phase 3.

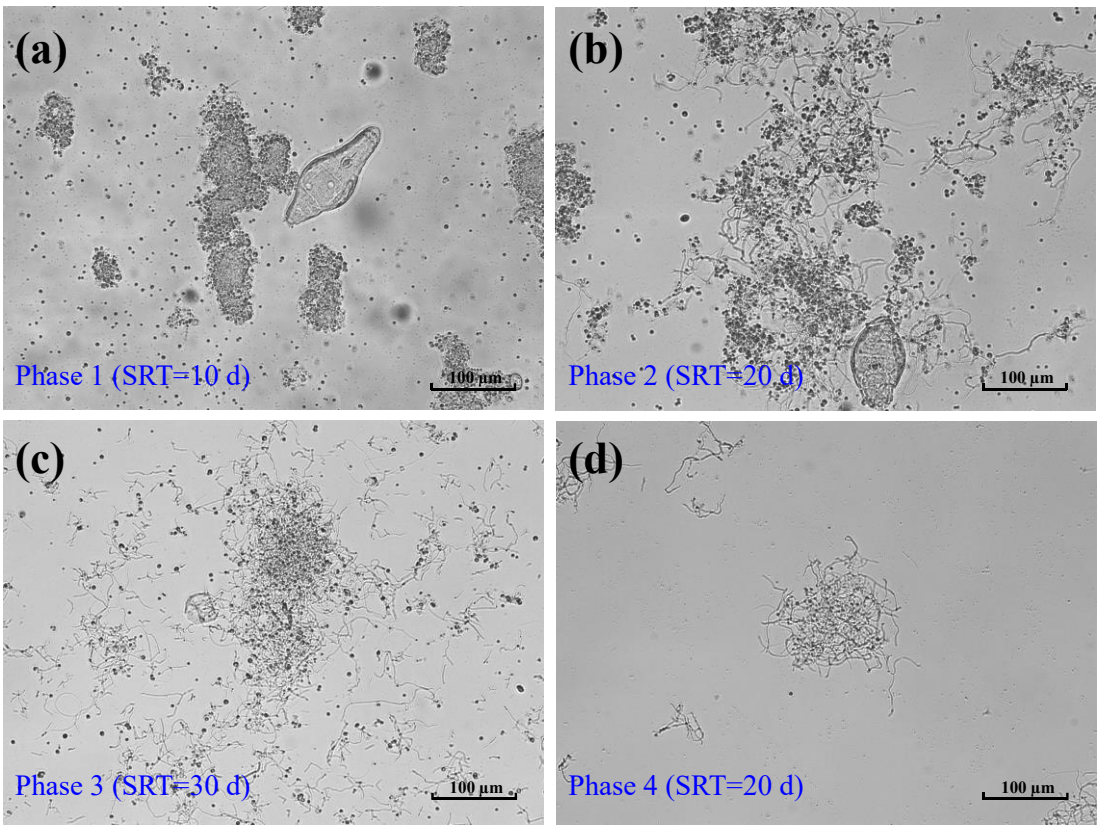

Figure 5-5 Microscopic images for micromorphology of the microalgal-bacterial consortia in the MB-MPBR at (a) Phase 1 (day 57), (b) Phase 2 (day 119), (c) Phase 3 (day 205), (d) Phase 4 (day 283) (HRT = 2.8 ± 0.2 d for Phases 1 to 3 and 5.8 ± 0.3 d for Phase 4).

5.4 Conclusions

This study showed that longer SRT led to higher biomass concentration and increased TP removal efficiency, which was attributed to the enhanced surface-adsorption under higher biomass concentration. The TN removal relied on microalgae assimilation, whereas they were nonlinearly correlating to SRT. SRT had little impact on COD removal, while significantly influenced the PSD and microscopic morphology of microalgal-bacterial consortium. High nutrient concentration negatively impacted the microalgae growth and nutrient removal, and thus influent dilution or a longer HRT is required to achieve effluent quality meets the discharge standards. In short, medium SRT in the range of 10-20 d benefits the reliable operation of MB-MPBRs.

5.5 References

Alcántara, C., Domínguez, J. M., García, D., Blanco, S., Pérez, R., García-Encina, P. A., Muñoz, R., 2015. Evaluation of wastewater treatment in a novel anoxic–aerobic algal–bacterial

photobioreactor with biomass recycling through carbon and nitrogen mass balances. *Bioresource Technology*. 191, 173-186.

APHA. 2005. *Standard Methods for the Examination of Water and Wastewater*. *twentieth ed*. American Public Health Association, American Water Works Association, Water Environmental Federation, Washington, USA.

Beuckels, A., Smolders, E., Muylaert, K., 2015. Nitrogen availability influences phosphorus removal in microalgae-based wastewater treatment. *Water Research*. 77, 98-106.

Cai, T., Park, S. Y., Racharaks, R., Li, Y., 2013. Cultivation of Nannochloropsis salina using anaerobic digestion effluent as a nutrient source for biofuel production. *Applied Energy*. 108, 486-492.

Chen, X., Li, Z., He, N., Zheng, Y., Li, H., Wang, H., Wang, Y., Lu, Y., Li, Q., Peng, Y., 2018. Nitrogen and phosphorus removal from anaerobically digested wastewater by microalgae cultured in a novel membrane photobioreactor. *Biotechnology for Biofuels*. 11(1), 190.

Choi, C., Lee, J., Lee, K., Kim, M., 2008. The effects on operation conditions of sludge retention time and carbon/nitrogen ratio in an intermittently aerated membrane bioreactor (IAMBR). *Bioresource Technology*. 99(13), 5397-5401.

Derakhshan, Z., Ehrampoush, M. H., Mahvi, A. H., Dehghani, M., Faramarzian, M., Eslami, H., 2019. A comparative study of hybrid membrane photobioreactor and membrane photobioreactor for simultaneous biological removal of atrazine and CNP from wastewater: A performance analysis and modeling. *Chemical Engineering Journal*. 355, 428-438.

Derakhshan, Z., Mahvi, A. H., Ehrampoush, M. H., Mazloomi, S. M., Faramarzian, M., Dehghani, M., Yousefinejad, S., Ghaneian, M. T., Abtahi, S. M., 2018. Studies on influence of process parameters on simultaneous biodegradation of atrazine and nutrients in aquatic environments by a membrane photobioreactor. *Environmental Research*. 161, 599-608.

Gao, F., Li, C., Yang, Z.-H., Zeng, G.-M., Feng, L.-J., Liu, J.-z., Liu, M., Cai, H.-w., 2016. Continuous microalgae cultivation in aquaculture wastewater by a membrane photobioreactor for biomass production and nutrients removal. *Ecological Engineering*. 92, 55-61.

Han, S.-S., Bae, T.-H., Jang, G.-G., Tak, T.-M., 2005. Influence of sludge retention time on membrane fouling and bioactivities in membrane bioreactor system. *Process Biochemistry*. 40(7), 2393-2400.

Honda, R., Teraoka, Y., Noguchi, M., Yang, S., 2017. Optimization of Hydraulic Retention Time

and Biomass Concentration in Microalgae Biomass Production from Treated Sewage with a Membrane Photobioreactor. *Journal of Water and Environment Technology*. 15(1), 1-11.

Huang, Z., Ong, S. L., Ng, H. Y., 2011. Submerged anaerobic membrane bioreactor for low-strength wastewater treatment: effect of HRT and SRT on treatment performance and membrane fouling. *Water Research*. 45(2), 705-13.

Karya, N. G. A. I., van der Steen, N. P., Lens, P. N. L., 2013. Photo-oxygenation to support nitrification in an algal–bacterial consortium treating artificial wastewater. *Bioresource Technology*. 134, 244-250.

Lee, C. S., Lee, S.-A., Ko, S.-R., Oh, H.-M., Ahn, C.-Y., 2015. Effects of photoperiod on nutrient removal, biomass production, and algal-bacterial population dynamics in lab-scale photobioreactors treating municipal wastewater. *Water Research*. 68, 680-691.

Lin, H., Peng, W., Zhang, M., Chen, J., Hong, H., Zhang, Y., 2013. A review on anaerobic membrane bioreactors: Applications, membrane fouling and future perspectives. *Desalination*. 314, 169-188.

Liu, J., Wu, Y., Wu, C., Muylaert, K., Vyverman, W., Yu, H.-Q., Muñoz, R., Rittmann, B., 2017. Advanced nutrient removal from surface water by a consortium of attached microalgae and bacteria: A review. *Bioresource Technology*. 241, 1127-1137.

Luo, Y., Le-Clech, P., Henderson, R. K., 2017. Simultaneous microalgae cultivation and wastewater treatment in submerged membrane photobioreactors: A review. *Algal Research*. 24, 425-437.

Marcilhac, C., Sialve, B., Pourcher, A.-M., Ziebal, C., Bernet, N., Béline, F., 2015. Control of nitrogen behaviour by phosphate concentration during microalgal-bacterial cultivation using digestate. *Bioresource Technology*. 175, 224-230.

Muñoz, R., Jacinto, M., Guieysse, B., Mattiasson, B., 2005. Combined carbon and nitrogen removal from acetonitrile using algal–bacterial bioreactors. *Applied Microbiology and Biotechnology*. 67(5), 699-707.

Nautiyal, P., Subramanian, K. A., Dastidar, M. G., 2014. Production and characterization of biodiesel from algae. *Fuel Processing Technology*. 120, 79-88.

Oswald, W. J. 1988. Micro-algae and waste-water treatment. in: *Micro-algal Biotechnology*, (Eds.) Borowitska, M. A., Borowitzka, L. J., Cambridge, pp. 305-328.

Ouyang, K., Liu, J. X., 2009. Effect of sludge retention time on sludge characteristics and

membrane fouling of membrane bioreactor. *Journal of Environmental Sciences-China*. 21(10), 1329-1335.

Ozgun, H., Dereli, R. K., Ersahin, M. E., Kinaci, C., Spanjers, H., van Lier, J. B., 2013. A review of anaerobic membrane bioreactors for municipal wastewater treatment: Integration options, limitations and expectations. *Separation and Purification Technology*. 118(0), 89-104.

Park, J., Jin, H.-F., Lim, B.-R., Park, K.-Y., Lee, K., 2010. Ammonia removal from anaerobic digestion effluent of livestock waste using green alga Scenedesmus sp. *Bioresource Technology*. 101(22), 8649-8657.

Praveen, P., Guo, Y., Kang, H., Lefebvre, C., Loh, K.-C., 2018. Enhancing microalgae cultivation in anaerobic digestate through nitrification. *Chemical Engineering Journal*. 354, 905-912.

Praveen, P., Loh, K.-C., 2019. Nutrient removal in an algal membrane photobioreactor: effects of wastewater composition and light/dark cycle. *Applied Microbiology and Biotechnology*.

State Environmental Protection Administration of China, 2002. Monitoring and analysis methods of water and wastewater (4th edition). China Environmental Science Press, Beijing.

Sun, L., Tian, Y., Zhang, J., Cui, H., Zuo, W., Li, J., 2018a. A novel symbiotic system combining algae and sludge membrane bioreactor technology for wastewater treatment and membrane fouling mitigation: Performance and mechanism. *Chemical Engineering Journal*. 344, 246-253.

Sun, L., Tian, Y., Zhang, J., Li, H., Tang, C., Li, J., 2018b. Wastewater treatment and membrane fouling with algal-activated sludge culture in a novel membrane bioreactor: Influence of inoculation ratios. *Chemical Engineering Journal*. 343, 455-459.

Sun, L., Tian, Y., Zhang, J., Li, L., Zhang, J., Li, J., 2018c. A novel membrane bioreactor inoculated with symbiotic sludge bacteria and algae: Performance and microbial community analysis. *Bioresource Technology*. 251, 311-319.

Van Thuan, N., Thi Thanh Thuy, N., Hong Hai, N., Nguyen, N. C., Bui, X.-T., 2018. Influence of microalgae retention time on biomass production in membrane photobioreactor using human urine as substrate. *2018*. 60(4), 5.

Xie, B., Gong, W., Yu, H., Tang, X., Yan, Z., Luo, X., Gan, Z., Wang, T., Li, G., Liang, H., 2018. Immobilized microalgae for anaerobic digestion effluent treatment in a photobioreactor-ultrafiltration system: Algal harvest and membrane fouling control. *Bioresource Technology*. 268, 139-148.

Xu, M., Bernards, M., Hu, Z., 2014. Algae-facilitated chemical phosphorus removal during high-density Chlorella emersonii cultivation in a membrane bioreactor. *Bioresource Technology*. 153, 383-387.

Xu, M., Li, P., Tang, T., Hu, Z., 2015. Roles of SRT and HRT of an algal membrane bioreactor system with a tanks-in-series configuration for secondary wastewater effluent polishing. *Ecological Engineering*. 85, 257-264.

Yang, J., Gou, Y., Fang, F., Guo, J., Ma, H., Wei, X., Shahmoradi, B., 2018. Impacts of sludge retention time on the performance of an algal-bacterial bioreactor. *Chemical Engineering Journal*. 343, 37-43.

Zhang, M., Yao, L., Maleki, E., Liao, B.-Q., Lin, H., 2019. Membrane technologies for microalgal cultivation and dewatering: Recent progress and challenges. *Algal Research*. 44, 101686.

Chapter 6 Effects of Solids Retention Time on Biomass Properties and Membrane Fouling of the Microalgal-Bacterial Membrane Photobioreactor (MB-MPBR)

Abstract: In this study, a microalgal-bacterial membrane photobioreactor (MB-MPBR) was operated treating synthetic anaerobic digestion effluent at three SRTs of 10, 20, and 30 d to investigate the biomass properties and membrane fouling over 300 days. Results showed that membrane fouling rate in MB-MPBR was nonlinearly correlated to SRT, and the highest membrane fouling was observed at SRT of 20 d. From the characterization of the mixed liquor suspensions, the functional groups of the samples from different SRTs were not significantly different. XPS results showed a significant difference in the surface composition of the microalgal-bacterial consortium at different SRTs. The biological flocs at SRT of 20 d had the largest floc size, moderate filament abundance, and the highest concentration of bound EPS and SMP. The highest membrane fouling at SRT of 20 d was mainly attributed to the higher concentration of EPS and SMP. Environmental stress and fierce competition between microalgae and bacteria were considered as the underlying reason for the increased production of EPS and SMP. The predominant fouling mechanism was gel layer formation. In brief, optimizing the SRT value to control the balanced growth of microalgae and bacteria and keep them at an appropriate ratio is the key to delay membrane fouling in MB-MPBR.

Keywords: Microalgal-bacterial membrane photobioreactor; SRT; Characterization; Membrane fouling

6.1 Introduction

The microalgal-bacterial consortium can simultaneously remove organics carbon and nutrients (N and P) from the sewage and thus has been widely applied in wastewater treatment (Alcántara et al., 2015; Gutzeit et al., 2005; Lee et al., 2015; Posadas et al., 2013; Tang et al., 2010). In recent years, microalgal-bacterial membrane photobioreactor (MB-MPBR), a novel modified MBR system combining the microalgal-bacterial biodegradation step with a membrane filtration module, has been proposed and applied for wastewater treatment (Sun et al., 2018a; Sun et al., 2018b; Sun et al., 2018c; Yang et al., 2018). In comparison to conventional membrane bioreactor (MBR) process, many advantages including enhanced nutrient removal efficiency, lower aeration energy consumption, and reduced membrane fouling can be enumerated for this system (Sun et al., 2018a; Sun et al., 2018c). However, membrane fouling is an inevitable problem that would restrict further development and widespread application of MB-MPBR. Therefore, investigation on the fouling performance of the membrane in MB-MPBR is significantly important.

Membrane fouling is a complex phenomenon caused by the unwanted deposition of particles, organics, and inorganics on the membrane surface (Aslam et al., 2017; Chen et al., 2020; Wang et al., 2014). It was directly or indirectly affected by numerous factors, including PSD, flocs morphology, EPS, and SMP (Erkan et al., 2016; Li et al., 2019; Lin et al., 2014; Zhang et al., 2015). In general, all these factors have a close correlation to various operating conditions, i.e. HRT, OLR, and SRT (Huang et al., 2011; Xue et al., 2015). Among these operating conditions, SRT is one of the most crucial operational parameters. In fact, SRT itself has no direct impact on membrane fouling. However, it does influence the biological properties of the biomass. It is well accepted that longer SRT corresponds to higher MLSS. Also, the floc size and microbial community are influenced by SRT (Ahmed et al., 2007; Ng & Hermanowicz, 2005; Su et al., 2011). Moreover, numerous studies have reported that SRT had critical effects on the production of EPS and SMP (Annop et al., 2014; Dereli et al., 2014; Duan et al., 2014; Faust et al., 2014; Fu et al., 2017; Hasani Zonoozi et al., 2015; Van den Broeck et al., 2012).

In MB-MPBR, the addition of microalgae led to a more complex ecological environment and population interaction. The microalgae and bacteria in the system are cooperative and competitive (Liu et al., 2017). The variation of SRT can not only affect the total concentration of the microalgal-bacterial consortium but also regulate the relative content and interaction between them. As two

types of microorganisms with different growth modes, microalgae and bacteria have different requirements for the environmental conditions. For example, prolonged SRT benefited the stabilization of bacteria but may significantly impede the growth of microalgae due to photo limitation. Under environmental stress, the microalgae/bacteria would produce more EPS and SMP to prevent them from harm (Zhang et al., 2016). Overall, the complex biological community and population interaction in MB-MPBR generally correspond to more complex membrane contaminants, which may lead to more complicated interactions with the membrane. Consequently, it is necessary to understand membrane fouling of the novel MB-MPBR system and develop targeted fouling control strategies. However, to our knowledge, the information regarding membrane fouling in MB-MPBR systems are limited, and no studies have been conducted to investigate the impact of SRT on biomass properties and membrane fouling in MB-MPBR, as the research and development of MB-MPBR are still in its very early stage.

This study, therefore, intended to investigate the effects of SRT (10, 20, and 30 d) on membrane fouling of an MB-MPBR system treating a synthetic anaerobic digestion effluent with high COD and nutrients (N and P) concentrations. The biological performance (biomass concentration, COD removal, and nutrients removal) of the MB-MPBR were reported in Chapter 5. Characterizations of the membrane performance of the MB-MPBR and sludge properties, including TMP, filtration resistance composition, PSD, micromorphology, SMP, EPS, XPS, and FTIR, were conducted and the role of sludge properties in membrane fouling was investigated.

6.2 Material and methods

6.2.1 MB-MPBR set-up and operation

The lab-scale submerged MB-MPBR set-up, as shown in Figure 5-1 (Chapter 5), had a working volume of 9.64 L. A flat sheet membrane module (supplied by SINAP Co. Ltd., Shanghai, China) was used for solid-liquid separation. The general characteristics of the membrane module and the basic operating parameters of the MB-MPBR are displayed in Table 6-1 and Table 6-2, respectively. Air containing 0.05% CO_2 was provided by an aeration pump to generate shear force for membrane fouling control. Moreover, a magnetic stirrer (Model 6795-61, Corning, USA) was placed at the reactor bottom to prevent biomass settling through gentle stirring. Continuous illumination was provided by four LED lamps placed outside the reactor. Pre-cultivated *Chlorella Vulgaris* and activated sludge were inoculated with an initial microalgal and bacterial

concentration of 1.02 and 3.06 g/L (1:3), respectively. The activated sludge (bacteria) seed was from an activated sludge plant treating pulp and paper wastewater from a local pulp and paper mill. The permeate was intermittently obtained by a peristaltic pump with an operational cycle of 3 min suction followed by 2 min relaxation.

Table 6-1 Specifications of the membrane module used in this study.

Module specification	Value
Total membrane surface area	0.03 m^2
Membrane materials	Polyvinylidene fluoride (PVDF)
Membrane type	Flat sheet
Mean membrane pore size	0.1 μm

Table 6-2 Basic operating parameters of the MB-MPBR.

Operating parameter	Value
Aeration rate	3.39 ± 0.16 L/min
Illumination intensity	8400 lux
Operating temperature	26.7-28.2 ℃
Operating pH	6.8-7.2
Flux	6.68 ± 0.32 L/(h·m^2)

The composition of the feed was listed in Table 5-1. The influent concentration of COD, TN, and TP were 1106.17 ± 20.05, 136.72 ± 8.17, and 24.63 ± 1.13 mg/L, respectively. The reactor was operated in sequence with three SRTs of 10, 20, and 30 d. The average MLSS concentration at the last two weeks was 1.34 ± 0.32, 2.25 ± 0.18, and 3.40 ± 0.15 g/L for SRTs of 10, 20, and 30 d, respectively. When the TMP reached 30 kPa, physical cleaning was conducted to recover the membrane permeability. At the end of each phase, permeability measurements were conducted, and a new membrane was used at the transition of phase.

6.2.2 Evaluation of membrane filtration resistance

The evaluation of membrane filtration resistance was conducted according to Darcy's law as follows (Lin et al., 2009):

$$R = \frac{\Delta P}{J\mu} \quad (6\text{-}1)$$

$$R_t = R_m + R_p + R_g \quad (6\text{-}2)$$

where, R represents the filtration resistance; ΔP is the trans-membrane pressure difference; J signifies the permeate flux; μ represents the permeate dynamic viscosity; R_t is the total filtration resistance; R_m, R_p, and R_g represent the filtration resistance of virgin membrane, pore-clogging, and gel layer, respectively. The procedure of the measurement for each resistance can refer to Section 4.2.2.

6.2.3 Analytical methods

6.2.3.1 Floc morphology and filamentous microorganisms

The micromorphology of the microalgal-bacterial consortium was observed and recorded by an inverted optical microscope (Olympus IX51, Japan) at the same time for quantification of filaments. For each sample, at least 30 images were randomly taken by a digital camera connected with the microscope.

The abundance of filamentous bacteria was determined based on the classification criteria previously reported (Jenkins et al., 2004). The number of 0 to 5 represents the abundance level of low to high.

6.2.3.2 Floc size distribution

The floc size distribution of the suspension was measured by a Malvern Mastersizer 2000 instrument (Worcestershire, UK) with a detection range of 0.02-2000 μm. Each sample was automatically measured in triplicate.

6.2.3.3 SMP and EPS extraction and analysis

SMP was prepared by centrifuging microalgal-bacterial suspension at 4,000 × g for 10 min and then filtrating the supernatant through 0.45 μm filter paper.

The bound EPS was extracted by a CER (Dowex^{TM} Marathon^{TM} C, Na^+ form, Sigma-Aldrich, Bellefonte, PA) method (Frølund et al., 1996). The microalgal-bacterial suspension with 0.25 g biomass was taken and centrifuged (Eppendorf Centrifuge 5430, Germany) at 4,000 × g for 10 min. After discarded the supernatant, the pellets were washed with a buffer solution and then centrifuged at 10,000 × g for 10 min. The buffer solution contained 2 mM Na_3PO_4, 4 mM NaH_2PO_4,

9 mM NaCl and 1 mM KCl at pH 7.0 (Frølund et al., 1996). The pellets were resuspended into the above buffer and then transferred into an extraction beaker containing 20 g clean CER (80 g/g MLSS). The beaker was put in an ice-water bath and stirred for 2 h. The supernatant obtained after centrifugation (18,700 × g for 20 min) was regarded as bound EPS (Lin et al., 2009).

The total SMP and bound EPS were normalized as the sum of protein and carbohydrates. The contents of protein and carbohydrates were determined colorimetrically according to Lowry's method and Gaudy's method, respectively (Gaudy, 1962; Lowry et al., 1951).

6.2.3.4 Surface composition analysis by XPS

An XPS spectrometer (AXIS Supra+, Kratos Analytical Ltd., UK) was used to measure the elemental composition on the microalgal-bacterial surface. The samples were pre-dried with a freezer dryer (Labconco Freezone 12, USA) before the measurement. The survey and elemental spectra were taken at low and high resolution, respectively. A software (ESCApe) provided by the company was adopted for data analysis.

6.2.3.5 Molecular composition analysis by FTIR

A Tenthesor 37 FTIR spectrometer (Bruker Optics Inc., Billerica, MA, USA) was used for the determination of the functional groups in the microalgal-bacterial consortium at different SRTs. Prior to the measurement, the suspensions were put into crucibles and heated at 105 ℃ for at least 48 h. The dried samples were then used for FTIR measurement.

6.2.3.6 Other measurements

A gas chromatography instrument (Shimazu, Mondel GC-2014, Japan) was used to determine the CO_2 concentration in the air around the MB-MPBR. Parameters of water quality, including MLSS, COD, TN, and TP, were measured according to the methods applied in Chapter 5.

6.2.4 Statistical analysis

SPSS 17.0 software was used for statistical analysis. An analysis of variance (ANOVA) was used to examine the statistically significant difference ($p < 0.05$) of SMP and EPS concentration at different SRTs. The student t-test was employed to analyze the content difference of the surface chemical composition for the microalgal-bacterial consortium.

6.3 Results and Discussion

6.3.1 MB-MPBR performance

The MB-MPBR system was operated at three different SRTs of 10, 20, and 30 d. The COD removal efficiency was slightly decreased with the increase in SRT (COD removal ranged from 93.66% to 89.87%) (Chapter 5). TP removal was improved under longer SRT due to the enhanced surface-adsorption with higher biomass concentration. TN removal efficiency had the same variation trend as that of the chlorophyll-a concentration since the TN removal relied on microalgae assimilation (Chapter 5). Both microalgae content and TN removal were nonlinearly correlating to SRT, and their highest values were achieved at SRT of 20 d (Chapter 5). These results suggested that MB-MPBR is a promising technology to simultaneously remove COD and nutrients (N and P) from the high strength anaerobically treated malting secondary wastewater. However, appropriate pre-treatment or longer HRT is required to obtain effluent meets the discharge standards due to the high concentration of pollutants in the sewage.

Under the same flux, TMP is proportional to filtration resistance and is a visual indicator for membrane performance. As shown in Figure 6-1, the variation of TMP exhibited two-step rise characteristics, that is, a slow increase of TMP followed by a sudden increase. In comparison, the fastest and slowest membrane fouling was observed at SRT of 20 and 30 d, respectively. This result suggested that SRT had a dramatic impact on membrane fouling in MB-MPBR while the membrane fouling rate was nonlinearly correlating to SRT.

At the end of each SRT operation, the permeability of the fouled membrane was measured after the cleaning. The compositions of the membrane filtration resistances under different SRTs are listed in Table 6-3. Since the ending TMP of each SRT was different, it is unreasonable to evaluate the membrane fouling with the filtration resistances directly. Nevertheless, the determination of filtration resistance can be used to evaluate the dominant fouling mechanism and figure out the contribution of pore-clogging and cake/gel layer to membrane fouling. Figure 6-2 shows that the dominant fouling mechanism was the formation of gel layer (formed from the accumulation of SMPs on membrane surface) rather than cake layer, although a small fraction of cake layer was also observed at SRT of 30 d. As illustrated in Table 6-3, gel layer resistance accounted for the highest proportion of the total resistance despite SRT and further verified that gel layer formation was the dominant fouling mechanism of the MB-MPBR. In addition, the

highest pore-clogging filtration resistance was observed at SRT of 20 d.

It is extensively accepted that membrane fouling formation is directly controlled by the physicochemical properties of biomass. Therefore, a series of characterizations, including floc size, micromorphology, XPS, EPS, SMP, and FTIR, were conducted for the microalgal-bacterial consortium to identify the major contributors to the different membrane performance.

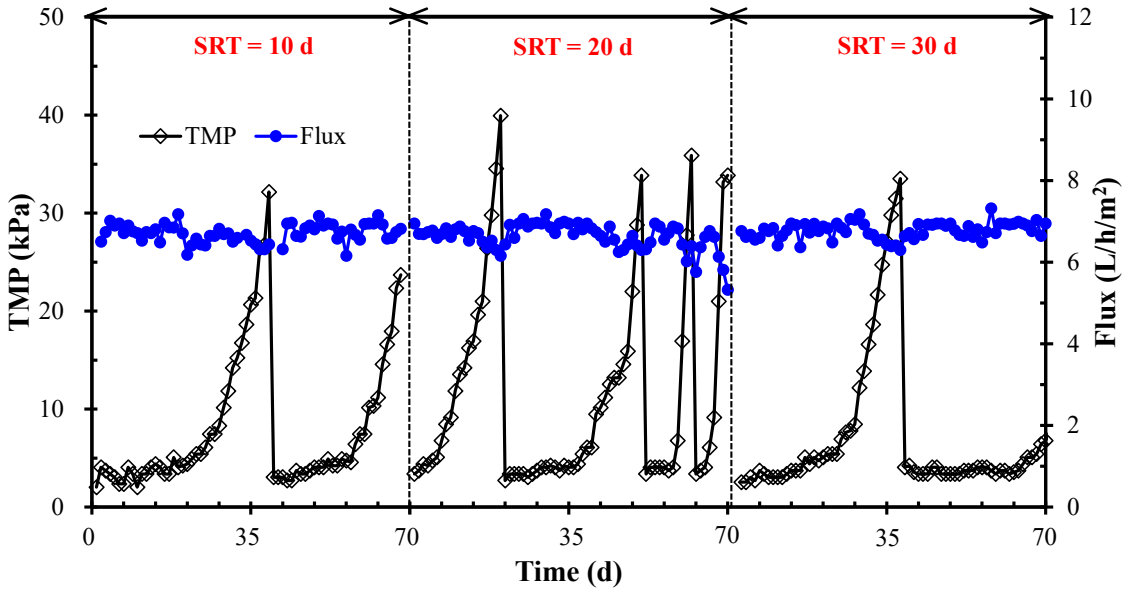

Figure 6-1 Variations of TMP and flux for the MB-MPBR at different SRTs.

Table 6-3 Compositions of membrane filtration resistances under different SRTs.

	R_m ($\times 10^{12}$ m^{-1})	R_p ($\times 10^{12}$ m^{-1})	R_g ($\times 10^{12}$ m^{-1})	R_t ($\times 10^{12}$ m^{-1})
Phase 1	0.479 (3.66%)[a]	1.946 (14.90%)[a]	10.636 (81.44%)[a]	13.060 (100%)[a]
Phase 2	0.475 (1.68%)[a]	3.460 (12.27%)[a]	24.256 (86.04%)[a]	28.190 (100%)[a]
Phase 3	0.464 (10.24%)[a]	0.203 (4.49%)[a]	3.859 (85.27%)[a]	4.526 (100%)[a]

[a] Percentage of the total resistance R_t shown in parentheses.

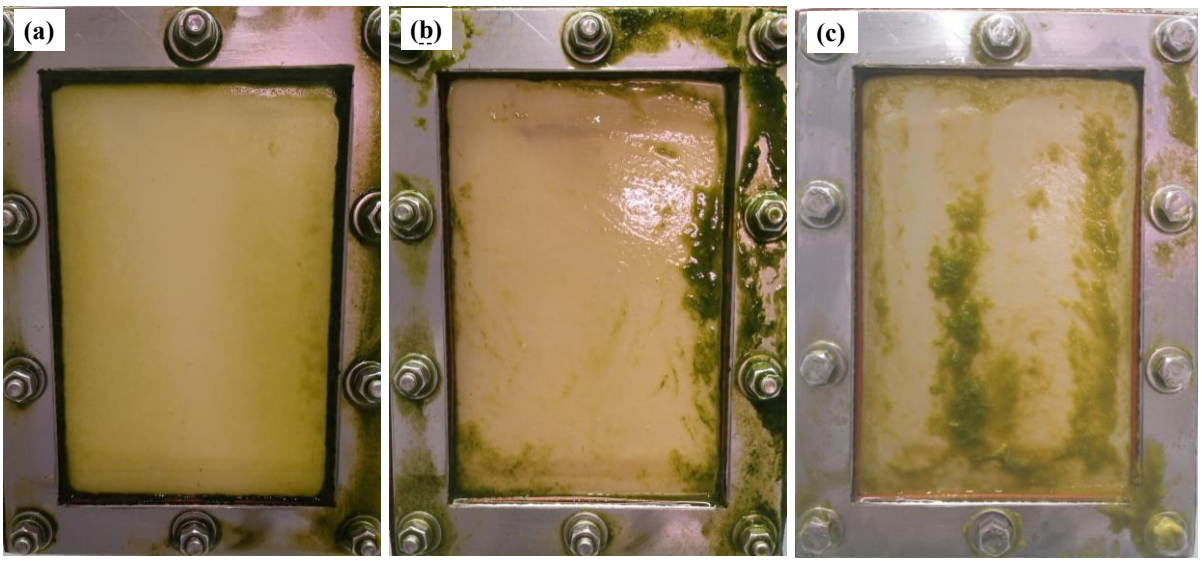

Figure 6-2 Optical images of the fouled membrane at SRT of (a) 10 d, (b) 20 d, and (c) 30 d.

6.3.2 Characterization of the microalgal-bacterial consortium under different SRTs

6.3.2.1 Floc size and morphology

The morphology of microalgal-bacterial consortium was analyzed by PSD and microscopic observation. Figure 6-3 shows the microalgal-bacterial flocs at different SRTs had similar unimodal shape but different proportion distribution. The largest mean particle size of 134.2 μm was found at SRT of 20 d. The difference in floc size was further demonstrated by microscopic observation. As displayed in Figure 6-4, microalgae and bacteria coexisted throughout the experimental period. The morphology of microalgal-bacterial consortium and the abundance of filamentous microorganisms varied with SRT. The biological flocs at SRT of 10 d had a low level (0-1) of filamentous bacteria and small-size *Chlorella Vulgaris* cells dispersed in the suspension or adhered to the surface of bacterial particles (Figure 6-4(a)). The prolonged SRT led to an increased abundance of filamentous bacteria (moderate and excessive level for SRTs of 20 and 30 d, respectively) (Figure 6-4(b-c)). Unlike filamentous bacteria, the density of microalgae increased at SRT of 20 d while sharply decreased at SRT of 30 d. Furthermore, many filamentous fragments were observed at SRT of 30 d, which was attributed to the enhanced interspecies competition of filamentous microorganisms under high biomass concentration. A larger fraction of colloidal particles (0.0.5-10 um) at SRT of 30 d, as compared to that of SRT of 10 and 20 d, also explained the observation (Figure 6-2) of a small fraction of cake layer was formed on the membrane surface, although gel layer formation was the dominant mechanism of membrane fouling at SRT of 30 d,

as smaller colloidal particles would be easily transported to and accumulated on the membrane surface.

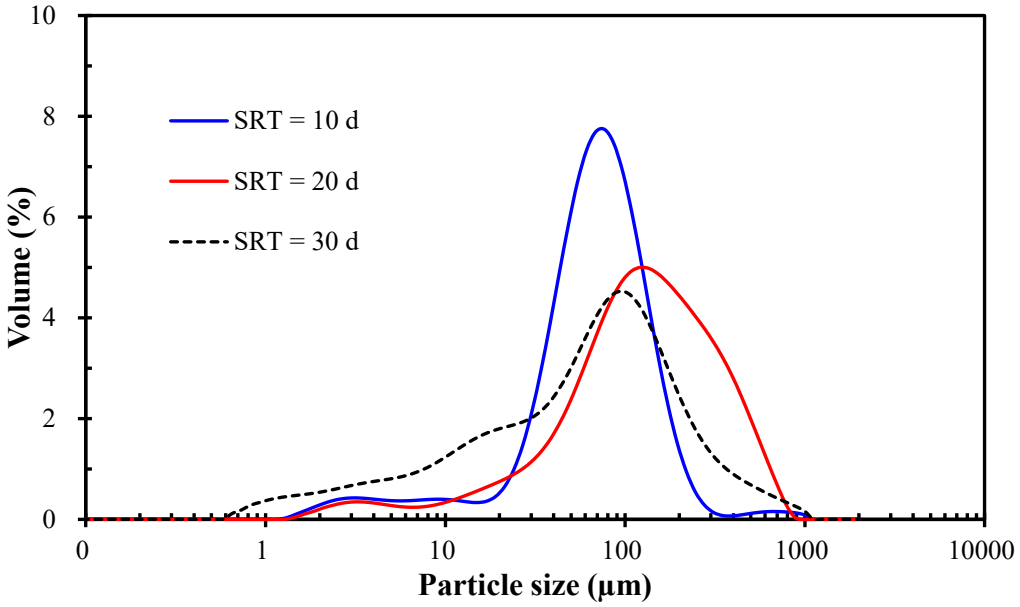

Figure 6-3 Particle size distribution of microalgal-bacterial suspended liquor at different SRTs.

For membrane related systems, particle size is an essential characteristic parameter playing a vital role in biomass filterability and membrane fouling formation (Cao et al., 2015; Wang et al., 2008). It is well accepted that smaller flocs would induce a faster membrane fouling because they can be easier attached to the membrane surface and formed a cake layer with a denser structure (Lin et al., 2009; Shen et al., 2015). Filamentous bacteria also have significant impacts on membrane fouling (Meng et al., 2009; Wang et al., 2010). Generally, a moderate level of filamentous bacteria is beneficial to membrane fouling control because they could serve as a backbone to promote the formation of large flocs (Hao et al., 2016; Meng et al., 2006). However, in this study, the biomass flocs at SRT of 20 had the largest floc size and moderate filament abundance but exhibited the fastest membrane fouling rate, which was inconsistent with other researchers' reports (Shen et al., 2015; Wang et al., 2010) and suggested that other factors, such as bound EPS and SMPs, might be more important than floc size in this case controlling membrane fouling. It is reasonable considering the formation of membrane fouling was not only associated with floc size and filamentous bacteria but also other factors like SMP and EPS. The different

fouling performance at different SRTs should be ascribed to the differences in other properties.

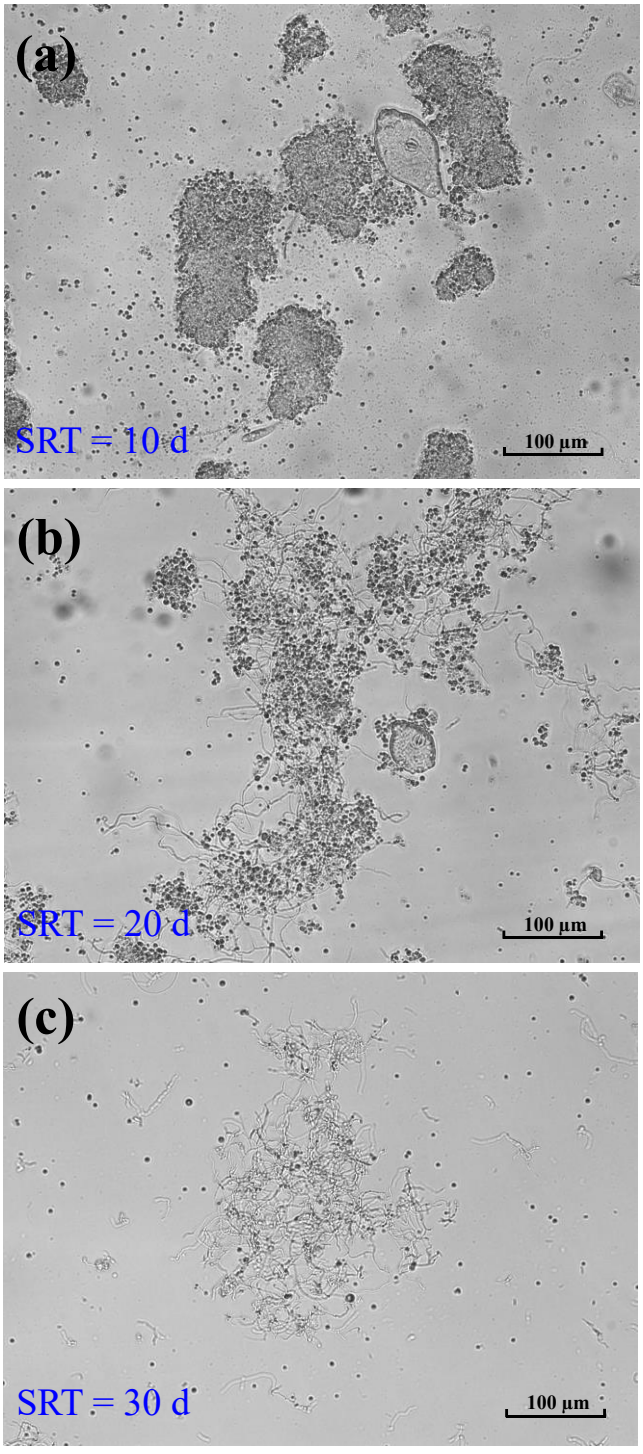

Figure 6-4 Microscopic morphology of microalgal-bacterial flocs at SRT of (a) 10 d, (b) 20 d, and (c) 30 d.

6.3.2.2 Surface composition analysis by XPS

Figure 6-5(a) shows the major elements on the surface of the microalgal-bacterial consortium were composed of C, O, and N. As shown in Figure 6-5(b-c), the C peak resolved into C 1s, C 1sA, C 1sB, and C 1sC can be attributed to four different bonds (Hao et al., 2016; Lin et al., 2011): C-(C, H) existed in lipids or amino acid side chains at a binding energy of 284.8 eV; C-(O, N) associated with ether, alcohol, amine, and amide at a binding energy of 286.3 eV; C=O and O-C-O from amide, carbonyl, carboxylate, ester, acetal, and hemiacetal at a binding energy of 288.5 eV; O=C-OH and O=C-OR at a binding energy of 289.3 eV. The O peak consisted of O 1s, O 1sA, and O 1sB can be attributed to three bonds (Hao et al., 2016; Lin et al., 2011): C-OH from hydroxide and C-O-C from hemiacetal at a binding energy of 530.7 eV; O=C in aldehyde, ketone, and amide at a binding energy of 531.4 eV; and O-C=O from ester, carboxylate, and acid anhydride at a binding energy of 534.0 eV. The N peaks (N 1s and N 1sA) can be decomposed into two different bonds (Hao et al., 2016; Lin et al., 2011): N-C in amide or amine at a binding energy of 400.1 eV and N-H bonds from ammonia or protonated amine at a binding energy of 402.9 eV.

The surface composition measured by XPS can be regarded as the building blocks of the surface polymer molecules. The automatic concentrations of C, O, and N on the surface of the microalgal-bacterial consortium at different SRTs were summarized in Table 6-2. The quantity of total C, O, and N was significantly different between SRT of 10 and 20 d, 30 and 10 d (Student t-test, $p < 0.05$). The microalgal-bacterial consortium at SRT of 10 d had less oxygen, less nitrogen, and more hydrocarbon moieties than that at SRT of 20 and 30 d. Although there was no significant difference in total C and O (Student t-test, $p > 0.05$), significant differences in the quantity of total N and decomposed bonds of C=O, O=C-OH, and C-O-C were observed between SRT of 20 and 30 d (Student t-test, $p < 0.05$). Overall, the XPS result strongly suggested there were significant differences in the surface properties of the microalgal-bacterial consortium at different SRTs.

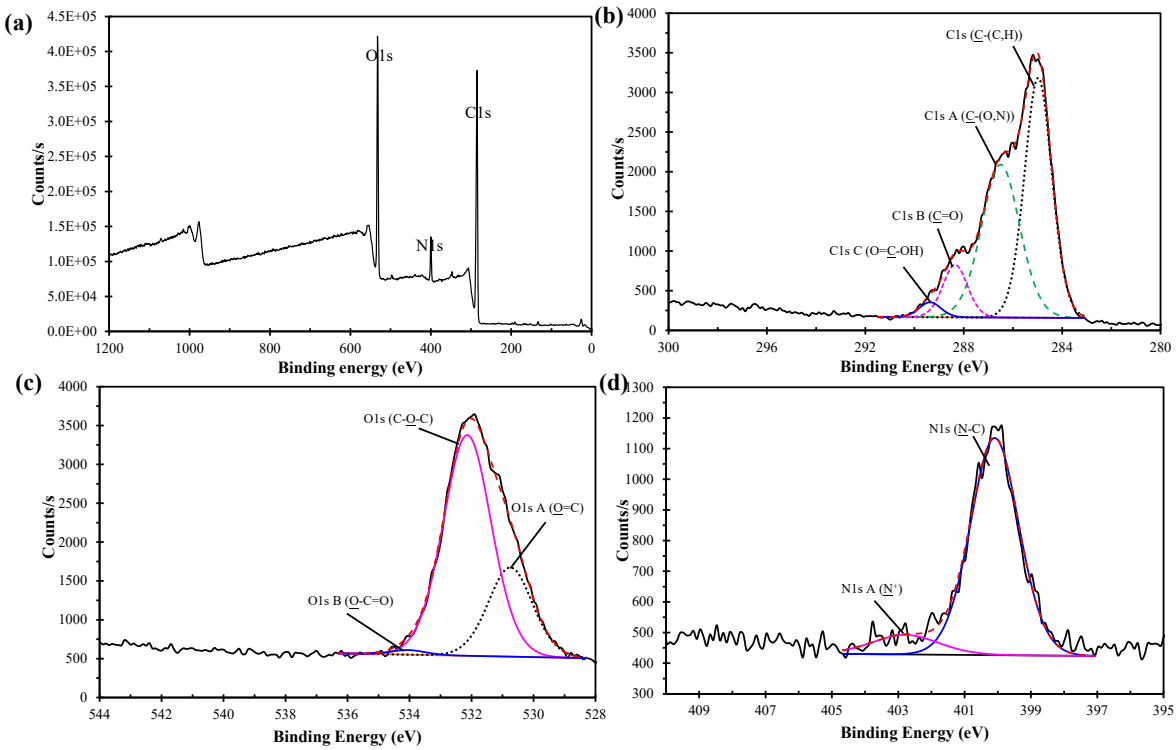

Figure 6-5 XPS spectra of microalgal-bacterial consortium, (a) whole spectra, (b) C1s spectra, (c) O1s spectra, and (d) N1s spectra.

6.3.2.3 EPS production and components

The bound EPS contents of the microalgal-bacterial consortium are illustrated in Figure 6-6. The total EPS were 25.29 ± 3.92, 47.05 ± 5.23, and 25.23 ± 3.15 mg/g MLSS for SRTs of 10, 20, and 30 d, respectively. Statistical analysis using ANOVA showed that the total EPS, carbohydrate, and protein at SRT of 20 d were significantly higher than the other two SRTs (ANOVA, $p < 0.05$). The highest protein content of bound EPS at SRT of 20 d is consistent with the highest total N content on the surface of sludge measured by XPS (Table 6-4). No significant differences were observed between SRT of 10 and 30 d in the content of total EPS, carbohydrate, and protein (ANOVA, $p > 0.05$). In general, higher EPS is associated with more severe membrane fouling (Ding et al., 2015; Kim et al., 2014; Lin et al., 2014; Xuan et al., 2010). In addition to the content of bound EPS, the PN/CH ratio also has significant influences on fouling resistance. In this study, the PN/CH was calculated to be 3.79 ± 1.55, 2.19 ± 0.40, and 3.06 ± 0.73 for SRTs of 10, 20, and 30 d, respectively. Apparently, the lowest and highest PN/CH values were observed at SRT of 20

and 10 d, respectively. Many studies have pointed out that higher PN/CH ratio in bound EPS corresponds to greater membrane fouling because the decreased floc hydrophobicity would promote the formation of the cake layer (Hao et al., 2016; Lee et al., 2003). In this study, the biomass samples possessed the highest bound EPS exhibited the fastest membrane fouling rate, although the PN/CH ratio was the lowest among the three SRTs. Furthermore, with the similar content of bound EPS, the biomass samples at SRT of 10 d showed more serious membrane fouling, which might be ascribed to the higher PN/CH ratio. Together with the current investigation with the results from the literature, it can be concluded that SRT had a notable impact on the concentration and component of bound EPS. The effects of EPS on membrane fouling resulted from the integrated effects of total EPS content and PN/CH ratio. The higher membrane fouling rate at SRTs of 10 and 20 d in Figure 6-1 could be at least partially explained by the higher PN/CH and total EPS concentration, respectively.

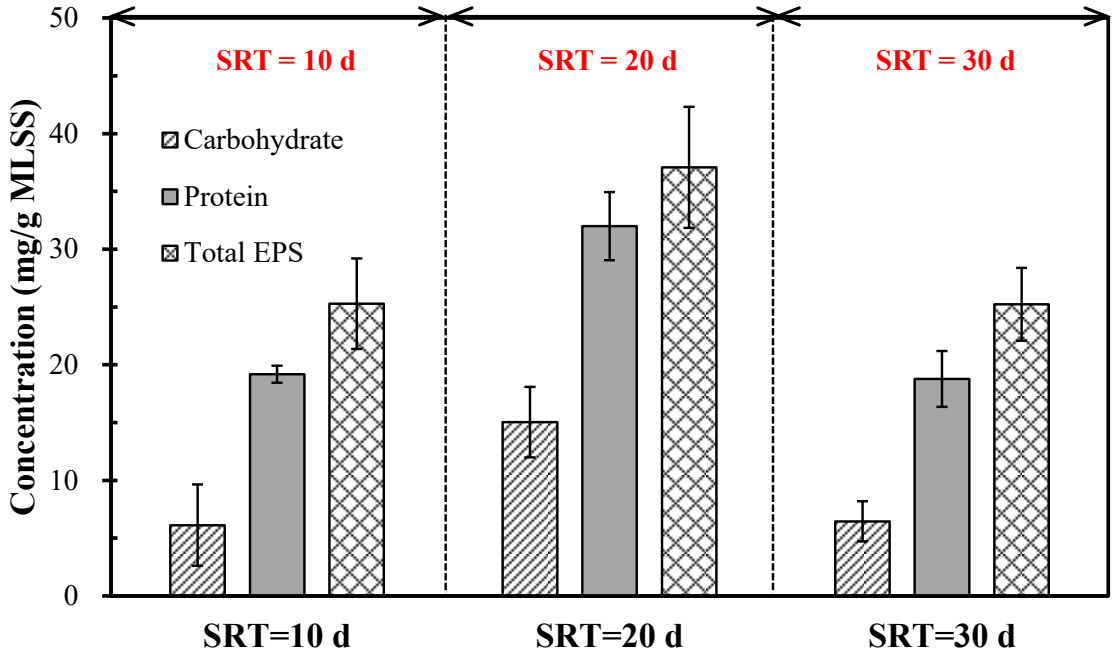

Figure 6-6 Comparison of bound EPS of the microalgal-bacterial consortium at different SRTs.

Table 6-4 Surface composition of the microalgae-sludge consortium determined by XPS: average atom fraction (%) excluding hydrogen.

Element component	SRT			Significant difference[1] of SRT		
	10 d	20 d	30 d	10 d and 20 d	20 d and 30 d	30 d and 10 d
Total C	71.61 ± 1.21	62.14 ± 0.17	61.06 ± 1.91	Y (0.000)	N (0.305)	Y (0.000)
C-(C,H)	35.04 ± 1.17	19.20 ± 1.69	17.64 ± 1.04	Y (0.000)	N (0.167)	Y (0.000)
C-(O,N)	26.42 ± 1.96	29.88 ± 1.39	30.02 ± 0.73	Y (0.016)	N (0.864)	Y (0.008)
C=O	8.28 ± 1.05	11.92 ± 1.05	5.28 ± 0.27	Y (0.001)	Y (0.000)	Y (0.001)
O=C-OH	1.86 ± 0.28	1.13 ± 0.19	8.12 ± 0.47	Y (0.002)	Y (0.000)	Y (0.000)
Total O	20.94 ± 0.66	28.62 ± 0.36	30.18 ± 1.87	Y (0.000)	N (0.151)	Y (0.000)
O=C	5.52 ± 0.48	8.08 ± 0.05	6.36 ± 0.93	Y (0.000)	Y (0.034)	N (0.093)
C-OH and C-O-C	15.16 ± 0.63	20.17 ± 0.43	23.33 ± 1.02	Y (0.000)	Y (0.001)	Y (0.000)
O-C=O	0.26 ± 0.05	0.36 ± 0.05	0.49 ± 0.10	Y (0.028)	N (0.051)	Y (0.001)
Total N	6.06 ± 0.51	7.51 ± 0.16	6.90 ± 0.39	Y (0.001)	Y (0.027)	Y (0.024)
N-C	5.40 ± 0.45	6.54 ± 0.17	5.67 ± 0.31	Y (0.001)	Y (0.003)	N (0.328)
N^+	0.66 ± 0.07	0.97 ± 0.07	1.23 ± 0.10	Y (0.000)	Y (0.005)	Y (0.000)

[1] Sig. value shown in parentheses. Sample number n = 6, 4, and 4 for SRTs of 10, 20, and 30 d, respectively.

6.3.2.4 SMP

Figure 6-7 presents the total SMP, soluble carbohydrate, and protein concentrations at different SRTs. Ranging from the highest amount, the concentration of carbohydrate and total SMP were SRT 20 d > SRT 10 d > SRT 30 d. Nevertheless, the protein content decreased with the increase in SRT. SMP is generally released by bound EPS hydrolysis and cell lysis. The highest value of SMP (28.24 ± 5.06 mg/L) at SRT of 20 d suggested the occurrence of serious decomposition of microalgal-bacterial consortium in that phase, which might be ascribed to the intensive competition between microalgae and bacteria. It was reported that accumulation of SMP in the bioreactors played an important role in permeate flux decline and membrane fouling gel layer formation (Meng et al., 2009; Teng et al., 2020). As the variation trend of TMP and SMP was the same for the three SRTs, it can be speculated that SMP should be an important reason for the different TMP in this study. This is verified by the visual observation of gel layer formation on membrane surfaces (Figure 6-2). Besides, SMP can penetrate into membrane pores due to its small size (Benyahia et al., 2013). As shown in Table 6-3, SMP values had a similar trend as the pore-clogging filtration resistance, indicating that SMP might be the primary contributor to the pore-clogging. As compared to Chapter 4, which suggested the dominant fouling mechanism was cake layer formation in that study, the quantity of SMPs in this study was 2-6 times higher than that in the study of Chapter 4. With such a high SMPs content, the relative importance of floc size and SMPs in controlling membrane fouling changed in this study. SMP played a vital role in controlling gel layer formation on the membrane surface in this study.

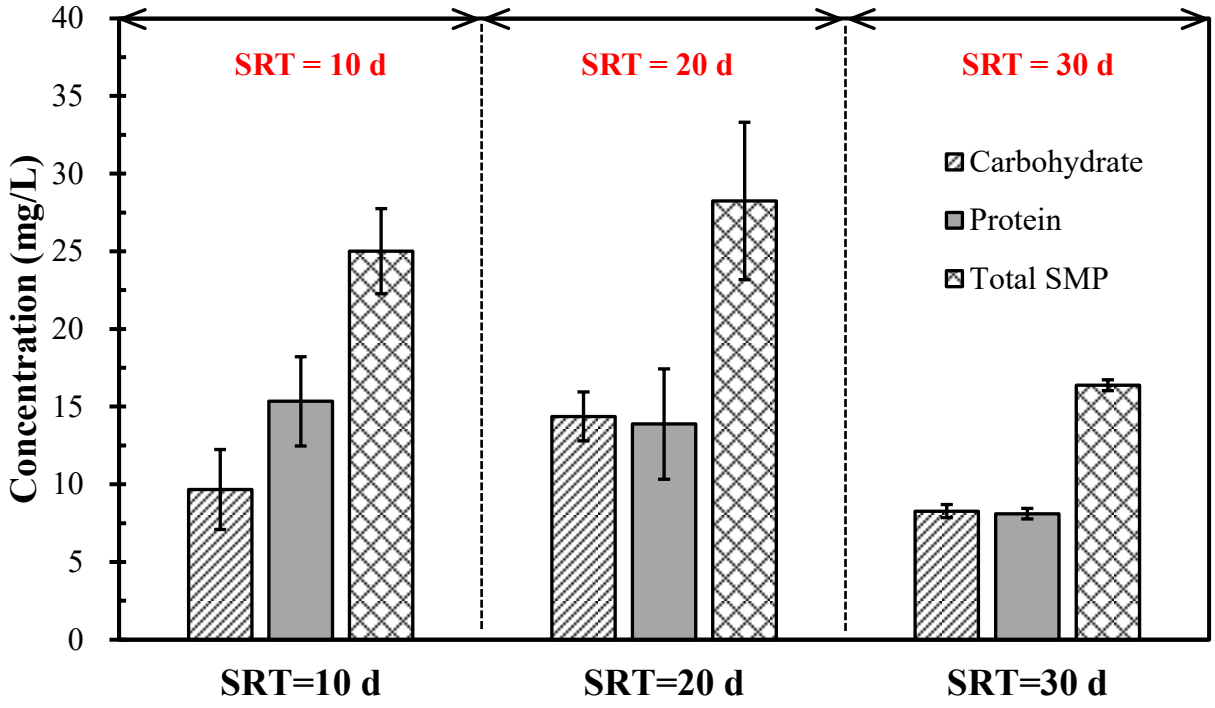

Figure 6-7 Comparison of SMP at different SRTs.

6.3.2.5 FTIR analysis

Figure 6-8 shows the FTIR spectra under different SRTs. All the three samples showed peaks around 3300 cm^{-1} associated with the symmetric stretching of O-H and N-H (Kumar et al., 2019). The bands at approximate 1640 and 1525 cm^{-1} corresponded to the C=O stretching of amides I and N-H bending of amides II belonging to protein groups (Lin et al., 2009). The peak of ~1405 cm^{-1} associated with C-O stretching of COO- groups (Dean et al., 2010). The peaks of 1225 cm^{-1} were due to P=O bonds associated with polysaccharides and nucleic acids (Mayers et al., 2013). The bands at 1030 cm^{-1} were attributed to carbohydrate and polysaccharides (Kumar et al., 2019). The FTIR measurements indicated that there was no great difference in functional groups among the three microalgal-bacterial samples from different SRTs. Therefore, the different fouling performance at different STRs cannot be explained by the difference in functional groups and should be ascribed to other factors.

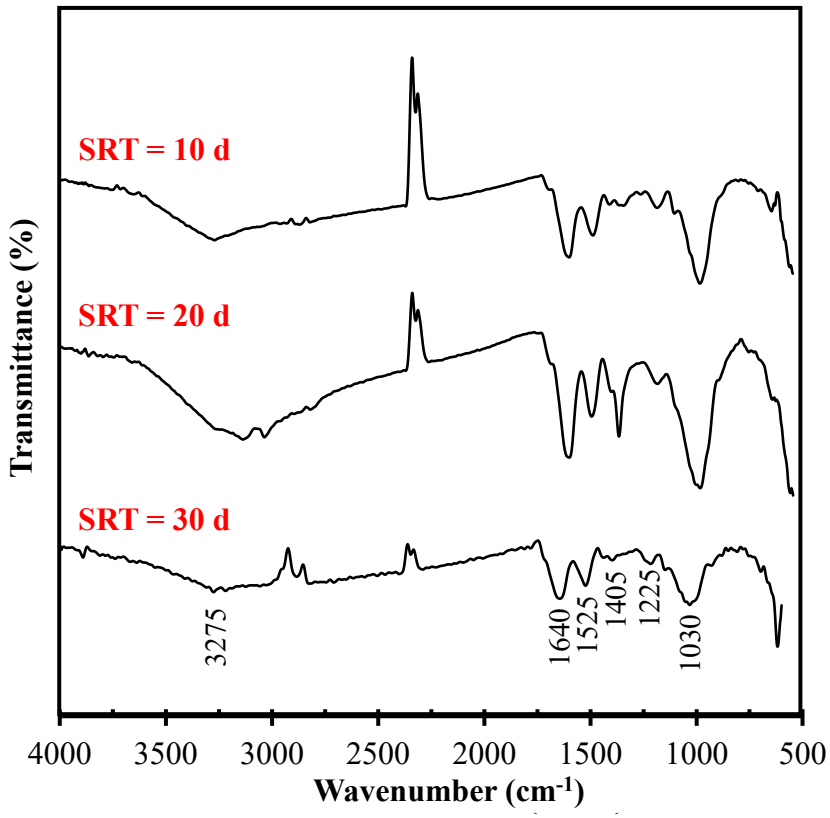

Figure 6-8 FTIR spectra of microalgal-bacterial consortium for the MB-MPBR at different SRTs.

6.3.3 Discussion

The experimental results suggested that SRT significantly affected the properties of microalgal-bacterial consortium and membrane fouling. In this study, the floc sample from SRT of 20 d had larger particle size and moderate filamentous bacteria, while possessed the highest membrane fouling rate. This is inconsistent with the findings reported in the previous literature regarding the effects of particle size and filamentous bacteria on membrane fouling. It is well accepted that larger floc size is in favor of membrane fouling mitigation because they had lower adhesive ability and can form a looser cake layer with higher filterability (Cao et al., 2015; Lin et al., 2009; Shen et al., 2015; Wang et al., 2008). Also, a moderate level of filaments in the biomass can avoid the formation of severe pore blocking and non-porous cake layer, and then retard the formation of membrane fouling (Hao et al., 2016; Meng et al., 2006). However, as shown in Figure 6-2, it was a gel layer instead of a cake layer that formed on the membrane surface. Numerous

studies have reported that gelling foulants, such as SMP and biopolymer clusters (BPC), were the main contributor to gel layer formation (Hong et al., 2014; Lin et al., 2014; Meng et al., 2009). Therefore, although the biomass flocs and gelling foulants coexisted in the MB-MPBR, the effect of floc itself on membrane fouling was negligible. It worth noting that EPS had no direct impacts on gel layer formation. Nevertheless, EPS hydrolysis was an important source of SMP (Li et al., 2013; Zhou et al., 2013). Therefore, the highest SMP concentration at SRT of 20 d should be the primary cause for the fastest membrane fouling at that phase. The difference in EPS content can be regarded as a secondary reason.

Although the SRT significantly influenced membrane fouling in MB-MPBR, the variation trend was different from that of the traditional MBR. In the traditional MBR system, many studies have reported evaluated SRT led to a lower membrane fouling rate because of the lower production of bound EPS, SMP, and colloidal (Liang et al., 2007; Ng & Hermanowicz, 2005; Ouyang & Liu, 2009). However, in this study, the foulants production and fouling rate neither monotonically increased nor decreased with the increasing SRT. The highest concentration of EPS and SMP, as well as membrane fouling rate, was achieved at SRT of 20 d. It suggested that the MB-MPBR had a different response to the variation of operating conditions as compared to that of MBR due to the addition of microalgae. In MB-MPBR, the relationship between microalgae and bacteria is complicated. They are cooperative and competitive. At SRT of 20 d, the growth status of microalgae and bacteria significantly shifted, indicating the competition between microalgae and bacteria was intensive. Apparently, such a turbulent and unfavorable condition promoted the production of EPS and SMP and then exacerbated the formation of membrane fouling. That is, the relatively stable growth of microalgae and bacteria is predominantly important to the membrane fouling control in MB-MPBR.

The above findings give some implications for MB-MPBR development and its membrane fouling control. As reported in the previous publications, the addition of microalgae in MBR favored the biological performance and membrane fouling control (Sun et al., 2018a; Sun et al., 2018c). However, it also makes the system become more complex. The cooperative and

competitive relationship between microalgae and bacteria means the growth of microalgae and bacteria is dynamically balanced. Any biased conditions may cause the unbalanced growth of microalgae and bacteria, which would lead to deteriorated treatment performance and severe membrane fouling. It was reported that too high proportion of microalgae/bacteria (e.g. microalgae/sludge mass ratio of 1:1) would exacerbate the cake layer formation of membrane fouling due to the small microalgal flocs size (Sun et al., 2018b). As shown in this study, the treatment performance worsened at SRT of 30 d owing to the overgrowth of bacteria even though the membrane fouling was decreased. Hence, there should exist an optimized ratio for microalgae and bacteria, under such a status, microalgae and bacteria cooperate, aggregate into a large particle, and possess low fouling propensity. Moreover, the stress from environmental conditions and fierce competition between microalgae and bacteria would stimulate their self-protection mechanism, and then promote the production of protective substances like EPS and SMP (Zhang et al., 2016). Therefore, pre-treatment may be required for the high strength wastewaters before pumping into the MB-MPBR bioreactor. In short, the optimized SRT should be able to control the balanced growth of microalgae and bacteria and keep them at an appropriate ratio. Take the treatment performance into consideration, the optimized SRT for this research should locate in the range of 10-20 d. This study strengthened our knowledge of membrane fouling in MB-MPBR and can guide the design, operation, development, and application of MB-MPBR for high strength wastewater treatment.

6.4 Conclusions

In MB-MPBR, SRT had a significant impact on membrane performance by controlling the biomass concentration and properties and the growth status of microalgae and bacteria. Membrane fouling rate was nonlinearly correlating to SRT. The fastest membrane fouling and highest pore-clogging filtration resistance were observed at SRT of 20 d. Characterization results showed that the biomass flocs at SRT of 20 d had the largest floc size and moderate filament abundance. The higher membrane fouling at SRT of 20 d was mainly attributed to the higher concentration of EPS and SMP. The dominant fouling mechanism in this study was gel layer formation. In brief,

optimizing the SRT value to control the balanced growth of microalgae and bacteria and keep them at an appropriate ratio is the key to delay membrane fouling in MB-MPBR.

6.5 References

Ahmed, Z., Cho, J., Lim, B.-R., Song, K.-G., Ahn, K.-H., 2007. Effects of sludge retention time on membrane fouling and microbial community structure in a membrane bioreactor. *Journal of Membrane Science*. 287(2), 211-218.

Alcántara, C., Domínguez, J. M., García, D., Blanco, S., Pérez, R., García-Encina, P. A., Muñoz, R., 2015. Evaluation of wastewater treatment in a novel anoxic–aerobic algal–bacterial photobioreactor with biomass recycling through carbon and nitrogen mass balances. *Bioresource Technology*. 191, 173-186.

Annop, S., Sridang, P., Puetpaiboon, U., Grasmick, A., 2014. Effect of solids retention time on membrane fouling intensity in two-stage submerged anaerobic membrane bioreactors treating palm oil mill effluent. *Environmental Technology*. 35(20), 2634-2642.

Aslam, M., Charfi, A., Lesage, G., Heran, M., Kim, J., 2017. Membrane bioreactors for wastewater treatment: A review of mechanical cleaning by scouring agents to control membrane fouling. *Chemical Engineering Journal*. 307, 897-913.

Benyahia, B., Sari, T., Cherki, B., Harmand, J., 2013. Anaerobic membrane bioreactor modeling in the presence of Soluble Microbial Products (SMP) – the Anaerobic Model AM2b. *Chemical Engineering Journal*. 228(0), 1011-1022.

Cao, T. A., Van De Staey, G., Smets, I. Y., 2015. Integrating activated sludge floc size information in MBR fouling modeling. *Water Science and Technology*. 71(7), 1073-1080.

Chen, Y., Shen, L., Li, R., Xu, X., Hong, H., Lin, H., Chen, J., 2020. Quantification of interfacial energies associated with membrane fouling in a membrane bioreactor by using BP and GRNN artificial neural networks. *Journal of Colloid and Interface Science*. 565, 1-10.

Dean, A. P., Sigee, D. C., Estrada, B., Pittman, J. K., 2010. Using FTIR spectroscopy for rapid determination of lipid accumulation in response to nitrogen limitation in freshwater microalgae. *Bioresource Technology*. 101(12), 4499-4507.

Dereli, R. K., Grelot, A., Heffernan, B., van der Zee, F. P., van Lier, J. B., 2014. Implications of changes in solids retention time on long term evolution of sludge filterability in anaerobic membrane bioreactors treating high strength industrial wastewater. *Water Research*. 59(0), 11-22.

Ding, Y., Tian, Y., Li, Z., Zuo, W., Zhang, J., 2015. A comprehensive study into fouling properties of extracellular polymeric substance (EPS) extracted from bulk sludge and cake sludge in a mesophilic anaerobic membrane bioreactor. *Bioresource Technology*. 192(0), 105-114.

Duan, L., Song, Y., Yu, H., Xia, S., Hermanowicz, S. W., 2014. The effect of solids retention times on the characterization of extracellular polymeric substances and soluble microbial products in a submerged membrane bioreactor. *Bioresource Technology*. 163(0), 395-398.

Erkan, H. S., Engin, G. O., Ince, M., Bayramoglu, M. R., 2016. Effect of carbon to nitrogen ratio of feed wastewater and sludge retention time on activated sludge in a submerged membrane bioreactor. *Environmental Science and Pollution Research*. 23(11), 10742-10752.

Faust, L., Temmink, H., Zwijnenburg, A., Kemperman, A. J. B., Rijnaarts, H. H. M., 2014. High loaded MBRs for organic matter recovery from sewage: Effect of solids retention time on bioflocculation and on the role of extracellular polymers. *Water Research*. 56, 258-266.

Frølund, B., Palmgren, R., Keiding, K., Nielsen, P. H., 1996. Extraction of extracellular polymers from activated sludge using a cation exchange resin. *Water Research*. 30(8), 1749-1758.

Fu, C., Yue, X., Shi, X., Ng, K. K., Ng, H. Y., 2017. Membrane fouling between a membrane bioreactor and a moving bed membrane bioreactor: Effects of solids retention time. *Chemical Engineering Journal*. 309, 397-408.

Gaudy, A. F., 1962. Colorimetric determination of protein and carbohydrate. *Industrial water & wastes*. 7, 17-22.

Gutzeit, G., Lorch, D., Weber, A., Engels, M., Neis, U., 2005. Bioflocculent algal–bacterial biomass improves low-cost wastewater treatment. *Water Science and Technology*. 52(12), 9-18.

Hao, L., Liss, S. N., Liao, B. Q., 2016. Influence of COD:N ratio on sludge properties and their

role in membrane fouling of a submerged membrane bioreactor. *Water Research*. 89, 132-141.

Hasani Zonoozi, M., Alavi Moghaddam, M. R., Maknoon, R., 2015. Operation of integrated sequencing batch membrane bioreactor treating dye-containing wastewater at different SRTs: study of overall performance and fouling behavior. *Environmental Science and Pollution Research*. 22(8), 5931-42.

Hong, H., Zhang, M., He, Y., Chen, J., Lin, H., 2014. Fouling mechanisms of gel layer in a submerged membrane bioreactor. *Bioresource Technology*. 166(0), 295-302.

Huang, Z., Ong, S. L., Ng, H. Y., 2011. Submerged anaerobic membrane bioreactor for low-strength wastewater treatment: effect of HRT and SRT on treatment performance and membrane fouling. *Water Research*. 45(2), 705-13.

Jenkins, D., G. Richard, M., T. Daigger, G. 2004. *Manual on the Causes and Control of Activated Sludge Bulking, Foaming, and other Solids Separation Problems 3rd Edition*. Lewis

Kim, B.-C., Nam, D.-H., Na, J.-H., Kang, K.-H., 2014. Analysis of extracellular polymeric substance (EPS) release in anaerobic sludge holding tank and its effects on membrane fouling in a membrane bioreactor (MBR). *Water Science and Technology*. 70(1), 82-88.

Kumar, S. S., Basu, S., Gupta, S., Sharma, J., Bishnoi, N. R., 2019. Bioelectricity generation using sulphate-reducing bacteria as anodic and microalgae as cathodic biocatalysts. *Biofuels*. 10(1), 81-86.

Lee, C. S., Lee, S.-A., Ko, S.-R., Oh, H.-M., Ahn, C.-Y., 2015. Effects of photoperiod on nutrient removal, biomass production, and algal-bacterial population dynamics in lab-scale photobioreactors treating municipal wastewater. *Water Research*. 68, 680-691.

Lee, W., Kang, S., Shin, H., 2003. Sludge characteristics and their contribution to microfiltration in submerged membrane bioreactors. *Journal of Membrane Science*. 216(1-2), 217-227.

Li, R., Lou, Y., Xu, Y., Ma, G., Liao, B.-Q., Shen, L., Lin, H., 2019. Effects of surface morphology on alginate adhesion: Molecular insights into membrane fouling based on XDLVO and DFT analysis. *Chemosphere*. 233, 373-380.

Li, Z., Tian, Y., Ding, Y., Chen, L., Wang, H., 2013. Fouling potential evaluation of soluble

microbial products (SMP) with different membrane surfaces in a hybrid membrane bioreactor using worm reactor for sludge reduction. *Bioresource Technology*. 140(0), 111-119.

Liang, S., Liu, C., Song, L., 2007. Soluble microbial products in membrane bioreactor operation: Behaviors, characteristics, and fouling potential. *Water Research*. 41(1), 95-101.

Lin, H., Liao, B.-Q., Chen, J., Gao, W., Wang, L., Wang, F., Lu, X., 2011. New insights into membrane fouling in a submerged anaerobic membrane bioreactor based on characterization of cake sludge and bulk sludge. *Bioresource Technology*. 102(3), 2373-2379.

Lin, H., Zhang, M., Wang, F., Meng, F., Liao, B.-Q., Hong, H., Chen, J., Gao, W., 2014. A critical review of extracellular polymeric substances (EPSs) in membrane bioreactors: Characteristics, roles in membrane fouling and control strategies. *Journal of Membrane Science*. 460(0), 110-125.

Lin, H. J., Xie, K., Mahendran, B., Bagley, D. M., Leung, K. T., Liss, S. N., Liao, B. Q., 2009. Sludge properties and their effects on membrane fouling in submerged anaerobic membrane bioreactors (SAnMBRs). *Water Research*. 43(15), 3827-3837.

Liu, J., Wu, Y., Wu, C., Muylaert, K., Vyverman, W., Yu, H.-Q., Muñoz, R., Rittmann, B., 2017. Advanced nutrient removal from surface water by a consortium of attached microalgae and bacteria: A review. *Bioresource Technology*. 241, 1127-1137.

Lowry, O. H., Rosebrough, N. J., Farr, A. L., Randall, R. J., 1951. Protein measurement with the folin phenol reagent. *Journal of Biological Chemistry*. 193, 265-275.

Mayers, J. J., Flynn, K. J., Shields, R. J., 2013. Rapid determination of bulk microalgal biochemical composition by Fourier-Transform Infrared spectroscopy. *Bioresource Technology*. 148, 215-220.

Meng, F., Chae, S.-R., Drews, A., Kraume, M., Shin, H.-S., Yang, F., 2009. Recent advances in membrane bioreactors (MBRs): Membrane fouling and membrane material. *Water Research*. 43(6), 1489-1512.

Meng, F., Zhang, H., Yang, F., Li, Y., Xiao, J., Zhang, X., 2006. Effect of filamentous bacteria on membrane fouling in submerged membrane bioreactor. *Journal of Membrane Science*. 272(1-

2), 161-168.

Ng, H. Y., Hermanowicz, S. W., 2005. Membrane bioreactor operation at short solids retention times: performance and biomass characteristics. *Water Research*. 39(6), 981-992.

Ouyang, K., Liu, J. X., 2009. Effect of sludge retention time on sludge characteristics and membrane fouling of membrane bioreactor. *Journal of Environmental Sciences-China*. 21(10), 1329-1335.

Posadas, E., García-Encina, P.-A., Soltau, A., Domínguez, A., Díaz, I., Muñoz, R., 2013. Carbon and nutrient removal from centrates and domestic wastewater using algal–bacterial biofilm bioreactors. *Bioresource Technology*. 139, 50-58.

Shen, L.-g., Lei, Q., Chen, J.-R., Hong, H.-C., He, Y.-M., Lin, H.-J., 2015. Membrane fouling in a submerged membrane bioreactor: Impacts of floc size. *Chemical Engineering Journal*. 269(0), 328-334.

Su, Y. C., Pan, J. R., Huang, C. P., Chang, C. L., 2011. Impact of sludge retention time on sludge characteristics and microbial community in MBR. *Water Science and Technology*. 63(10), 2250-2254.

Sun, L., Tian, Y., Zhang, J., Cui, H., Zuo, W., Li, J., 2018a. A novel symbiotic system combining algae and sludge membrane bioreactor technology for wastewater treatment and membrane fouling mitigation: Performance and mechanism. *Chemical Engineering Journal*. 344, 246-253.

Sun, L., Tian, Y., Zhang, J., Li, H., Tang, C., Li, J., 2018b. Wastewater treatment and membrane fouling with algal-activated sludge culture in a novel membrane bioreactor: Influence of inoculation ratios. *Chemical Engineering Journal*. 343, 455-459.

Sun, L., Tian, Y., Zhang, J., Li, L., Zhang, J., Li, J., 2018c. A novel membrane bioreactor inoculated with symbiotic sludge bacteria and algae: Performance and microbial community analysis. *Bioresource Technology*. 251, 311-319.

Tang, X., He, L. Y., Tao, X. Q., Dang, Z., Guo, C. L., Lu, G. N., Yi, X. Y., 2010. Construction of an artificial microalgal-bacterial consortium that efficiently degrades crude oil. *Journal of*

Hazardous Materials. 181(1), 1158-1162.

Teng, J., Shen, L., Xu, Y., Chen, Y., Wu, X.-L., He, Y., Chen, J., Lin, H., 2020. Effects of molecular weight distribution of soluble microbial products (SMPs) on membrane fouling in a membrane bioreactor (MBR): Novel mechanistic insights. *Chemosphere*. 248, 126013.

Van den Broeck, R., Van Dierdonck, J., Nijskens, P., Dotremont, C., Krzeminski, P., van der Graaf, J. H. J. M., van Lier, J. B., Van Impe, J. F. M., Smets, I. Y., 2012. The influence of solids retention time on activated sludge bioflocculation and membrane fouling in a membrane bioreactor (MBR). *Journal of Membrane Science*. 401–402(0), 48-55.

Wang, J., Guan, J., Santiwong, S. R., Waite, T. D., 2008. Characterization of floc size and structure under different monomer and polymer coagulants on microfiltration membrane fouling. *Journal of Membrane Science*. 321(2), 132-138.

Wang, Z., Ma, J., Tang, C. Y., Kimura, K., Wang, Q., Han, X., 2014. Membrane cleaning in membrane bioreactors: A review. *Journal of Membrane Science*. 468(0), 276-307.

Wang, Z., Wang, P., Wang, Q., Wu, Z., Zhou, Q., Yang, D., 2010. Effective control of membrane fouling by filamentous bacteria in a submerged membrane bioreactor. *Chemical Engineering Journal*. 158(3), 608-615.

Xuan, W., Bin, Z., Zhiqiang, S., Zhigang, Q., Zhaoli, C., Min, J., Junwen, L., Jingfeng, W., 2010. The EPS characteristics of sludge in an aerobic granule membrane bioreactor. *Bioresource Technology*. 101(21), 8046-8050.

Xue, W., Tobino, T., Nakajima, F., Yamamoto, K., 2015. Seawater-driven forward osmosis for enriching nitrogen and phosphorous in treated municipal wastewater: Effect of membrane properties and feed solution chemistry. *Water Research*. 69, 120-130.

Yang, J., Gou, Y., Fang, F., Guo, J., Ma, H., Wei, X., Shahmoradi, B., 2018. Impacts of sludge retention time on the performance of an algal-bacterial bioreactor. *Chemical Engineering Journal*. 343, 37-43.

Zhang, D., Trzcinski, A. P., Kunacheva, C., Stuckey, D. C., Liu, Y., Tan, S. K., Ng, W. J., 2016. Characterization of soluble microbial products (SMPs) in a membrane bioreactor (MBR)

treating synthetic wastewater containing pharmaceutical compounds. *Water Research*. 102, 594-606.

Zhang, M., Liao, B.-q., Zhou, X., He, Y., Hong, H., Lin, H., Chen, J., 2015. Effects of hydrophilicity/hydrophobicity of membrane on membrane fouling in a submerged membrane bioreactor. *Bioresource Technology*. 175(0), 59-67.

Zhou, Z., Meng, F., Lu, H., Jia, X., 2013. Denitrification-caused suppression of soluble microbial products (SMP) in MBRs used for biological nitrogen removal. *AIChE Journal*. 59(10), 3569-3573.

Chapter 7 Conclusions and future work

1.1 Conclusions

Microalgal-bacterial membrane photobioreactor (MB-MPBR) is a novel technology developed recently by integrating membrane separation process into the microalgal-bacterial consortium. As compared with traditional MBR, it takes some distinctive advantages of improved nutrient removal efficiency, reduced aeration energy consumption, and mitigated membrane fouling. As a new technology, MB-MPBR is still in its very early stage of research and development and should overcome lots of challenges before realizing industrial applications. However, seldom studies have investigated the processing performance, condition optimization, and membrane fouling of MB-MPBR for wastewater treatment. Therefore, this thesis investigated the effects of combined HRT (nutrients loading rate) and N/P ratio variation, and solo SRT variation on the biological performance and membrane fouling of MB-MPBR for wastewater treatment.

HRT and N/P ratio significantly affected the biological performance of MB-MPBR for municipal wastewater treatment. The underlying reason was the different nutrient loading rate resulted from the various combinations of HRT and N/P ratio. A lower N/P ratio (3.9:1) and HRT (2 d) promoted the biomass yield. A COD and ammonia-N removal efficiency of over 96% and 99% respectively was achieved under all tested conditions, regardless of N/P ratio and HRT. The TN and TP removal varied under different conditions, but a low level of TN (< 10 mg/L) and TP (< 1 mg/L) was achieved under the appropriate conditions and met the discharge standards of effluent in a single stage.

In MB-MPBR, N/P ratio also had a significant impact on membrane performance by controlling the growth balance of microalgae and bacteria and their biological properties. A lower N/P ratio of 3.9:1 led to a more quickly TMP increase under the same HRT and influent TN concentration. The dominant fouling mechanism was cake layer formation. Characterization results showed that smaller particle size and changes in surface composition (e.g. bound EPS

composition) under the lower N/P ratio were the primary contributors to the faster increase in membrane fouling. XPS, FTIR, and microscopic analysis demonstrated that the underlying reason for the decreased floc size was attributed to the strengthened competitiveness and overgrowth of microalgae at P-rich conditions. In brief, optimizing the operating conditions, such as appropriate nutrients loading rate and COD/N/P ratio, to balance the microalgae and bacteria growth at an appropriate ratio is the key for membrane fouling control in MB-MPBRs.

For the treatment of high strength anaerobic digestion effluent, longer SRT led to higher biomass concentration and increased TP removal efficiency, which was attributed to the enhanced surface-adsorption under higher biomass concentration. The TN removal relied on microalgae assimilation, whereas they were nonlinearly correlating to SRT. SRT had little impact on COD removal, while greatly influenced the PSD and microscopic morphology of microalgal-bacterial consortium. High nutrient concentration negatively impacted the microalgae growth and nutrient removal, and thus influent dilution or a longer HRT is required to achieve effluent quality meets the discharge standards. In short, intermedium SRT in the range of 10-20 d benefits the reliable operation of MB-MPBRs.

In addition, SRT had a significant impact on membrane performance by controlling the biomass concentration and properties and the growth status of microalgae and bacteria. Membrane fouling rate was nonlinearly correlating to SRT. The predominant fouling mechanism was gel layer formation. The fastest membrane fouling and highest pore-clogging filtration resistance were observed at SRT of 20 d. Characterization results showed that the biomass flocs at SRT of 20 d had the largest floc size and moderate filament abundance. The higher membrane fouling at SRT of 20 d was mainly attributed to the higher concentration of EPS and SMP. In brief, optimizing the SRT value to control the balanced growth of microalgae and bacteria and keep them at an appropriate ratio is the key to delay membrane fouling in MB-MPBR.

Overall, MB-MPBR is a promising technology to simultaneously remove COD and nutrients from wastewater. For the treatment of municipal wastewater with medium nutrients strength, it is

feasible to use MB-MPBR to achieve a high-quality effluent meets discharge standards in a single system. As for high-strength wastewater like anaerobic digestion effluent, influent dilution or a longer HRT is required to achieve satisfactory effluent quality. In MB-MPBR system, the coexistence of microalgae and bacteria can effectively improve the removal efficiency of nutrients and achieve high-quality effluent in a single step, which can reduce the capital costs. Besides, the cooperation of microalgae and bacteria can reduce the energy demand of mechanical aerations for CO_2 and O_2 deliveries, and hence be regarded as a safer and more cost-effective alternative of mechanical aeration. As a new technology, MB-MPBR is still at its very early stage of research and development and requires more study to overcome lots of challenges before realizing engineering applications. In this thesis, the optimal operating conditions were not achieved. However, this research has strengthened our understanding of MB-MPBR technology and is a pioneering study that can help promote the development of sewage treatment technology.

1.2 Future work

MB-MPBR technology is a novel system developed for simultaneous COD and nutrients (N and P) removals from wastewater. Although MB-MPBR takes many distinctive advantages for wastewater treatment, it should overcome a lot of challenges before satisfying industrial applications. To date, we have inadequate knowledge about MB-MPBR, which will significantly hinder its further development and wider application. Therefore, more researchers are urgently required with the intention of enhancing the system performance and commercial feasibility of MB-MPBR technology.

Currently, MB-MPBR research is limited to the treatment of artificial wastewater with low or medium nutrients strength. Studies on wastewater with high nutrients strength, such as concentrates, are rare. Further research is needed to examine various wastewaters to assess further practical implementation of MB-MPBR.

Except for HRT, N/P ratio, and SRT, the treatment effectiveness and membrane fouling of MB-MPBR are affected by other conditions, such as pH, temperature, toxic compound load, need

to be investigated for MB-MPBRs. Besides, these operating conditions may have complicated interactions, and holistic evaluation is required to sort out the complex relationship between them.

Illumination is essential for microalgae photosynthetic activity. However, MB-MPBR is characterized by high biomass concentrations that may cause self-shading. Therefore, further studies regarding the reactor design with the purpose of effective light penetration in MB-MPBRs are recommended.

The cooperative interaction of microalgae and bacteria leads to less or no demand for aeration. However, in MB-MPBR, the function of aeration is not only providing O_2/CO_2 but also mixing the biomass and scouring membrane to prevent foulants adhesion. Therefore, special attention should be given to the assessment of the economic viability of different aeration types and rates. The feasibility of using oxygen released from microalgae for bacteria growth with no external aeration should be investigated to save aeration energy.

The microalgal-bacterial interactions associate with complicated chemical reactions, their effects on the biological performance of MB-MPBRs needs to be further investigated.

Membrane fouling is inevitable, in which EPS and SMP are considered as the major contributors. However, in MB-MPBR, the existence of microalgae may lead to the production of new foulants, which may correspond to new fouling mechanism. Further work is needed to evaluate the influencing factors and underlying mechanisms of membrane fouling in MB-MPBRs.